# Lithoclass and shear wave velocity characterisation of terps

Aalbersberg, G.; Meijles, Erik

# Lithoclass and shear wave velocity characterisation of terps: an assessment in relation to earthquake risks

Dr. G. Aaldersberg and dr. E.W. Meijles

**Salisburt Archäologie GmbH and**

**Faculty of Spacial Sciences, Rijksuniversiteit Groningen**

Datum October 2020

Editors Jan van Elk

# General Introduction

The ground acceleration experienced as a result of the earthquakes induced by the production of gas from the Groningen gasfield is locally dependent on the shallow geological and soil conditions. This is called the site-response. Erik Meijles of the Rijksuniversiteit Groningen prepared an introduction to the quaternary geology of the Groningen area (Ref. 1 and 2).

Deltares studied the shallow geological and soil conditions using the Geotop model and numerous cone-penetration tests performed by Fugro and Wiersema (Ref. 3 to 8) and prepared a detailed model of the shallow subsurface below Groningen (Ref. 9 to 16). However, these studies and models do not address man-made changes to the shallow subsurface. An important man-made change to the shallow subsurface in Groningen is the dwelling mound or terp (regionally called 'wierde'). These are especially important, because these often form the village centers with relatively high population densities. In addition, many buildings on the terps are old and of cultural importance.

As part of the NAM-led studies program, geographers and archeologists of the Rijksuniversiteit Groningen investigated the lithological composition and geometry of terps in the province of Groningen (Ref. 17). This first report provides a database and classification of terps with modelled texture classes of the clastic sediment component of all terps in Groningen. Also micro-scale data on anthropogenic lithology of a selection of terps in the province are provided.

Based on shallow geological cores and geophysical measurements detailed lithological description have been prepared for eight selected terps in Groningen (Ref. 18). The current report describes the lithology and shear-wave velocity derived from these measurements for development of a site-response for terps.

More information on the modelling of the earthquake response of buildings located on terps can be found in reference 19.

# References


1 A geological history of Groningen's subsurface - eng, Erik Meijles, Rijksuniversiteit Groningen, NAM, June 2015.

2 De ondergrond van Groningen: een geologische geschiedenis, Erik Meijles, Rijksuniversiteit Groningen, NAM, June 2015.

3 CPT in Thinly Layered Soils - Validation Tests and Analysis for Multi Thin Layer Correction, D.A. de Lange, Deltares, Aug 2018.

4 Campaign to acquire SCPT at the location of the G-stations of the Seismic Monitoring Network (operated by KNMI), FUGRO, FUGRO, Nov 2019.

5 Digital data campaign to acquire SCPT at the location of the G-stations of the Seismic Monitoring Network (operated by KNMI), FUGRO, FUGRO, Nov 2019.

6 Dataset describing the shallow geology Vs for GMM V6, Pauline Kruiver, Deltares, Mar 2019.

7 Digital data second campaign to acquire SCPT at the location of the G-stations of the Seismic Monitoring Network (operated by KNMI), FUGRO, FUGRO, Aug 2020.

8 Second Campaign to acquire SCPT at the location of the G-stations of the Seismic Monitoring Network (operated by KNMI), FUGRO, FUGRO, Aug 2020.

9 Geological schematisation of the shallow subsurface of Groningen. For site response to earthquakes for the Groningen gas field. part 1, Pauline Kruiver, Ger de Lange, Ane Wiersma, Piet Meijers, Mandy Korff, Jan Peeters, Jan Stafleu, Ronald Harting, Roula Dambrink, Freek Busschers and Jan Gunnink, Deltares and NAM, June 2015.

10 Geological schematisation of the shallow subsurface of Groningen. For site response to earthquakes for the Groningen gas field. part 2, Pauline Kruiver, Ger de Lange, Ane Wiersma, Piet Meijers, Mandy Korff, Jan Peeters, Jan Stafleu, Ronald Harting, Roula Dambrink, Freek Busschers and Jan Gunnink, Deltares and NAM, June 2015.

11 Geological schematisation of the shallow subsurface of Groningen. For site response to earthquakes for the Groningen gas field. part 3, Pauline Kruiver, Ger de Lange, Ane Wiersma, Piet Meijers, Mandy Korff, Jan Peeters, Jan Stafleu, Ronald Harting, Roula Dambrink, Freek Busschers and Jan Gunnink, Deltares and NAM, June 2015.

12 Modifications of the Geological model for Site response at the Groningen Field, P. Kruiver, Deltares, June 2016.

13 Geophysical measurements of shear wave velocity at KNMI accelerograph stations in the Groningen gas field area, July 2016.

14 Assessment of dynamic properties for peat - Factual Report, dr.ir. C. Zwanenburg and M. Konstantinou, Deltares, Oct 2017.

15 Dynamic behaviour of Groningen peat - Analysis and parameter assessment, M. Konstantinou, dr.ir. C. Zwanenburg and dr.ir. P. Meijers, Deltares, Oct 2017.

16 Background document NAM database of subsurface information - Version date of database - 29 March 2018, Pauline Kruiver, Fred Kloosterman, Ger de Lange, Pieter Doornenbal, Deltares, Mar 2018.

17 Terp composition in respect to earthquake risk in Groningen, Dr. ir. E.W. Meijles, Dr. G. Aalbersberg, and Prof. dr. H.A. Groenendijk, RUG, Mar 2016.

18 Archeologisch en seismisch onderzoek naar de lithologie en opbouw van acht wierden in de provincie Groningen - Gemeente Hogeland, Delfzijl en Westerkwartier, Dr. G. Aaldersberg en drs H.W. Veenstra, RAAP Archeologisch Adviesbureau, Feb 2021.

19 Study of the impact of Wierden soil on Groningen buildings fragility, Francesco Cavalieri, Antonio A. Correia and Helen Crowley, Mozayk, November 2020.

NAM

| | | | |
|---|---|---|---|
| **Title** | Lithoclass and shear wave velocity characterisation of terps: an assessment in relation to earthquake risks | **Date** | October 2020 |
| | | **Initiator** | NAM |
| **Autor(s)** | Dr. G. Aaldersberg and dr. E.W. Meijles | **Editors** | Jan van Elk |
| **Organisation** | Salisburt Archäologie GmbH and Faculty of Spacial Sciences, Rijksuniversiteit Groningen | **Organisation** | NAM |
| **Place in the Study and Data Acquisition Plan** | Study Theme: Ground Motion Preduction<br>Comment:<br>The ground acceleration experienced as a result of the earthquakes induced by the production of gas from the Groningen gasfield is locally dependent on the shallow geological and soil conditions. This is called the site-response. Erik Meijles of the Rijksuniversiteit Groningen prepared an introduction to the quaternary geology of the Groningen area.<br>Deltares studied the shallow geological and soil conditions using the Geotop model and numerous cone-penetration tests performed by Fugro and Wiersema and prepared a detailed model of the shallow subsurface below Groningen. However, these studies and models do not address man-made changes to the shallow subsurface. An important man-made change to the shallow subsurface in Groningen is the dwelling mound or terp (regionally called 'wierde'). These are especially important, because these often form the village centers with relatively high population densities. In addition, many buildings on the terps are old and of cultural importance.<br>As part of the NAM-led studies program, geographers and archeologists of the Rijksuniversiteit Groningen investigated the lithological composition and geometry of terps in the province of Groningen. This first report provides a database and classification of terps with modelled texture classes of the clastic sediment component of all terps in Groningen. Also micro-scale data on anthropogenic lithology of a selection of terps in the province are provided.<br>Based on shallow geological cores and geophysical measurements detailed lithological description have been prepared for eight selected terps in Groningen. The current report describes the lithology and shear-wave velocity derived from these measurements for development of a site-response for terps.<br>More information on the modelling of the earthquake response of buildings located on terps can be found in a separate report. | | |

| | |
|---|---|
| **Directliy linked research** | (1) Hazard Assessment.<br>(2) Fragility assessment of buildings in the Groningen region (located on terpen). |
| **Used data** | Data of the University of Groningen. |
| **Associated organisation** | Raap Archeologisch Adviesbureau<br>Deltares<br>Mozayk |
| **Assurance** | Internal assurance RUG |

# Lithoclass and shear wave velocity characterisation of terps: an assessment in relation to earthquake risks

Project phase 2

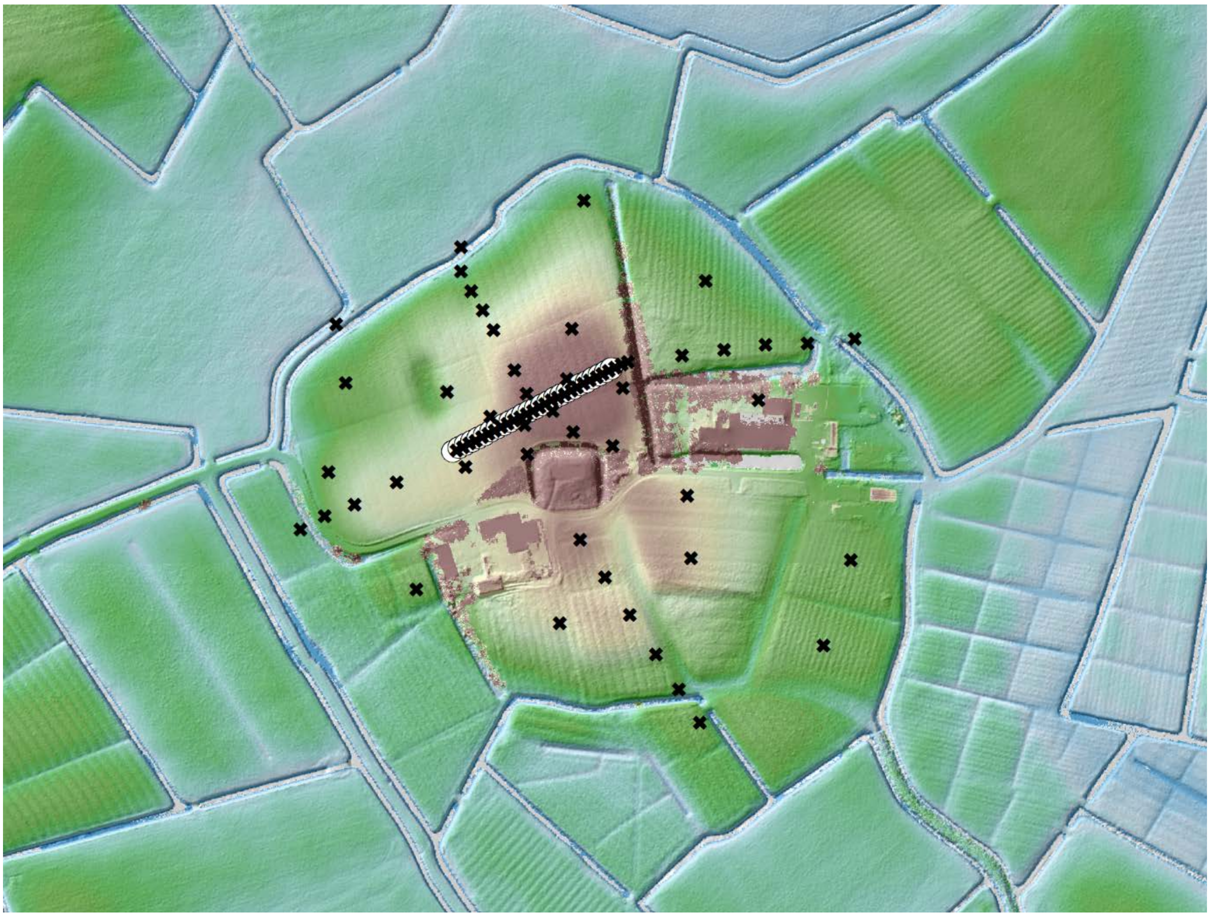

G. Aalbersberg
Salisburt Archäologie GmbH
Hanns-Martin-Schleyerstraße 3
D-48301 Nottuln (Dld.)

E.W. Meijles
Faculty of Spatial Sciences
Rijksuniversiteit Groningen
PO Box 800
9700 AV Groningen
The Netherlands

October 2020

# Contents

# 1 Introduction and problem description

The northern Netherlands, and the northern part of the Groningen province in particular, are currently experiencing subsidence and induced earthquakes caused by extraction of natural gas from the Groningen gas field. The shallow geology of this area predominantly consists of unconsolidated heterogenic Holocene deposits of coastal and tidal origin on (peri)glacial sediments dating from the Pleistocene. Since such soft sediments are characterised by low, small strain shear wave velocities ($v_s$ typically around 200 m/s), they are known to amplify earthquakes (Kruiver *et al.*, 2017a). In order to predict the geohazards of ground shaking and liquefaction at the surface, a ground motion model (GMM) was developed (Bommer *et al.*, 2017; Van Elk *et al.*, 2018). The GMM in turn is based on the detailed 3D geological GeoTOP voxel model, containing lithostratigraphical and lithoclass attributes derived from on a large archive of geological core data (Stafleu *et al.*, 2012; Stafleu *et al.*, 2016). It models the lithoclasses for the uppermost 50 m of the subsurface with a horizontal resolution of 100 m and a vertical resolution of 0.5 m. Lithology or lithoclass is one of the most important parameters determining the shear wave velocity of a particular layer, and therefore of the transmission and the amplification of earthquake waves reaching the surface. For application in the GMM, GeoTOP was used to classify the heterogeneous natural layers into geological zones. Typical sequences of geological units were converted to representative voxel stacks for the province of Groningen. Details of this procedure are described in Kruiver *et al.* (2017a).

However, an important aspect still missing from the model are the layers associated with terps, anthropogenic dwelling mounds occurring in abundance in the northern coastal area. Terps, locally called wierden in Groningen, are manmade mounds created between the middle Iron Age and Late Medieval period as a defence against flooding (Bazelmans *et al.*, 2012; Nieuwhof *et al.*, 2019). They are relatively small, typically around 10 ha, and an altitude of several metres above their direct surroundings. Although the total area of the terps in the northern Netherlands is limited in terms of percentage cover, their significance should not be underestimated, as well over 900 terps occur in the province of Groningen alone. They form the core on which many densely built village centres are situated, and thus have relatively high population densities compared to surrounding rural areas. In addition, a substantial amount of the (built) cultural heritage of the province is located on or associated with terps, including 12th century churches, typical regional housing and village layouts with high heritage values (Bazelmans *et al.*, 2012). It is therefore no surprise, that for the terps, their population and their heritage, earthquakes are a potential threat.

Given their relatively small size in comparison to the average coring interval in the available mapping data (c. 330 m), terps are seldom characterised in 2D or 3D geological mapping. In addition, the anthropogenic nature of these terps means that they are not representative of the natural sediments, and are as such of limited value to the mapping of past landscapes. Consequently, if at all, they are only classified as "anthropogenic" without any further lithological information. This means that the terps in the province of Groningen are insufficiently represented in the GeoTOP model and the GMM, which poses a serious problem in earthquake assessment.

In order to include terps in the GeoTOP model and GMM and thus provide accurate assessments of the behaviour of earthquake waves within the terp and the impacts they have on buildings and people, first of all the lithology, geometry and elevation of the terps needs to be established. Secondly, an assessment of typical shear wave velocities in the terps is needed. These data can then be added to the voxel stacks of the GMM model to assess to what extent the terps may (further) amplify earthquake motions.

From archaeological observations, it is apparent that terp lithology can be very heterogeneous as they were built of almost any available material. Plaggen (Dutch for sods) were cut from the diverse salt marsh deposits in the immediate surroundings of the terp to form the majority of the terp body. It also contained varying amounts of soil from the digging of pits and ditches on and near the terp, and, most importantly, cattle manure (Miedema, 1983; Knol, 1993; Bazelmans *et al.*, 2012; Nieuwhof, 2019).

In the spring of 2016, a desk study was carried out as an inventory of available data and an initial estimate of terp lithology based on geomorphological, soil and altitude maps and archaeological sources (Meijles *et al.*, 2016). Although they concluded that a GIS-based approach provided a good first assessment of the lithology and that it was theoretically possible to assess composition for each terp in the area, no fieldwork was carried out to test the outcome empirically. Furthermore, the composition of terps was shown to vary at the regional scale as well as within individual terps themselves, leading to the conclusion that detailed information on lithoclass variation at regional and terp scales was required to provide data for input in earthquake models. Moreover, since the GIS-based approach used soil maps as its primary source, the contribution of manure to the total volume of the terp body could not be assessed. The available data however suggested that this contribution could be considerable. In addition, the research only resulted in an assessment of typical lithoclasses, but did not include shear wave velocity measurements. Given the lithological differences between anthropogenic and natural sediments, assigning $v_s$ values from literature to terp layers was considered too imprecise or impossible.

Therefore, this project aims to assess the lithological composition and typical shear wave velocities of terps in the province of Groningen. It consists of archaeo-lithological hand coring and micro-seismic measurements on a representative set of terps. By combining these datasets, a statistical representation of lithoclasses and their distribution within the terp body was created, providing the input for the GMM.

Chapter 2 of this report presents a brief characterisation of geological and archaeological history of the research area. After the description of the methodology of the seismic and archaeological investigations and statistical analyses in chapter 3, chapter 4 presents the results for each location. Chapter 5 provides a synthesis of the results as well as a comparison between the lithological results of the current project and those of soil map modelling. Finally, conclusions and recommendations can be found in chapter 6.

# 2 Geological and anthropogenic origin of the study area

The study area comprises the Holocene coastal plain north of the city of Groningen, which forms part of the belt of coastal plains stretching from the province of Fryslân in the west to northwestern Germany in the east. The geological development of this area is complex and governed by (amongst others) rising relative sea-level during the Holocene, position and morphology of the barrier islands, and sediment supply. Based on core data and $^{14}$C-dating, Roeleveld (1974) provided a lithostratigraphical and chronostratigraphical framework for the area on which later research has been based.

Pleistocene deposits and morphology dating from the Saalian and Weichselian form the basement on which the Holocene development of the coastal plain took place. During the second part of the Saalian glaciation (Drente Stadial; OIS-6; c. 200 – 120 ka BP), the outline of the present-day landscape was formed by the Scandinavian ice sheet. Not only did the glaciers deposit an extensive sheet of basal till (Drente Fm, Gieten Mbr) across the northern provinces, successive advances from the northeast and northwest created a series of ice-pushed and subsequently re-moulded ridges of which the Hondsrug-complex is the most prominent (Rappol, 1984; Van den Berg and Beets, 1987). The city of Groningen is situated on this Hondsrug-complex, which to the north of the city dips towards the northeast and becomes invisible by a cover of Holocene deposits. A comparatively small subcrop of Pleistocene deposits and part of the Hondsrug-complex, often referred to as the 'Winsumer High', occurs near Winsum/Ranum (c. 11 km north-north-east of Groningen). Other, small glaciogenic ridges can be found near Noordhorn, the Schildmeer area and Midwolda/Winschoten. Immediately east of the Hondsrug complex, the Hunze valley was carved out by the advancing ice and later meltwater streams.

Deposits from the Eemian Interglacial are known only from cores. High sea levels during this period led to the deposition of marine sediments, in particular in the deeper basins in between the glaciogenic ridges as well as in the Hunze valley.

In the following Weichselian Glacial, the Scandinavian ice-sheet did not reach the northern Netherlands, but the severe climatic conditions during the Late Pleniglacial and Younger Dryas Stadial in particular permitted a scant vegetation cover only leading to erosion and aeolian deposition ('coversand', Boxtel Fm, Wierden Mbr).

The climatic amelioration at the start of the Holocene and the retreat of the Scandinavian ice-sheet not only allowed the vegetation to develop from arctic tundra into mixed forest and the landscape to stabilize, but also led to rapidly rising relative sea-levels (Meijles *et al.*, 2018). As a consequence, regional groundwater levels also rose leading to peat formation (Nieuwkoop Fm, Basal Peat Bed) in closed depressions and at the intersection of the groundwater table and the Pleistocene topography. With rising sea-levels, peat formation moved land inward, ultimately covering a substantial part of the Pleistocene topography. At around 6000-5000 BC, a notable change in landscape occurred with the development of a large tidal and intertidal area in the northern coastal area. Although the general trends are the same, from this moment onwards, the various physiogeographical regions follow their own paths in landscape genesis.

The western part of the coastal plain (Hunsingo), formed the Hunze estuary and remained under marine influence right until embankment during the Middle Ages. As a result, a considerable sequence of clastic tidal sediments has been deposited; moreover, erosion by the deeply incised Hunze and tidal channels has removed much of the Late Pleistocene and early Holocene deposits and peat layers. Initially, the Hunze drained northwards through a large tidal outlet near Pieterburen. Saltmarsh barriers and natural levees bordering the channels were slightly higher than their surroundings and therefore provided the inhabitable locations for the first settlers to build their farmsteads. The first terps were constructed on these sites, mainly built out of sods taken from their direct environment. This situation persists, with continuously rising relative sea-level and a coastline gradually moving northwards, until the development of the Lauwerszee and the subsequent change of the Hunze-system to its present, westerly course around 800 AD. From this moment onward, marine influence steadily decreases until embankment in the Middle Ages all but ends it. In this period, many more terps were constructed and many existing terps were enlarged and heightened to raise further above flood levels. Many terps grew from single farmstead terps to the size of villages. The highest points were taken up by farms and houses, whereas the flanks served as arable lands and grassland.

From a geological point of view, the development of the eastern part, also called Fivelingo, is broadly similar to that of the western part, but the presence of a peat layer (Nieuwkoop Fm, Hollandveen Mbr) intercalated in the sequence of tidal deposits points to a return to freshwater back-barrier swamps. Start and end of the peat formation have been dated to c. 4000 BC and 500 BC respectively, although these dates obviously vary locally.

From the Middle Ages onward, man started playing a more active role in the development of the coastal landscape of northern Groningen by embanking, ditching and reclaiming the higher saltmarsh areas (Bazelmans *et al.*, 2012; Nieuwhof and Schepers, 2016). At the same time, terps were still inhabited and even raised since the embankments were breached or overtopped occasionally leading to flooding and inundation. Later still, coastal aggradation was helped and probably accelerated by building wooden structures in the intertidal zone to minimize wave action and allowing more sediment to settle. As a result, the coastline moved northwards in a stepwise fashion, with each embanked section or polder slightly higher than the previous.

On several occasions during the following centuries however, and most recently at Christmas 1717, dikes and saltmarsh barriers were breached leading to extensive flooding and loss of lives and livestock even up to the city of Groningen. The current landscape of the Dollard area, in the eastern part of the coastal plain, consists of a succession of reclaimed polders in two embayments caused by a series of catastrophic floods in the early 16$^{th}$ century.

The interaction between geological processes and anthropogenic use resulted in a pattern in which many terps are located on one of the saltmarsh barriers in the study area, and thus provide additional chronological information on the dating of these saltmarsh barriers. It must be noted however, that this information is based on pottery typology, and a lack of recent exposures, cores or other ways of finding pottery may well mean datable material related to the earliest phases has not or not yet been found. Starting dates therefore must be used with a certain degree of caution.
The coastal aggradation described above has led to a distinct south to north increase in median particle size also visible on the soil map, which is expected to be reflected in terp lithology. However, local topography will have played an important role in the actual characteristics of the sediment available for plaggen and terp building.

During the first quarter of the 20$^{th}$ century, extensive quarrying of the terps for their organic-rich soil (which was sold as fertilizer in the poor sandy regions) inevitably led to finds, kindling an occasional interest into a more or less scientific approach. The Ezinge terp is probably the most famous example of this early archaeological research, where finds and the remains of buildings and other structures were documented both in horizontal planes and sections (e.g. Van Giffen 1926; 1928). The sections still provide one of the best (but still limited) sources of lithological information and the general terp development. More recent work on temporary exposures in terps in the province Fryslân has shown that terp development can be summarized in two distinct phases. A first phase was characterised by the gradual accumulation of manure-rich occupation layers and layers composed of plaggen to raise the surface. During the second phase, the surface was raised by adding plaggen and in some cases, levelling the terp somewhat by spreading material from the top of the terp over its flanks (see for instance Nicolai, 2019; De Langen & Mol, 2016). This latter phase is thought to date from the 13th century, when embankment provided the houses and buildings sufficient protection against flooding for them to move to the lower flanks of the terps. The addition of material therefore created extra surface for agriculture on the most fertile locations in the landscape while also providing more flooding protection for the crops. Smaller, single homestead terps on the other hand are usually younger and generally consist of a single “terp layer”.

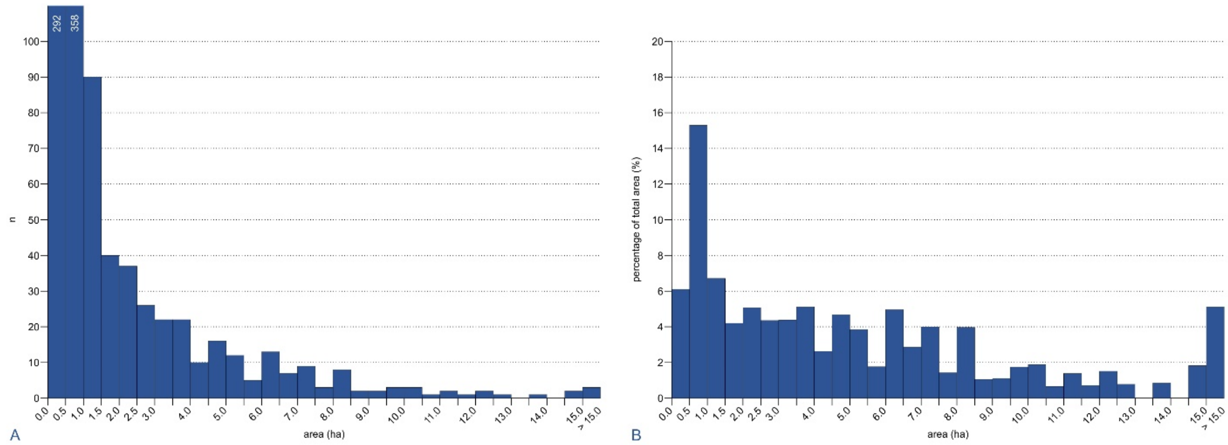


*Figure 2.1: A: Frequency distribution of terp area (class size 0.5 ha); B: Percentage of total area per size class.*

A large number of terps has been mapped out by the Province of Groningen in the 1980s and 1990s (Miedema, 1983, 1990), which, with an additional survey in the late 2010s, resulted in a database of 900 terps within the province. Figure 2.1 clearly shows that the majority of terps (n= 650) has an area < 1.0 ha and can be classified as “small”. Usually a single farmstead (house and outbuildings) is or was located on such terps, and in general, they are considered to be created during the youngest phase of terp development. Despite the high number of objects, this class only represents slightly over 20 % of total terp area. The anthropogenic layers in this type of terp are relatively thin and therefore their effect on seismic waves is expected to be relatively small. In this phase of the research, it is not meaningful to select such terps.

The category of large terps comprises most of the terps underlying the present-day villages (so-called “dorpsterpen”). In many instances, these terps probably started out as one or several smaller house terps, which later merged. In some cases, as for instance Ulrum and possibly Grote Houw, a similar merging of terps occurred once more leading to very large twin terps sometimes with a quite distinctive development history.

All terps between classes “large” and “small” can be considered as medium terps. In many instances, their development resembles that of large terps. However, in contrast to the larger terps, these terps did not develop any further and sometimes seem to have been abandoned. The reason for this abandonment is unknown; perhaps the larger terps provided sufficient space for the population.

The above description not only shows that the geological subsurface is geographically very heterogeneous; it also shows the large variability in size and composition of terps. Although many terps have been investigated for archaeological purposes, there is limited structured data available on lithoclass composition on a substantial number of terps to provide a quantitative view on terp composition and its variability.

# 3 Methodology

## 3.1 Approach

As Meijles *et al.* (2016) have shown, the amount of reliable and detailed lithological data for terps in the Groningen coastal plain (both in terms of number of location and quality) is insufficient to be used for improving the current GMM models. They recommended conducting field tests combining geoarchaeological coring and the collection of seismic data on a number of locations to investigate the relation between terp lithology and seismic properties of the anthropogenic layers.

Shallow micro seismicity data with a high horizontal resolution should provide a detailed 2D spatial picture of the seismic properties, and in particular of the shear wave velocity ($v_s$) of terp layers. Archaeo-lithological coring along the micro seismicity profiles provides accurate descriptions of the lithology as well as depths of layer boundaries, and will be used for the statistical comparison with micro seismicity data.

## 3.2 Terp selection criteria

Following the recommendations formulated by Meijles *et al.* (2016), a representative sample based on expert knowledge and location of different terps was selected from the current terp database:

- ideally, the selection should include locations in all major physiogeographical regions within the coastal zone identified in the prior report. The distinct developments of these areas define the characteristics of both the natural sequences and the sediments available for building the terps;

- the available lithological data from terps and current understanding of their development suggests a marked difference between small, single-farm terps and medium to large terps. The former category is thought to consist of just a few layers of anthropogenic material (leading to relatively low mounds); the latter terps may or may not contain manure layers, depending on age and location, and are relatively high. This latter category is also the most relevant to the research at this stage, as a substantial part of the historic buildings are located on medium to large terps. Furthermore, as the effect of anthropogenic layers in general on seismic wave transmission is as yet unknown, it was assessed that detecting such effects would be easier using locations with comparatively thick anthropogenic layers;

- research has already shown that inter-terp variability can be very high, even between locations in the same region and of the same age. As an example, Ezinge and Englum, located approximately only 1,5 km from each other, show substantially different compositions, with the lower anthropogenic layers at Englum having a considerably higher manure content than at Ezinge. Simple extrapolation of terp composition models to all locations with similar ages within a certain area may well be problematic. A large sample size, or at least several locations within the same region, is recommended;

- the use of built-up terps has the obvious advantage of a direct link between the measured data and (potential) earthquake damage. However, the use of built-up terps also has significant drawbacks. The presence of foundations and subsurface infrastructure such as sewers potentially hampers core and geophone location selection, but may also cause reflection and/or refraction of seismic waves adding another layer of uncertainty to the measurements. Finally, the amount of noise, and the vibrations caused by traffic, will be considerably higher on built-up terps;

- extensive commercial quarrying of terps for the use of “terp earth” as fertilizer in the late 19th and early 20th century AD has left many large and medium terps damaged to some extent, and in several cases (for instance Rottum) only small but relatively high pedestals around the church and other buildings remain. The response of such pedestals to seismic shaking will undoubtedly differ from that of more or less intact terps, but this would add more parameters to the interpretation of the measurement data. Therefore quarried terps should not be part of the selection;

- finally, social considerations have played an important role in terp selection. As with the choice for built-up terps or terps with a minimum of buildings, selecting locations in the worst hit part of the coastal plain (i.e. the wider Middelstum-Loppersum area) would probably provide a more direct link between measurements, actual earthquake information and damage. However, given the extent of earthquake-related damage and its effects on the inhabitants, it was anticipated that they would be less willing to cooperate with the project. Therefore, only locations outside the Middelstum-Loppersum area were selected.


*Figure 3.1: Example of quarrying a terp (Westeremden) in the early 20th century, leaving a steep face and a pedestal-shape terp body (Picture Collectie Groninger Archieven, www.beeldbankgroningen.nl (1173-143-102))*

## 3.3 Shear wave velocity data acquisition and modelling

Seismic microtremor measurements at the selected terps were performed using active and passive surface wave techniques (Geovision, 2019a). Hammer and accelerated weight drop sources were used for active Rayleigh wave acquisition and a shear wave vibrator for passive Love wave acquisition. All measurements were carried out by Rossingh Drilling and Geophysics (Gasselte, The Netherlands). Multi-channel analysis of surface wave (MASW) data were collected and then developed into 1D $v_s$ models using the passive source Rayleigh and Love wave data, accelerated weight drop (1D MASW) and 2D MASW data. The data were also developed into 2D $v_s$ profiles using the active source Rayleigh and Love wave data collected along approximately 120 m long transects on each terp. Full details on data acquisition and resulting models can be found in Geovision (2019a,b,c).

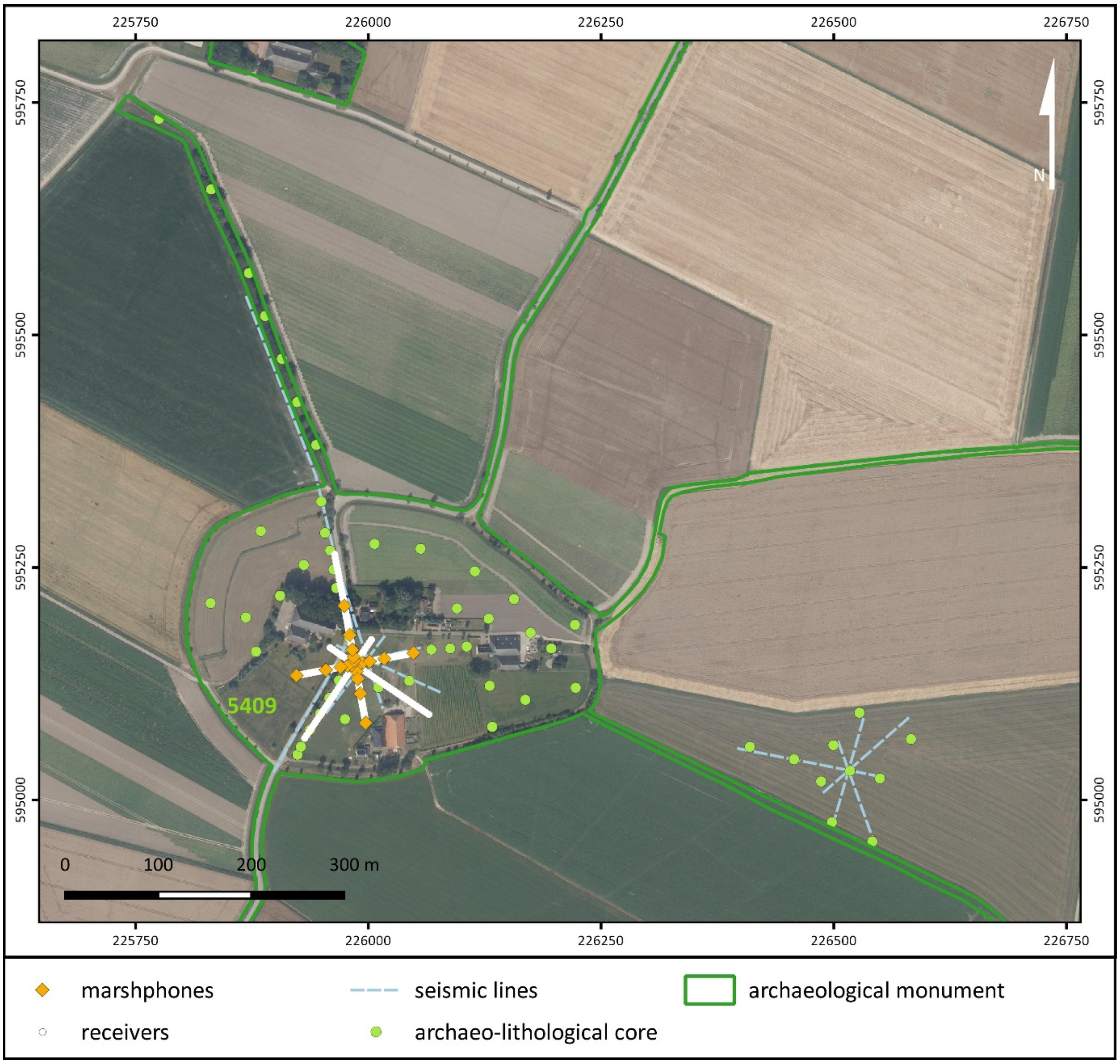


*Figure 3.2: Location Groot Maarslag. Overview of seismic lines, seismic receivers and archaeo-lithological cores).*

## 3.4 Experimental setup

In a pilot project, the terp Groot Maarslag was the first location to be investigated in the autumn of 2017. Here, the seismic receiver network consisted of four approximately 128 m long lines arranged in a star-shaped pattern (Figure 3.2). On the main, more or less north-south oriented line and a line perpendicular to the NS-line sensors were placed at 1 m intervals. On the two other lines, oriented northwest-southeast and northeast-southwest, the sensor interval was 4 m. The main line was extended a further 70 m north to the edge of the terp and from there c. 430 m to the northwest along the cycling path. Cores were taken only at the locations of the marshphones on the four main lines. In addition, 30 cores extended the main north-south line to the edges of the terp and filled in the areas not covered by the seismic receiver network. Cores were also taken at each of the receiver points of the off-wierde trial set-up to the southeast of the terp, and a further 7 cores at 50 m to 100 m intervals along the seismic line to the north of the terp.

After processing the Groot Maarslag data, several changes were made to the receiver array (Figure 3.3 ). Most importantly, the number of receiver points was reduced drastically, and instead of the star-shaped pattern, a single, c. 120 m long main line with seismic receivers every metre was deployed with additional receivers on a more or less radial pattern at greater intervals. The changes in the set-up of the seismic receiver network are reflected in the following changes to the archaeo-lithological coring strategy, which was used for the remaining seven locations:

- With receivers placed every metre on the main line, coring each receiver location would be extremely time consuming and lead to a large amount of data but not necessarily to more relevant information. Therefore it was decided to use a 4 m interval on the main line. All receiver locations outside the main line were cored.

- Where a core location happened to be positioned on deep cut features such as wells, a replacement core was taken nearby (max. 2 m) because it was assumed that such feature fills are not representative for the general terp lithology and could have a negative impact on the correlation between lithological and $v_s$-profiles.

- With an approximate length of 120 m, the main sensor line only covers the central part of the terps. For archaeological purposes as well as for a better understanding of the distribution of the various anthropogenic layers however, a section through the entire terp is more informative. At either end therefore, the main line was extended with several cores. Outside the main line, several more cores were taken for the same reason in the spaces between receiver points;

- Where possible, cores were taken just outside the terp to have some impression of the sequence of natural deposits.

- In order to gain some insight in the natural deposits, and in particular of the contact between Pleistocene and Holocene sediments underneath the terp, at each location a core was taken on the edge of the terp with a minimum depth of c. 5 m below surface level. Only at Amsweer and Biessum the top of the Pleistocene deposits (in each case coversands belonging to the Boxtel Fm, Wierden Mbr) was reached; in all other locations this proved impossible or impractical even at the lowest points of the terps.

Archaeo-lithological coring was carried out by the first author in cooperation with RAAP Archeologisch Adviesbureau b.v. (Weesp/Drachten, The Netherlands) using a 3 cm Ø gouge auger. Core descriptions are conform NEN5106 and relevant archaeological standards.

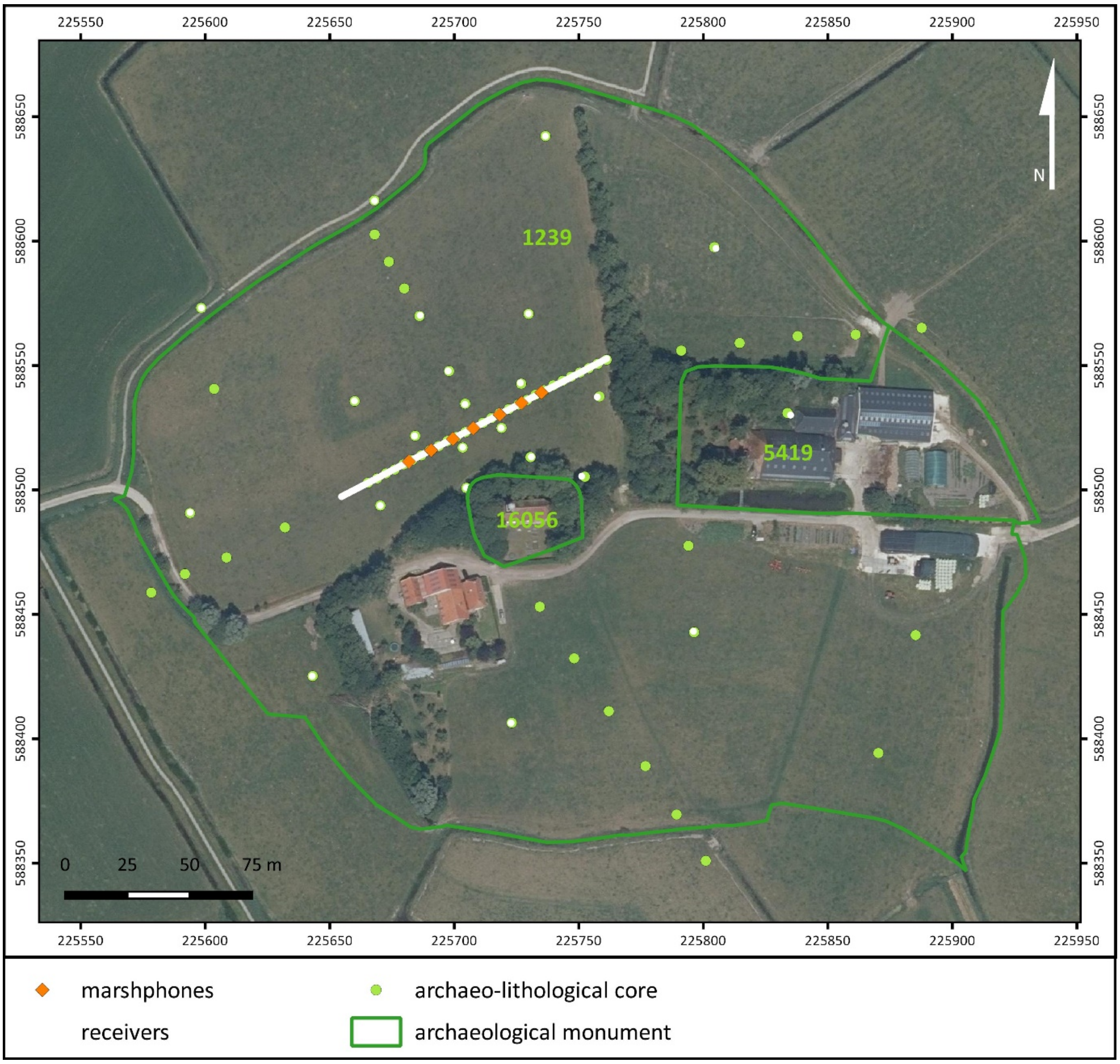


*Figure 3.3: Location Fransum: example of the seismic receiver setup and archaeo-lithological core locations.*

## 3.5 Lithoclass and shear wave assessment

As the GeoTOP model, which underlies the GMM, uses fewer lithoclasses than the NEN5104-based description system used for the archaeo-lithological descriptions, core descriptions had to be reclassified to allow direct comparisons (Table 3.1). Furthermore, the GeoTOP classification does not contain a class for manure for obvious reasons. This has been solved by using GeoTOP class 0, defined as anthropogenic, for manure.

The majority of anthropogenic sand layers consists of very fine or extremely fine sand, and therefore these layers are reclassified as GeoTOP class 5 (fine sand). The two anthropogenic sand layers consisting of medium fine sand are also placed in this category.

A second step in data processing prior to the statistical analyses is required by the significant difference in vertical detail between the archaeo-lithological data and the $v_s$-models. In general it can be stated that the smallest unit in the $v_s$-model as provided by Geovision has a vertical resolution of at least 0.5 m. In contrast, layers with a thickness of several centimetres are not unusual in archaeo-lithological core descriptions. In order to be able to make direct statistical comparisons, both datasets have been resampled using the method shown in Figure 3.4, which combines seismic units and archaeological layers into what has been termed 'functional horizons'. For each horizon, lithological parameters and $v_s$ (Rayleigh) were added. As the figure also shows, is that resampling likely results in a large amount of very thin horizons. To avoid overrepresentation of $v_s$ resulting from these thin horizons, the statistical analyses only used horizons (samples) with a thickness over 20 cm. Of the total of 1800 individually identified functional horizons, 1232 horizons (68%) were over 20 cm and used in the analysis. In terms of total thickness, 690 m of cores were used out of the in total 740 m of coring (93%).

*Table 3.1: Reclassification of NEN5104-lithoclasses into GeoTOP-lithoclasses.*

| GeoTOP lithoclass | description | NEN5104 lithoclass | description |
|---|---|---|---|
| 0 | manure | n.a. | all manure layers irrespective of (clastic) admixture components |
| 1 | peat/organic material | Vkm | peat |
| | | Vk1 | slightly clayey peat |
| | | Vk3 | strongly clayey peat |
| | | Vz1 | slightly sandy peat |
| | | Vz3 | strongly sandy peat |
| 2 | clay | Ks1 | slightly silty clay |
| | | Ks2 | moderately silty clay |
| 3 | sandy clay | Ks3 | strongly silty clay |
| | | Ks4 | extremely silty clay |
| | | Kz1 | slightly sandy clay |
| | | Kz2 | moderately sandy clay |
| | | Kz3 | strongly sandy clay |
| | | Zkx | clayey sand |
| 5 | fine sand | Zs1 | slightly silty sand |
| | | Zs2 | moderately silty sand |
| | | Zs3 | strongly silty sand |
| | | Zs4 | extremely silty sand |

All functional horizons over 20 cm were consequently used as single samples for statistical analyses. ANOVA was used to assess significant differences in mean $v_s$ values per lithoclass per terp and between terps. Ordinary multiple linear regression was used to assess strength and significant correlations between shear wave velocity as dependent variable and sample depth, lithoclass and terp as independent variable. The statistical analyses were carried out in SPSS 25.

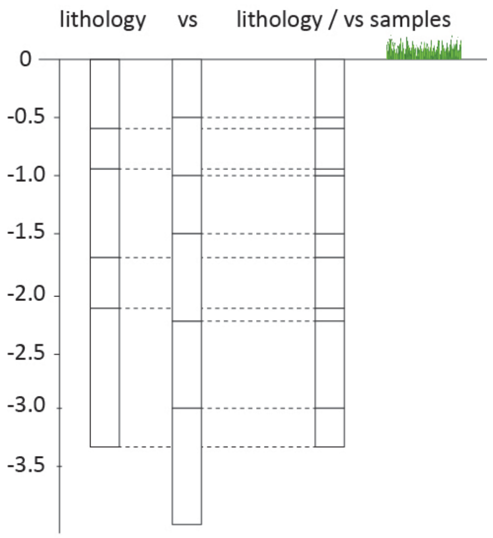


*Figure 3.4: Lithology and $v_s$ sampling strategy*

# 4 Results

## 4.1 Terp selection

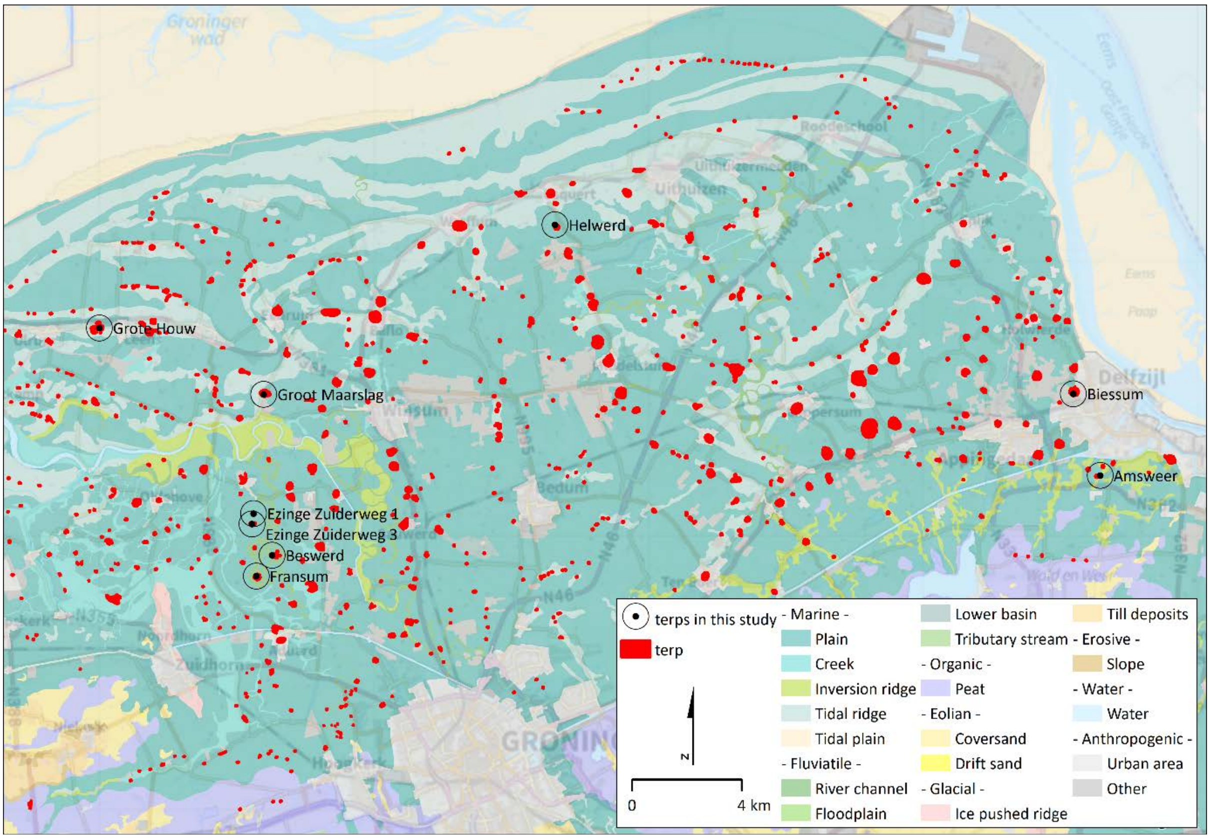


*Figure 4.1: Location of the investigated terps, superimposed on the geomorphological map (Koomen & Maas, 2004). Red dots represent major terps in the area.*

Application of the criteria formulated in paragraph 3.2 resulted in a selection of nine archaeologically intact, medium to large terps with a minimum number of buildings, in the western and north-eastern coastal plain (Figure 4.1; Table 4.1), covering a wide range of different occupation periods (Figure 4.2). A full description of each location and the results of the archaeo-lithological results is published as a separate archaeological report (Aalbersberg & Veenstra, in prep.).

Locations Biessum, Fransum, Ezinge-Zuiderweg 1 and Ezinge-Zuiderweg 3 are located at relatively short distances of each other in the southwestern part of the coastal plain. This cluster, consisting of locations with different sizes, Biessum being the largest and Ezinge-Zuiderweg 1 the smallest, was selected to address possible differences and similarities in stratigraphy and available source material. At location Ezinge-Zuiderweg 1 only seismic measurements were carried out. There are no archaeo-lithological cores available for this location, and this terp has been omitted from the analysis.

Groot Maarslag is located more or less halfway between the cluster described above and the younger saltmarsh barrier on which Grote Houw is situated. Location Grote Houw was selected because it is representative of the sandy west-east saltmarsh barrier on which several larger villages are situated. Prior research on the location and the surrounding region suggests it is considerably younger than terps located further to the south, and the location therefore might show a different sequence of anthropogenic layers. Finally, in terms of available lithological and archaeological information this terp is probably the best known of all selected locations, having been the focus of multidisciplinary research into (amongst others) soil erosion (Huisman *et al.*, 2017).

Location Helwerd represents the northern part of Fivelingo, and in particular the terps and villages on the extensive saltmarsh barrier complex defining the landscape. Locations Amsweer and Biessum were selected to represent the eastern part of Fivelingo. An additional criterion for Amsweer is its proximity to the industrial estates of Delfzijl. Investigating a location close to this area may also provide information on the risk of earthquake-related damage to the factories nearby.

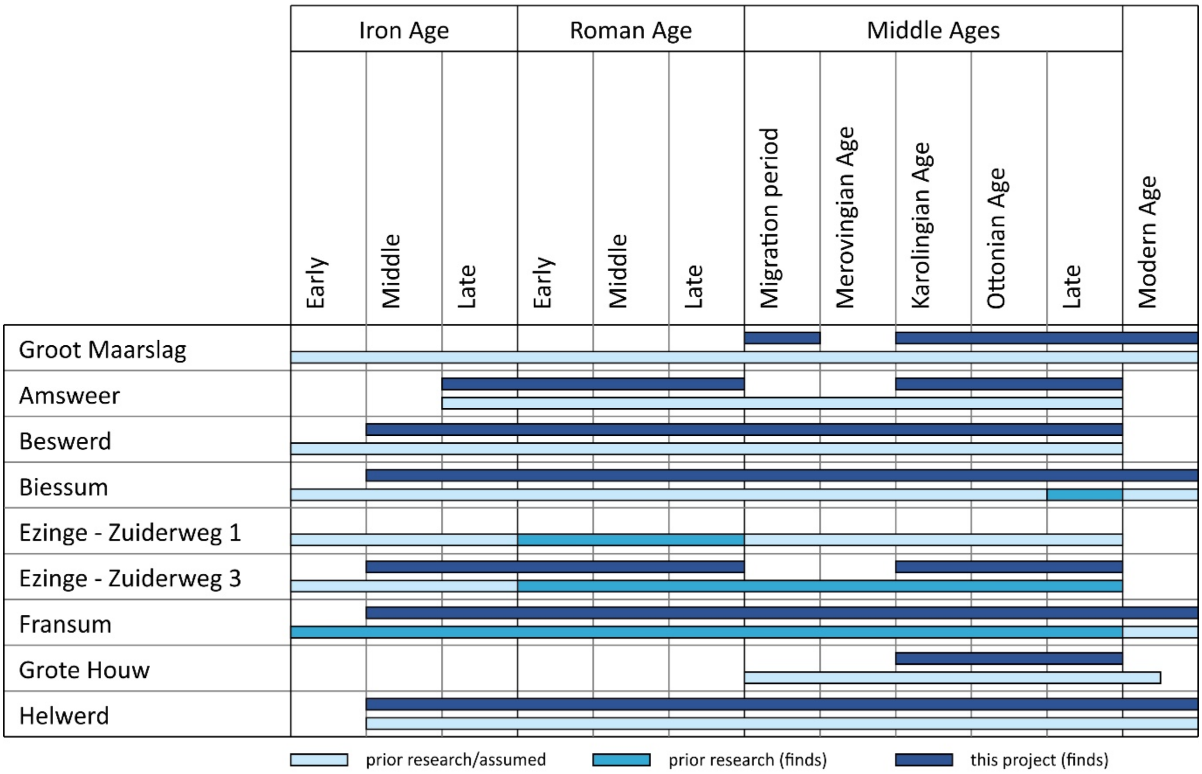


*Figure 4.2: Dating of the research locations, based on prior and current research. After Aalbersberg & Veenstra (in prep.).*

*Table 4.1: General characteristics of the selected terps.*

| location | coordinates (RD) | area (ha) | height[1] (m NAP) | height[1] (m) | Pleistocene (m) | buildings | remarks |
|---|---|---|---|---|---|---|---|
| Amsweer | 256349 / 592158 | c. 5.5 | 1.25 | 2.5 | 5 | none | Location chosen because of its' proximity to the Delfzijl industrial area. Not to be confused with the Amsweer (village) terp, c. 380 m northwest of this location |
| Beswerd | 226395 / 589289 | c. 6.9 | 2.7 | 2.4 | 14.5 | few | Two farmsteads on the eastern and southern flanks of the terp |
| Biessum | 255479 / 595227 | c. 8.5 | 2.20 | 3.2 | 6.5 | several | Several buildings around the perimeter, but almost none in the central part of the terp. The surrounding area is lowered by clay extraction; the relative height may be overestimated |
| Ezinge Zuiderweg 1 | 225609 / 590720 | c. 2.5 | 2.65 | 2.0 | 12 | none | Seismic survey only, no archaeo-lithological coring. The terp was left out of the archaeo-lithological analysis |
| Ezinge Zuiderweg 3 | 225552 / 590402 | c. 5.5 | 2.65 | 2.0 m | 12 | one | Farmstead on the eastern flank of the terp |
| Fransum | 225741 / 588499 | 8.6 | c. 3.20 | 2.6 m | 15 | few | Two farmsteads on flanks of the terp, and a (restored) 13th century church on centre of the terp. |
| Groot Maarslag | 226013 / 595180 | c. 10.6 | c. 3.75 | 2.9 m | 14 | few | Three farmsteads and several houses, both on the centre and the flanks of the terp |
| Grote Houw | 220057 / 597535 | c. 4.0 | c. 3.85 | 2.8 m | 27 | few | Part of a larger complex of terps. Three farmsteads on the northern part, none in the investigated part. This location was used for a study into (a.o.) erosion susceptibility (Huisman *et al.*, 2017) |
| Helwerd | 236638 / 601264 | c. 6.3 | 2.60 / 3.10 | 2.1 m | 14.5 | none | It is unclear whether this location consists of two terps separated by a north-south ditch, or that it is a single mound with a ditch resulting from quarrying |

## 4.2 Groot Maarslag (pilot)

### *4.2.1 General terp description*

Location Groot Maarslag is a more or less oval terp, measuring c. 440 m in an east-west direction and c. 300 in a north-south direction. Its highest point, at c. 3.75 m +NAP (Dutch Ordnance Datum), lies somewhat eccentric near the crossroads between the main road and the smaller road leading to the houses built on the terp and the farm on the eastern flank. Two more farmsteads are present, one on the southern flank and one just to the east of the crossroads. Around Groot Maarslag, the typical radial ditch pattern outside the terp thought to have been present around all larger terps still can be traced. Furthermore, the road/path encircling the foot of the terp and two small arable fields ('valge') to the northwest and southwest of the terp are still present.

The terp is located on a saltmarsh barrier or natural levee on the eastern side of the former, northernly course of the Hunze-system. As a result, the location was situated in a tidal landscape for most of the Holocene. Only after the development of the Lauwerszee and the subsequent change of the Hunze-system to its present, westerly course around 800 AD did the marine influence decrease. Archaeologically, little is known about Groot Maarslag. During the digging of trenches for fiberglass cables, stacks of plaggen were seen in at least two places on the terp (T. Sibma, Antea Group, pers. comm.).

### *4.2.2 Archaeo-lithological characterisation*

According to the data available from DINOloket (Data en Informatie van de Nederlandse Ondergrond), the depth of the contact between Pleistocene and Holocene sediments varies between c. 10 m -NAP and c. 20 m -NAP. This variation reflects the position of Groot Maarslag between the Pleistocene subcrop near Winsum and Ranum to the northeast and the area where the Hunze-system has eroded deeper into the subsoil, particularly to the south and west. As most of the DINOloket cores in the immediate vicinity of Groot Maarslag are only 5 m deep, it is hard to get a clear picture of the lower part of the Holocene sequence. However, it seems safe to assume that the majority of the Holocene sediments consists of clastic tidal sediments, locally, where erosion has been relatively slight, underlain by a thin layer of basal peat.

The top of the Holocene sequence is well documented, both in the data from DINOloket as in the coring carried out outside the terp during this project. To the northeast of the terp, the tidal deposits consist of laminated, strongly to extremely silty, very fine sand with intercalated clayey layers. These sediments are characteristic of channel, subtidal and intertidal environments, and are interpreted as the filling of the northern Hunze-system estuary. The base of these deposits has not been reached; the lowest point at which they occur is c. 7.40 m -NAP. The upper metre is formed by saltmarsh deposits reflecting the abandonment of this estuary. To the southeast, cores show a similar general sequence, although the lithological variation is greater.

The Groot Maarslag terp itself consists of anthropogenic layers with a combined thickness of up to 3.25 m. The majority of the layers consists of extremely silty clay and very fine sand (Figure 4.3). Patterns in the distribution of the various lithologies seem absent, with the exception of the north-western quadrant where the anthropogenic sequence consists of a basal manure layer, a layer of very fine sand and an upper layer of extremely silty clay. Whether this pattern is real or apparent remains uncertain. The coring at the other locations with a smaller coring interval (4 m) has shown that even at such short distances correlation between cores to be difficult.

Underneath the centre of the terp, a substantial manure layer with a thickness between 0.25 m and c. 2.00 m forms the base of the anthropogenic layers. With an extent of approximately 150 m x 130 m, it far exceeds the dimensions of manure layers at other locations which usually measure between

25 m and 45 m. Biessum (Paragraph 4.5), with a recorded with of 80 m, comes closest. An explanation for this extent cannot be given based on the cores only. However, it is possible that, as the Biessum section also demonstrates, the pattern consists of two or more separate manure layers. Because of the wider coring interval (10-20 m) used at Groot Maarslag, the edges of separate manure layers easily could have been missed. Nevertheless, it is safe to conclude that manure forms a substantial portion of the Groot Maarslag terp.

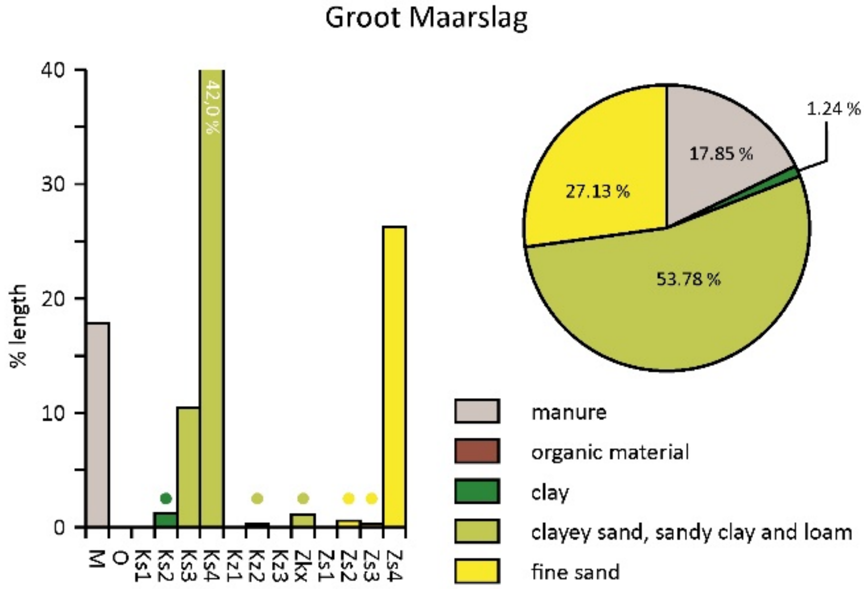


*Figure 4.3: Terp lithoclass proportions of Groot Maarslag. Left: frequency distribution NEN5104 lithoclasses and manure. Dots denote values < 2%; right: percentages of GeoTOP lithoclasses.*

Although the cores yielded a wide variety of archaeological material, including charcoal, burnt clay and bone, dateable pottery is surprisingly scarce. All fragments date from the period between the Migration period and the Late Middle Ages/present day, and the 15 sherds picked up from the surface also fall in this period. The typical and easily recognisable pottery from the Iron Age/Roman Age is absent, placing the first phase of occupation with some certainty in the Migration period or Early Medieval period.

### *4.2.3 Shear wave velocity variability*

The terp Groot Maarslag mainly consisted of clayey sand, sandy clay and loam (GeoTOP lithoclass 3), fine sand (lithoclass 5) and manure (lithoclass 0; *Figure* 4.3). Medium fine sand was not found in the transect, and clay (lithoclass 2) was only found in one sample. The proportion of the clay and fine sand was slightly higher beneath the terp (Table 4.2). Average shear wave velocity values were significantly higher in the terp than below, with an average of 94 m/s in the terp and 78 m/s underneath. The variation within the terps seems to be substantially higher in the terp than below, with a standard deviation of 18 m/s.

$V_s$ values appear to be significantly different between lithoclasses within the terp ($p < 0.003$). However, this effect is attributed to only a single clay sample with a relatively high $v_s$ value. When removed, the ANOVA analysis returns a non-significant difference between lithoclasses in the terp. It can therefore be concluded, that there is not enough evidence to suggest that the variation in $v_s$ value can be attributed to lithoclass variation.

Although the average $v_s$ values between lithoclasses underneath the terp vary from 88 to 103 m/s, the ANOVA shows that these differences are not statistically significant, probably due to the high internal variation as reflected in high standard deviations. This is also shown for $v_s$ values next to the terp (Table 4.3), where relatively high standard deviations prevent statistically significant difference between the lithoclasses clay; clayey sand, sandy clay and loam and fine sand. The average $v_s$ values in the terp, however, are not only significantly lower than the values below, but also in comparison to the samples taken next to the terp. On the contrary, it can be seen from Table 4.3 that there is no significant difference in $v_s$ values between off and beneath terp observations.

*Table 4.2: ANOVA results for $v_s$ values per lithoclass for Groot Maarslag*

| Groot Maarslag | | | | **$v_s$ (m/s)** | | **ANOVA** | |
|---|---|---|---|---|---|---|---|
| | **lithoclass** | **code** | **n** | **mean** | **std.** | **F** | **p** |
| **all samples** | natural | 0 | 23 | 94.3 | 18.0 | 35.771 | 0.000** |
| | anthropogenic | 1 | 79 | 77.7 | 9.1 | | |
| | total | | 102 | 81.5 | 13.5 | | |
| **all samples** | manure | 0 | 21 | 74.5 | 6.9 | 8.359 | 0.000** |
| | organic material (peat) | 1 | 0 | | | | |
| | clay | 2 | 8 | 100.0 | 21.1 | | |
| | clayey sand, sandy clay and loam | 3 | 48 | 81.5 | 11.1 | | |
| | fine sand | 5 | 25 | 81.4 | 14.2 | | |
| | medium fine sand | 6 | 0 | | | | |
| | total | | 102 | 81.5 | 13.5 | | |
| **within terp** | manure | 0 | 21 | 74.5 | 6.9 | 5.151 | 0.003** |
| **(anthropogenic)** | organic material (peat) | 1 | 0 | | | 1.993[1] | 0.143 |
| | clay | 2 | 1 | 106.2 | | | |
| | clayey sand, sandy clay and loam | 3 | 36 | 79.1 | 7.4 | | |
| | fine sand | 5 | 21 | 77.3 | 11.2 | | |
| | medium fine sand | 6 | 0 | | | | |
| | total | | 79 | 77.7 | 9.1 | | |
| | [1]*when removing lithoclass clay* | | | | | | |
| **under terp** | manure | 0 | 0 | | | 1.436 | 0.261 |
| **(natural)** | organic material (peat) | 1 | 0 | | | | |
| | clay | 2 | 7 | 99.1 | 22.6 | | |
| | clayey sand, sandy clay and loam | 3 | 12 | 88.4 | 16.7 | | |
| | fine sand | 5 | 4 | 103.3 | 5.5 | | |
| | medium fine sand | 6 | 0 | | | | |
| | total | | 23 | 94.3 | 18.0 | | |

Regardless of lithoclass, the general tendency is that $v_s$ values increase with depth (Figure 4.4). A linear regression analysis shows that this is significant ($p < 0.000$) but not very strong ($R^2 = 0.18$). This is almost entirely due to the strength of the regression of the off-terp samples ($p < 0.000$; $R^2 = 0.77$), since the regressions within and below the terp separately produce non-significant regression results ($R^2 < 0.05$). The increase in $v_s$ with depth appears to be better interpreted as a step-wise increase at around the depth of the terp basis (Figure 4.4).

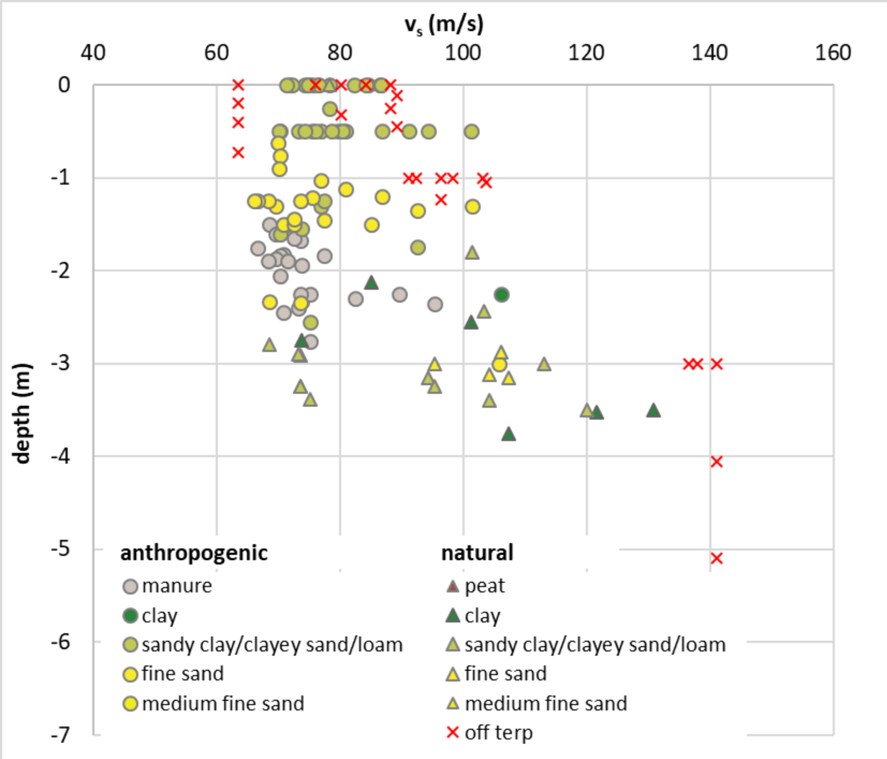


*Figure 4.4: $v_s$ values per lithoclass plotted against depth below soil surface for Groot Maarslag*

*Table 4.3: Off and in-terp ANOVA results for $v_s$ values per lithoclass for Groot Maarslag*

| Groot Maarslag | | | | $v_s$ (m/s) | | ANOVA | |
|---|---|---|---|---|---|---|---|
| | **lithoclass** | **code** | **n** | **mean** | **std.** | **F** | **p** |
| **all off-terp samples** | clay | 2 | 2 | 102.3 | 54.7 | 0.666 | 0.525 |
| | clayey sand, sandy clay and loam | 3 | 2 | 75.9 | 17.4 | | |
| | fine sand | 5 | 19 | 97.7 | 24.5 | | |
| | total | | 23 | 96.2 | 26.2 | | |
| **all samples** | off terp | -1 | 23 | 96.2 | 26.2 | 19.024 | 0.000 |
| | below terp | 0 | 23 | 94.3 | 18.0 | | |
| | terp | 1 | 79 | 77.7 | 9.1 | | |
| | total | | 125 | 84.2 | 17.4 | | |
| **fine sand** | off terp | -1 | 19 | 97.7 | 24.5 | 11.884 | 0.001 |
| | below terp | 0 | 4 | 103.3 | 5.5 | | |
| | terp | 1 | 21 | 77.3 | 11.2 | | |
| | total | | 44 | 88.5 | 20.8 | | |

Visual inspection of the 2D $v_s$ profiles in combination with the archaeo-lithoclass cores (Figure 4.5 and Figure 4.6) show, that for both profiles, there is little variation parallel to the soil surface at 4 m depth, where $v_s$ values average at 120 to 140 m/s. Deeper in the profiles, $v_s$ values linearly increase with depth more or less homogeneously, although the increase is more distinct underneath the terp than next to the terp (Figure 4.6). For example, at 10 m below the surface of the terp, $v_s$ values are typically around 180 m/s, whereas at the same depth below the soil surface next to the terp they are around 130 to 140 m/s.

The low values in the terp are remarkable. At around the terp basis, there is a sharp decline in $v_s$ values upwards. Just below the terp base (indicated by the red line in Figure 4.5), $v_s$ values are around 100 m/s, whereas just above the base typical $v_s$ values are 85 m/s or lower. This is only visible in the eastern section of the terp, however, and may be strongly related to the presence of relatively thick manure layers (soil cores 4 through 8 and 10). As in some terps, $v_s$ values increase again with decreasing depth, here, this is not the case. The horizontal variation in the terp is limited, which is different from most other terps. In the off terp profile (Figure 4.6), there is also hardly any variation in horizontal direction, but $v_s$ values near the soil surface are substantially higher than in the terp.

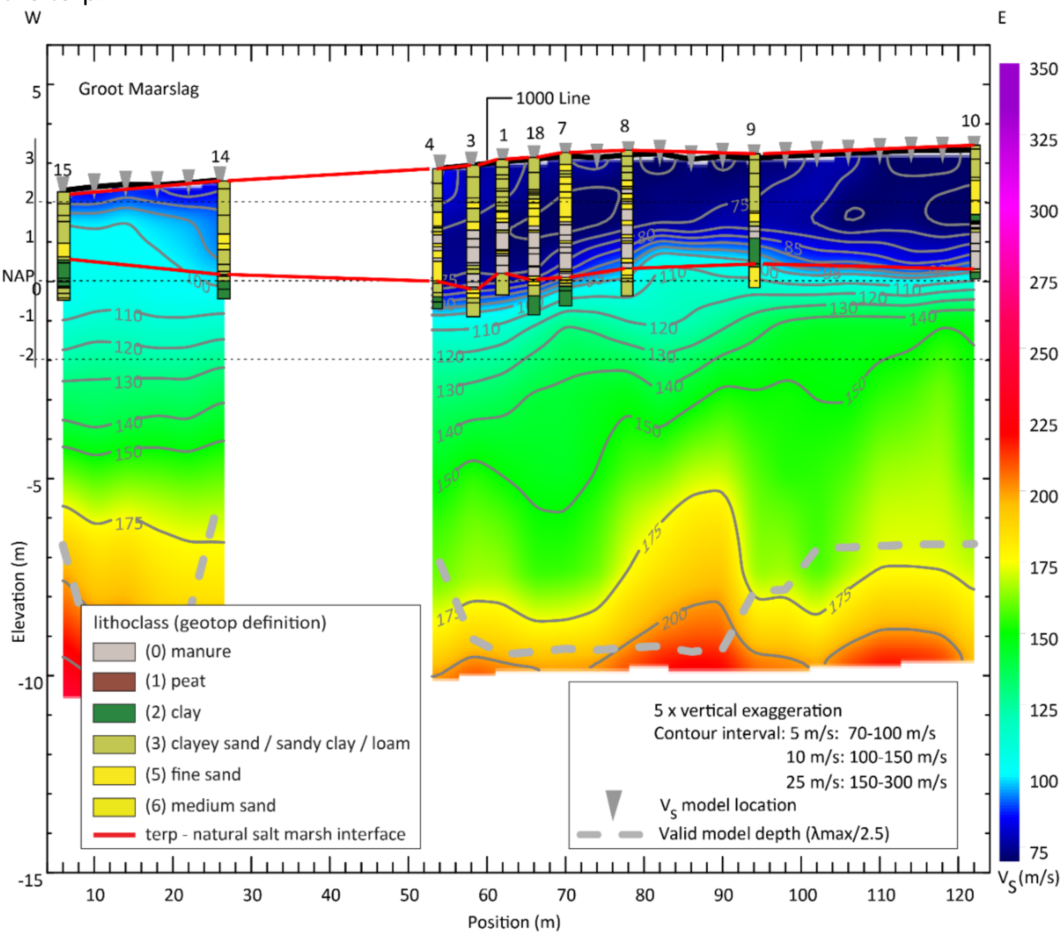


*Figure 4.5: Rayleigh wave 2D profile with archaeo-lithological corings for Groot Maarslag (on terp; adapted after Geovision, 2019b)*

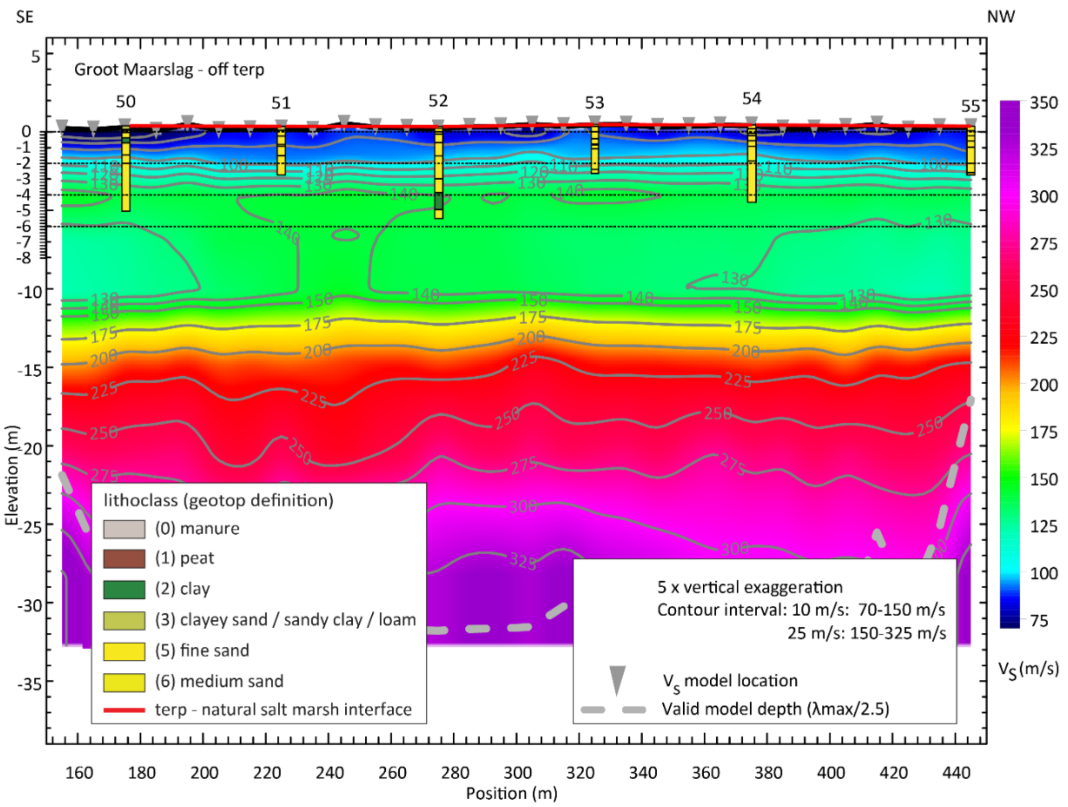


*Figure 4.6: Rayleigh wave 2D profile with archaeo-lithological corings for Groot Maarslag (off terp; adapted after Geovision, 2019c)*

## 4.3 Amsweer

### *4.3.1 General terp description*

The Amsweer location is a more or less rectangular terp, measuring approximately 140 m x 98 m. It is unclear whether these are the original shape and dimensions, or that this shape is a result of the older (pre-1965 but post-terp) pattern of ditches still recognisable on LIDAR images. According to local inhabitants, at some point in recent history an attempt to level the terp has been made. Although the damage within the terp cannot be undone, the terp profile and shape have been restored afterwards.

From a geomorphological point of view, the Amsweer terp lies on an (tidal) palaeo-channel ridge, part of a complex of higher topographical elements including saltmarsh ridges on the southern bank of the Ems estuary. This complex itself was created during the expansion of the intertidal area between c. 500 BC and c. 0 BC/AD (Roeleveld, 1974; Vos & De Vries, 2013), and the tidal channel must have been active around this time. The silting up of the channel and inversion of the relief to form the ridge must therefore be of a later date, perhaps somewhere during the Late Roman or Medieval periods. Archaeologically, little is known about the location. Although ARCHIS 3 mentions several inspections, with or without coring, datable finds have not been recorded.

### *4.3.2 Archaeo-lithological characterisation*

The base of the natural sequence around and between the Amsweer terp consists of fine and very fine sands, interpreted as aeolian deposits (“coversand”; Boxtel Fm, Wierden Mbr). The top of these Pleistocene deposits lies at approximately 4.6 m -NAP (c. 3.5 m below surface level outside the terp). An up to 2.0 m thick peat layer consisting of mesotrophic and oligotrophic peat types with thin, intercalated clay layers in the lower half and upper 20 cm (Nieuwkoop Fm, Basisveen Bed) forms the base of the Holocene sequence. The clay layers and mesotrophic peat types in the upper 20 cm reflect the change from oligotrophic conditions to an environment with increasing marine influences. A slightly over 1.0 m thick clay layer and a tidal channel underlying the terp record the transformation of a freshwater landscape into an intertidal area. The increasing silt content points to a gradually more dynamic salt marsh environment whereas subaerially weathered ('ripened') clay layers indicate periods during which sedimentation rates slowed enough to allow this kind of initial soil formation. The top of the clay layer consists of strongly to very strongly silty clay, both below and outside the terp.

The terp itself consists mainly of clay with varying silt content and a maximum thickness of c. 2.45 m. Sandy layers are rare (Figure 4.7). Generally, the base of the anthropogenic layers is less silty than the top, and this difference is most clear on the northern flank. In the central part and elsewhere silty and less silty layers alternate without apparent pattern. Only 8 cores yielded manure layers, with a maximum thickness of 0.35 m. Therefore, there is no presence of a continuous, thick manure layer, such as in some other locations.

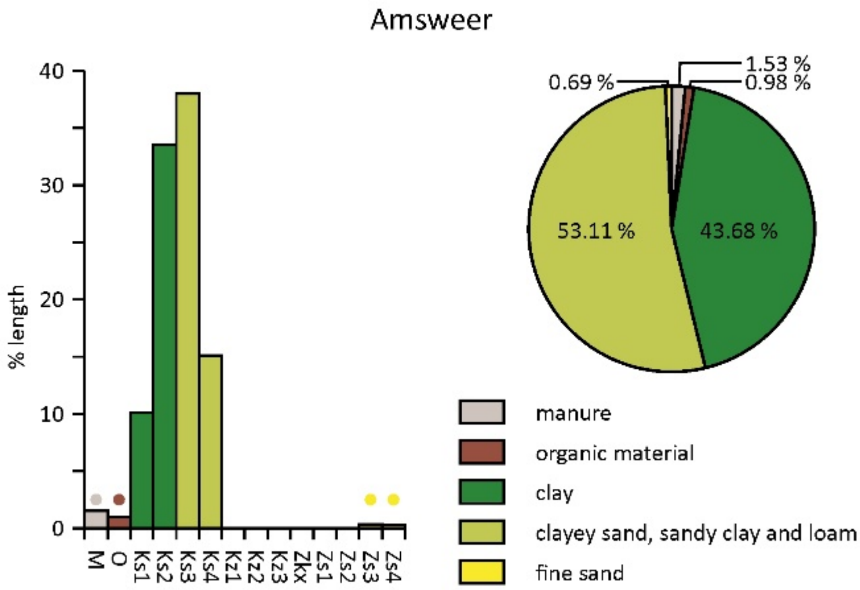


*Figure 4.7: Terp lithoclass proportions of Amsweer. Left: frequency distribution NEN5104 lithoclasses and manure. Dots denote values < 2%; right: percentages of GeoTOP lithoclasses.*

The cores have yielded a small number of datable pottery fragments. Surprisingly, almost half of them date from the Late Iron Age to Roman Age, a period during which the tidal channel is supposed to be active. Whether these finds reflect an occupation phase prior to terp construction, perhaps on the natural levees flanking the channel, or have been introduced with soil from elsewhere used for heightening (several sherds were found within 1 m below surface level) is not clear. The other finds date from the Karolingian period to Late Middle Age.

### *4.3.3 Shear wave velocity variability*

The terp Amsweer shows a statistically significant difference in $v_s$ values between the natural subsurface deposits (77 m/s on average) and the anthropogenic terp above (68 m/s), although the absolute difference seems limited. The variation within the terp is relatively low, with a low standard deviation in comparison with the subsurface (Table 4.4). The general tendency of $v_s$ with depth is a very subtle increase with depth from just above 60 m/s at the terp surface to around 70 m/s at 2 m below the surface. At greater depths, into the natural subsurface, the rate continues to increase to over 100 m/s at 5 m in depth (Figure 4.8). In the terp, the correlation is very weak but significant ($R^2$

= 0.14, p < 0.000). In the natural deposits below the terp, the correlation is somewhat stronger ($R^2$ = 0.24; p < 0.000), indicating that 24% of the variation in $v_s$ is explained by depth only.

Manure and peat layers show relatively low $v_s$ values, whereas in clastic sediments, values are generally higher. However, the differences between the lithoclasses are not statistically different. It has to be noted, however, that of the 158 sample only 10% were composed of organic material (peat and manure together), which means that there are relatively little data to assess possible $v_s$ differences within the terp.

*Table 4.4: ANOVA results for $v_s$ values per lithoclass for Amsweer*

| Amsweer | | | | $v_s$ (m/s) | | ANOVA | |
|---|---|---|---|---|---|---|---|
| | **lithoclass** | **code** | **n** | **mean** | **std.** | **F** | **p** |
| **all samples** | natural | 0 | 74 | 76.8 | 18.1 | 17.512 | 0.000** |
| | anthropogenic | 1 | 85 | 68.2 | 4.3 | | |
| | total | | 159 | 72.2 | 13.4 | | |
| **all samples** | manure | 0 | 3 | 68.9 | 3.8 | 1.355 | 0.244 |
| | organic material (peat) | 1 | 13 | 69.4 | 18.9 | | |
| | clay | 2 | 93 | 74.2 | 14.8 | | |
| | clayey sand, sandy clay and loam | 3 | 44 | 68.6 | 5.4 | | |
| | fine sand | 5 | 2 | 80.0 | 16.5 | | |
| | medium fine sand | 6 | 3 | 72.5 | 24.6 | | |
| | total | | 158 | 72.2 | 13.5 | | |
| **within terp (anthropogenic)** | manure | 0 | 3 | 68.9 | 3.8 | 0.187 | 0.905 |
| | organic material (peat) | 1 | 0 | | | | |
| | clay | 2 | 40 | 68.5 | 4.9 | | |
| | clayey sand, sandy clay and loam | 3 | 41 | 67.8 | 3.8 | | |
| | fine sand | 5 | 1 | 68.3 | | | |
| | medium fine sand | 6 | 0 | | | | |
| | total | | 85 | 68.2 | 4.3 | | |
| **under terp (natural)** | manure | 0 | 0 | | | 1.091 | 0.368 |
| | organic material (peat) | 1 | 13 | 69.4 | 18.9 | | |
| | clay | 2 | 53 | 78.5 | 18.1 | | |
| | clayey sand, sandy clay and loam | 3 | 4 | 77.3 | 10.2 | | |
| | fine sand | 5 | 1 | 91.6 | | | |
| | medium fine sand | 6 | 3 | 72.5 | 24.6 | | |
| | total | | 74 | 76.8 | 18.1 | | |

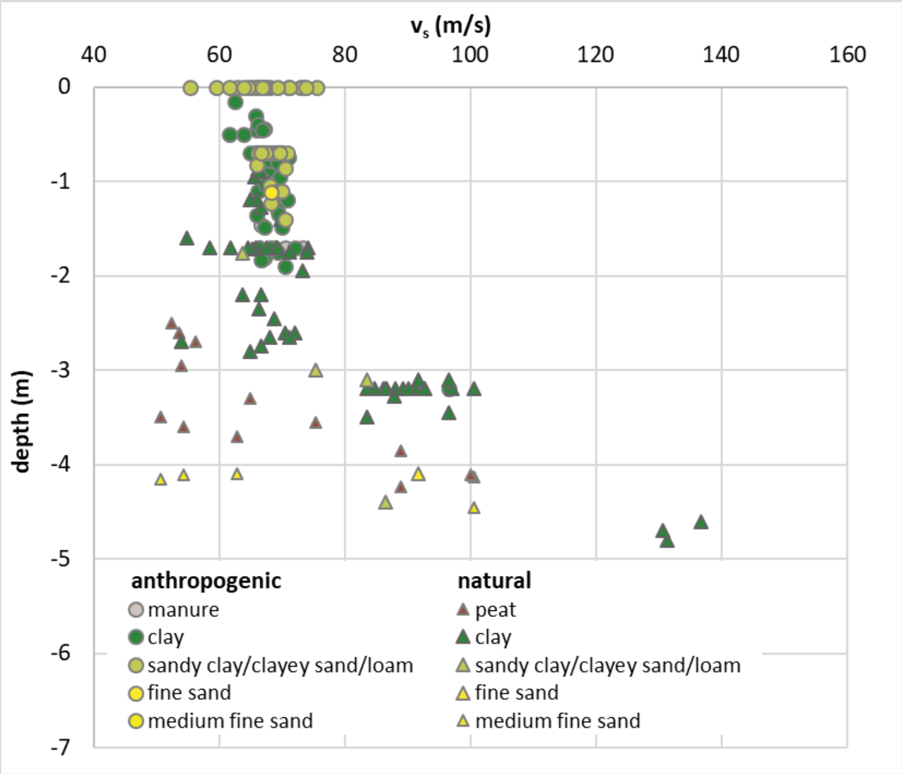


*Figure 4.8: $v_s$ values per lithoclass plotted against depth below soil surface for Amsweer*

Visual inspection of the terp profile (Figure 4.9) learns that shear wave velocity values appear homogeneous just a couple of meters below the terp basis, at 4 to 6 m below the soil surface. The homogeneity is parallel to the surface, but not parallel to the horizontal plane. Typical $v_s$ values at this depth fluctuate around 110 m/s, although towards the northern section of the terp a sharp decrease in $v_s$ values with depth make it slightly more difficult to interpret properly from the figure. In the zone directly underneath the terp (indicated in the figure by a red line), the horizontal variability remains low in the southern section of the terp, but there is a relatively sharp decrease in $v_s$ values with decreasing depth. Within the terp, in horizontal direction typical $v_s$ values are just below 70 m/s. This is also generally valid below the terp, except for the natural peat layers in soil profiles 638 to 643. Shear wave values appear to be substantially lower to around 50-55 m/s. Although the ANOVA analysis shows that peat samples do not appear to be significantly lower, it can be seen from the figure that there seems to be some offset: the low $v_s$ values appear at and just above the depth of the peat layers, and therefore the propagation of the Rayleigh waves seem to affect the upper layers also.

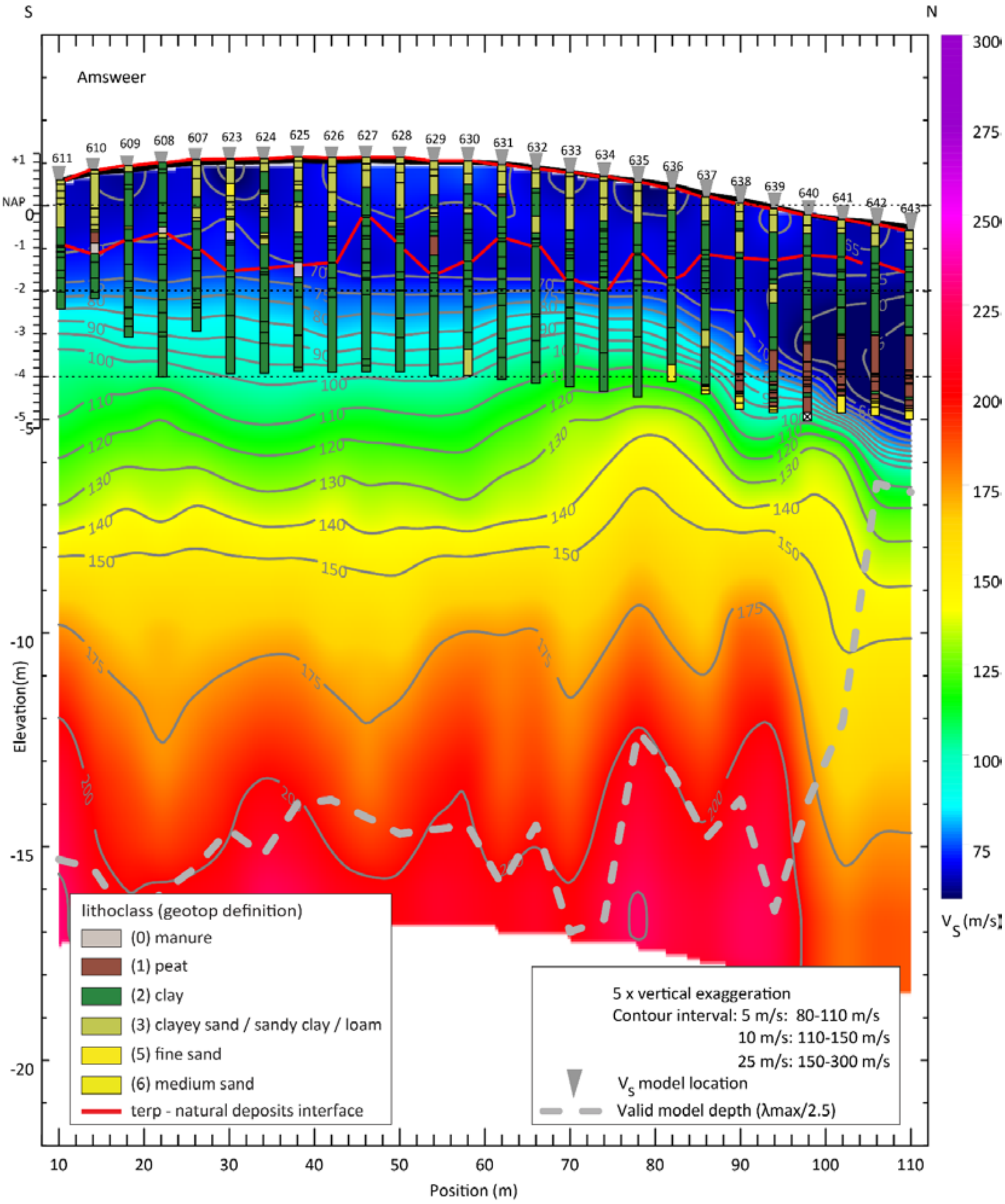


*Figure 4.9: Rayleigh wave 2D profile with archaeo-lithological corings for Amsweer (adapted after Geovision, 2019a)*

## 4.4 Beswerd

### *4.4.1 General terp description*

Beswerd is a more or less round terp with a c. 225 m diameter according to LIDAR images; using the ditch visible on topographic maps as the terp boundary however results in diameter of c. 330 m. The presence of farmsteads on the southern and eastern flanks suggests some damage to the terp body, but otherwise it appears to be intact.

This location is situated in an area with a complicated landscape history. According to the palaeo-geographical maps by Vos & De Vries (2013), the location lies in a tidal landscape, the seaward extension of the Hunze-system, for a substantial part of the Holocene. Only relatively late, at some stage between 1500 BC and 500 BC, marine activity decreases somewhat and salt marshes develop.

At the same time, the drainage system shifts to a more northern course as opposed to the north-eastern followed until then. The tidal meanders belonging to this northern drainage system are still visible both on LIDAR images and in the present-day topography. With the formation of the Lauwerszee embayment around 800 AD and re-routing of the Hunze-system via the Reitdiep to this embayment, the landscape around the Beswerd location changed into a far more active tidal environment until embankment during the Middle Ages.

Based on finds from several projects, ARCHIS 3 dates the location to the Iron Age to Middle Ages. Archaeological observations during the building of a new barn next to the farmstead on the southern flank of the terp indicate the farmstead is located on a Late Medieval expansion of the terp.

### *4.4.2 Archaeo-lithological characterisation*

Based on core information from the wider area around the location, the depth of the boundary between Pleistocene and Holocene deposits lies between 7.5 m -NAP and 11.0 m -NAP. Locally, a thin basal peat layer occurs, but much of this peat layer will have been removed by later erosion associated with the formation of the Hunze-estuary. The major part of the Holocene sequence consists of marine to inter- and supratidal clays. The top of this substantial clastic layer, as far as investigated during this project, consists of intertidal deposits (laminated very fine to extremely fine sand) followed by a c. 1 m thick layer of salt marsh deposits (silty clay with sand laminae, very fine sand with clay laminae and intergrades between those two).
The majority of the anthropogenic layers within the terp body consists of moderately to strongly silty clay (Figure 4.10). Some sandy layers occur as well, but seem to be confined to the centre of the terp. Although the differences in terms of lithological composition are small, the upper part of the anthropogenic layers appears to be slightly siltier than the base. This difference is most marked in the central area of the terp; on the flanks it is less clear or absent.
Underneath the central area, a c. 35 m wide and 0.6 m thick manure layer forms the base of the anthropogenic layers. In several cores, the manure layer is thicker and probably represents two or more phases. Finds from the cores date from the Middle Iron Age to the Late Middle Age, confirming the long period of occupation of the location suggested by earlier research.

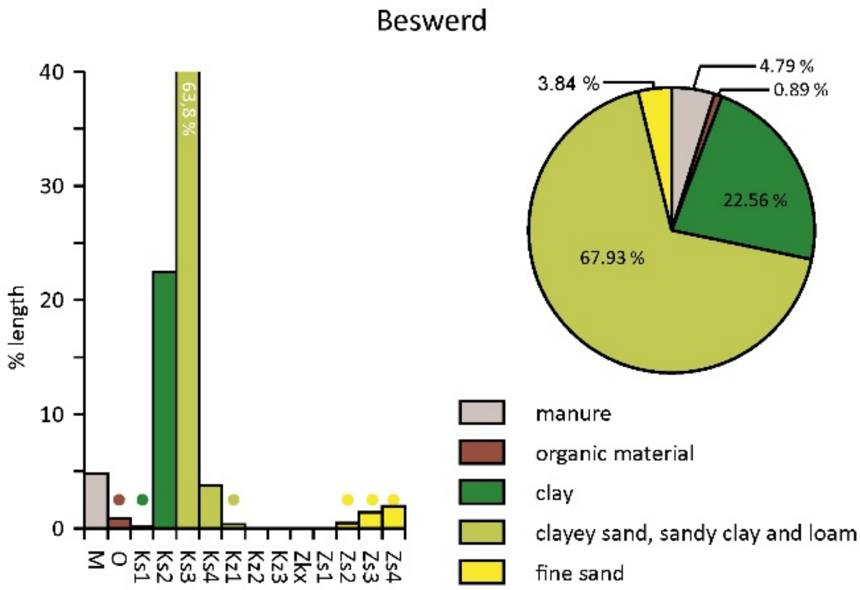


*Figure 4.10: Terp lithoclass proportions of Beswerd. Left: frequency distribution NEN5104 lithoclasses and manure. Dots denote values < 2%; right: percentages of GeoTOP lithoclasses.*

### 4.4.3 Shear wave velocity variability

The difference in typical $v_s$ values in the Beswerd terp is substantial and highly significantly different (Table 4.5). Typical values for the anthropogenic terp deposits are around 86 m/s, but do show a relatively high variation with a standard deviation of around 20 m/s. The natural subsurface shows a $v_s$ average of 123 m/s. Within the anthropogenic terp deposits, the difference between lithoclasses is significant, in which clayey sand, sandy clay and loam and fine sand appear to be lowest ($v_s = 80$ m/s). Clay and manure samples are somewhat higher with $v_s$ values of 98 and 104 m/s, resp. Below the terp, the only occurring lithoclass (fine sand) is again higher ($v_s = 121$ m/s). The terp shows a significant and statistically strong increase in $v_s$ with depth, in which 54% of the variation in $v_s$ is explained by depth alone (Figure 4.11; $R^2 = 0.54$; $p < 0.000$). There is no difference in rate within and below the terp.

From the visual interpretation of the terp profile (Figure 4.12), it is clearly visible that the horizontal variation within the terp is substantial. Typical shallow $v_s$ values are 60-70 m/s between soil profiles 315-327 and 303-307. But values are higher between soil profiles 308-314, with typical $v_s$ values of 80 to 90 m/s. This is not directly explained by the lithoclasses at shallow depth, which shows a rather homogeneous composition of clayey sands. However, at greater depth, the composition of the terp below the zones with zones of lower $v_s$ values consists of clay or manure deposits, whereas the zone with higher $v_s$ values does only show sandy lithoclasses. At this depth at around 4 m below the terp surface, there is no horizontal variation in $v_s$ values, which seems to be constant at around 120 m/s.

*Table 4.5: ANOVA results for $v_s$ values per lithoclass for Beswerd*

| Beswerd | | | | $v_s$ (m/s) | | ANOVA | |
|---|---|---|---|---|---|---|---|
| | **lithoclass** | **code** | **n** | **mean** | **std.** | **F** | **p** |
| **all samples** | natural | 0 | 31 | 123.3 | 13.0 | 99.503 | 0.000** |
| | anthropogenic | 1 | 123 | 85.7 | 19.9 | | |
| | total | | 154 | 93.3 | 24.0 | | |
| **all samples** | manure | 0 | 11 | 103.9 | 21.9 | 41.989 | 0.000** |
| | organic material (peat) | 1 | 0 | | | | |
| | clay | 2 | 30 | 97.5 | 17.1 | | |
| | clayey sand, sandy clay and loam | 3 | 78 | 78.8 | 16.4 | | |
| | fine sand | 5 | 35 | 118.5 | 20.3 | | |
| | medium fine sand | 6 | 0 | | | | |
| | total | | 154 | 93.3 | 24.0 | | |
| **within terp (anthropogenic)** | manure | 0 | 11 | 103.9 | 21.9 | 12.489 | 0.000** |
| | organic material (peat) | 1 | 0 | | | | |
| | clay | 2 | 30 | 97.5 | 17.1 | | |
| | clayey sand, sandy clay and loam | 3 | 78 | 78.8 | 16.4 | | |
| | fine sand | 5 | 4 | 81.5 | 29.9 | | |
| | medium fine sand | 6 | 0 | | | | |
| | total | | 123 | 85.7 | 19.9 | | |
| **under terp (natural)** | manure | 0 | 0 | | | n/a | n/a |
| | organic material (peat) | 1 | 0 | | | | |
| | clay | 2 | 0 | | | | |
| | clayey sand, sandy clay and loam | 3 | 0 | | | | |
| | fine sand | 5 | 36 | 120.8 | 13.7 | | |
| | medium fine sand | 6 | 0 | | | | |
| | total | | 36 | 120.8 | 13.7 | | |

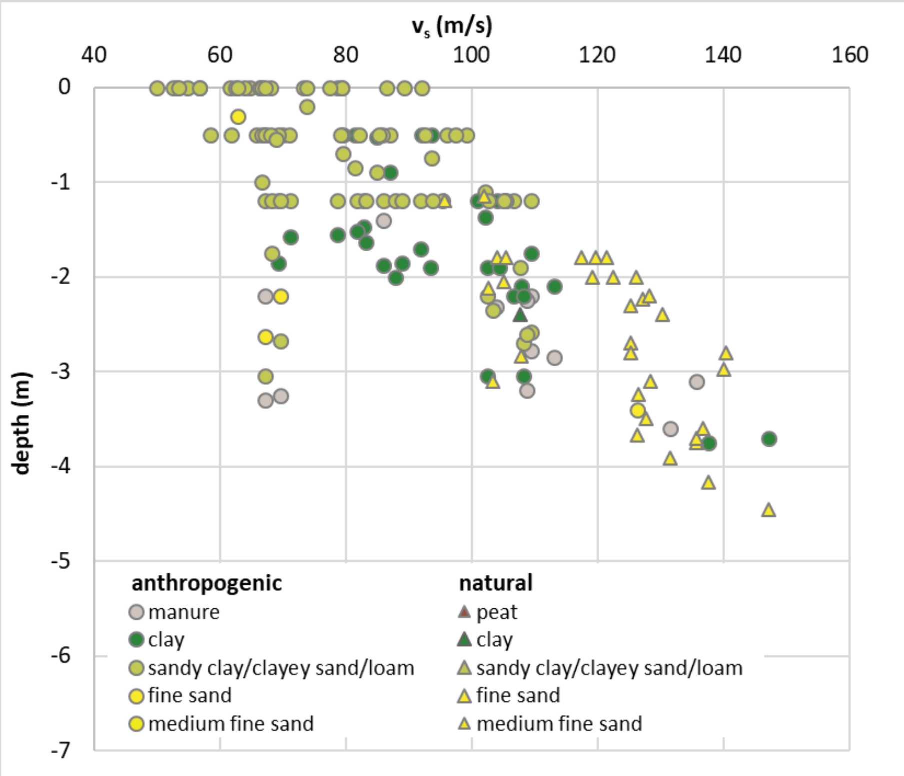


*Figure 4.11: $v_s$ values per lithoclass plotted against depth below soil surface for Beswerd*

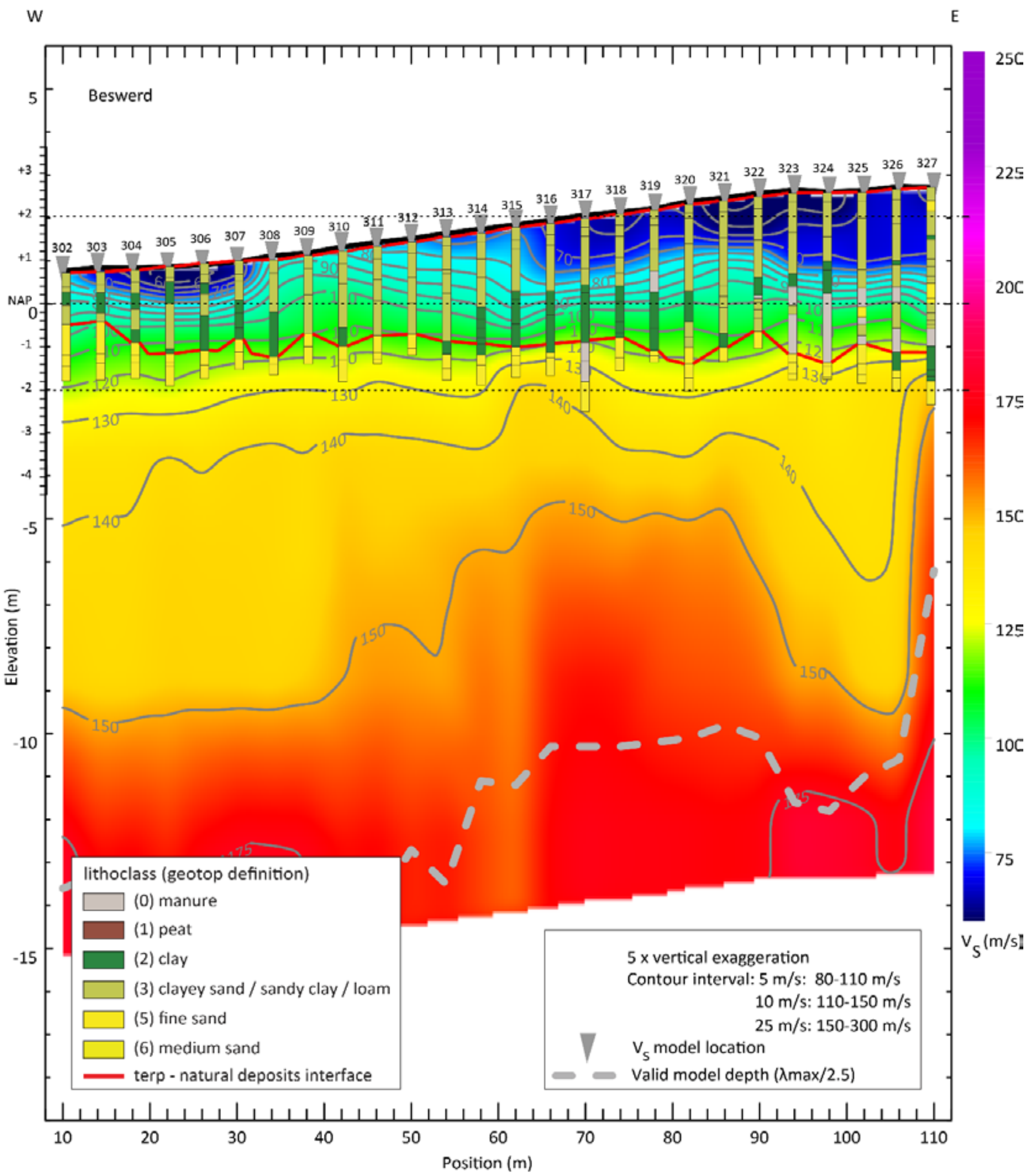


*Figure 4.12: Rayleigh wave 2D profile with archaeo-lithological corings for Beswerd (adapted after Geovision, 2019a)*

## 4.5 Biessum

### *4.5.1 General terp description*

Biessum is a large, round terp located just to the west of the town of Delfzijl (Figure 4.1). Taking the road encircling the terp as its perimeter, the terp diameter is approximately 300 m. LIDAR images however suggest the south-eastern to south-western edge of the terp may well lie several 10's of metres further from the centre. It is also possible that this area outside the circular road is (part of) a 'valge', a zone of communal arable fields. In contrast to the other location with more or less lens-shaped terps, the highest point of Biessum is not located in the centre, where surface level is c. 2.25 m +NAP, but on the southern and eastern edges, at 2.80 m +NAP.

According to the palaeo-geographical maps of Vos & De Vries (2013), Biessum is located in a saltmarsh region for a considerably part of the Holocene. Although the size of the marsh area steadily decreases, it is not until a moment between 1500 BC and 500 BC that marine influences appear and the landscape changes into a saltmarsh behind a narrow saltmarsh barrier. However, earlier reconstructions by Roeleveld (1974) show that earlier, roughly between 6000 $^{14}$C-years BP and 4400 $^{14}$C-years BP (c. 4000 BC-2400 BC), the location formed part of an intertidal to supratidal landscape. Between 500 BC and embankment in the later Middle Age and Modern Age, the area remains under marine influence.

The archaeological information on Biessum in ARCHIS 3 is limited. Although finds appear to be limited to the Late Middle Age, the description dates the location to period between Iron Age and present day. It is remarkable that although Biessum is a fairly large terp, it doesn't have a church. Biessum is also a very good example of the radial pattern of ditches on and outside the terp.

### *4.5.2 Archaeo-lithological characterisation*

A core on the southern edge provides some insight in the landscape development at the location. Here, the contact between Late Pleistocene coversands (Boxtel Fm, Wierden Mbr) and the overlying Holocene clay and peat sequence lies at approximately 4.40 m -NAP. The basal peat found at Amsweer (Paragraph 4.3) is missing here, and a c. 0.50 m thick clay layer forms the base of the Holocene sequence. This clay layer probably represents the first marine phase indicated by Roeleveld (1974). A 0.57 m thick layer of *Phragmites*-peat is all that remains of the long period with extensive freshwater marshes. A second layer of clastic tidal deposits forms the top of the Holocene sequence. In a 400 m wide zone underneath the terp, these deposits consist of silty, very fine sand laminated with clay and silt layers, and interpreted as tidal channel deposits. As the sections clearly show, the top of the tidal channel deposits forms a pronounced ridge, confirming the description in ARCHIS 3 that the terp is located on a palaeo-channel ridge. Outside the tidal channel, the upper clay layers are interpreted as intertidal and lower saltmarsh deposits at the base to upper saltmarsh deposits at the top.

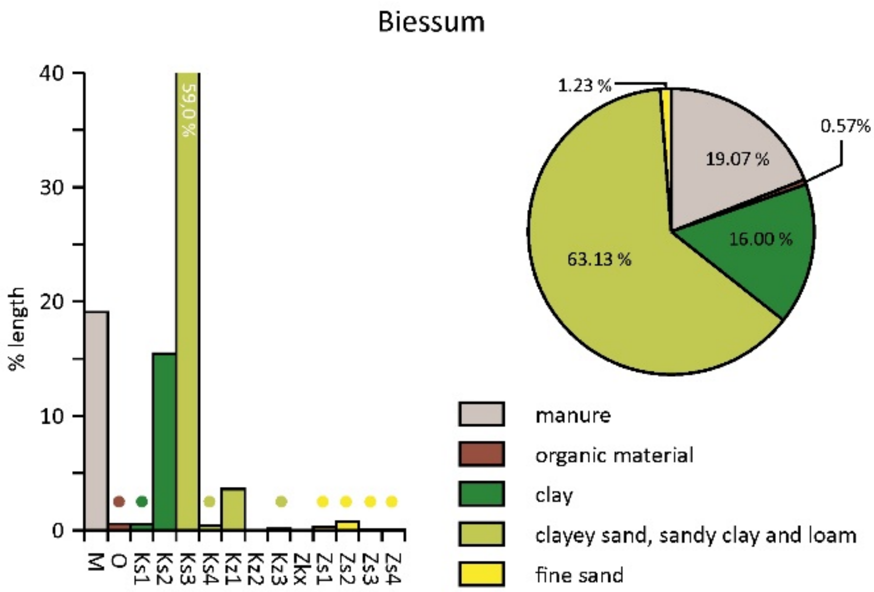


*Figure 4.13: Terp lithoclass proportions of Biessum. Left: frequency distribution NEN5104 lithoclasses and manure. Dots denote values < 2%; right: percentages of GeoTOP lithoclasses.*

The terp body consists of an up to 3.75 m thick sequence of anthropogenic layers, predominantly composed of silty to strongly silty clay (classes Ks2 and Ks3; Figure 4.13). As in other locations, the upper part of the anthropogenic layers appears to be somewhat siltier than the lower parts. The pattern is far from clear however, not in the least because a substantial manure layer forms the base of the terp north of the centre. This manure layer is found in a c. 80 m wide zone, and between 0.70 m and 2.35 m thick. A second, smaller manure layer can be found to the south of the centre. Overall, manure forms 19% of the total composition, the highest percentage of all investigated locations. Several deep features cut through the lower anthropogenic layers into the underlying natural deposits.

The oldest finds in the cores date from Middle Iron Age, placing the earliest occupation phase on Biessum in this period. Almost all other periods are also represented in the finds, suggesting the location was indeed inhabited throughout the Iron Age, Roman period, Middle Ages and the present day.

### *4.5.3 Shear wave velocity variability*

Although the difference in $v_s$ values between the terp Biessum and its subsurface is significantly different ($p < 0.05$), the absolute difference between the natural and anthropogenic lithoclasses seems limited with 78 vs 73 m/s, resp., with $v_s$ of anthropogenic lithoclasses being only slightly higher. When taking into account only all samples from within and below the terp, it is clear that manure (GeoTOP lithoclass 0) has an average $v_s$ value of 71 m/s, which is significantly lower than clay (lithoclass 2; $v_s$ = 81 m/s). There is no significant difference with the other lithoclasses fine sand and clayey sand, sandy clay and loam. When only taking into account the in-terp samples, there are no significant differences. The lithoclasses 2 (clay) and 5 (fine sand) are significantly different beneath the terp (Table 4.6).

There is a significant yet very weak increase of $v_s$ values with depth ($R^2$ = 0.08; $p < 0.000$), which loses its significance when carrying out the regression analysis on the in terp and below terp samples separately. This suggests that it is mainly the stepwise significant difference in $v_s$ values between in terp and below terp, and the increase with depth is an indirect effect.

*Table 4.6: ANOVA results for $v_s$ values per lithoclass for Biessum*

| Biessum | | | | $v_s$ (m/s) | | ANOVA | |
|---|---|---|---|---|---|---|---|
| | **lithoclass** | **code** | **n** | **mean** | **std.** | **F** | **p** |
| **all samples** | natural | 0 | 35 | 78.2 | 8.0 | 10.612 | 0.001** |
| | anthropogenic | 1 | 98 | 73.1 | 8.1 | | |
| | total | | 133 | 74.4 | 8.4 | | |
| **all samples** | manure | 0 | 28 | 70.8 | 4.5 | 8.896 | 0.000** |
| | organic material (peat) | 1 | 0 | | | | |
| | clay | 2 | 27 | 80.9 | 6.6 | | |
| | clayey sand, sandy clay and loam | 3 | 56 | 73.8 | 9.9 | | |
| | fine sand | 5 | 22 | 72.7 | 5.4 | | |
| | medium fine sand | 6 | 0 | | | | |
| | total | | 133 | 74.4 | 8.4 | | |
| **within terp (anthropogenic)** | manure | 0 | 28 | 70.8 | 4.5 | 1.958 | 0.126 |
| | organic material (peat) | 1 | 0 | | | | |
| | clay | 2 | 13 | 77.1 | 5.9 | | |
| | clayey sand, sandy clay and loam | 3 | 53 | 73.1 | 9.7 | | |
| | fine sand | 5 | 4 | 75.4 | 7.4 | | |
| | medium fine sand | 6 | 0 | | | | |
| | total | | 98 | 73.1 | 8.1 | | |
| **under terp (natural)** | manure | 0 | 0 | | | 29.735 | 0.000** |
| | organic material (peat) | 1 | 0 | | | | |
| | clay | 2 | 14 | 84.4 | 5.2 | | |
| | clayey sand, sandy clay and loam | 3 | 3 | 86.5 | 2.3 | | |
| | fine sand | 5 | 18 | 72.1 | 4.9 | | |
| | medium fine sand | 6 | 0 | | | | |
| | total | | 35 | 78.2 | 8.0 | | |

The visual interpretation of the terp profile (Figure 4.15), it is clearly visible that there is some horizontal variation within the terp. Although at around 5 m -NAP (generally 7 m depth from the surface) $v_s$ values appear rather constant at 130-140 m/s, the variation near the surface is more substantial. On the southern end of the terp (core numbers 203-244) show typical $v_s$ values of 60 m/s, whereas towards the northern end (core numbers 234/233 and 219-217) this appears to be much higher, with values of 85-90 m/s. Also, although $v_s$ values only decrease with decreasing depth to the south, in the north $v_s$ values appear to increase with decreasing depth in the upper 2 to 3 meters. This may be due to the presence of a relatively thick manure layer, which is with up to 1.5 m much thicker than the southern end, where typical thicknesses are of around 0.5 m. Also, the natural deposits beneath the terp seem to be sandier towards the north, which seem to have lower $v_s$ values than (sandy) clay in this profile (Table 4.6). Above the manure layers in the terp, $v_s$ values are slightly higher, indicating that $v_s$ values tend to increase after passing through manure layers. Below the terp, at around 5 m below the terp surface, the variation parallel to the surface is minimal, averaging at 90 m/s, although near the southern tip, this is slightly higher with around 110 m/s.

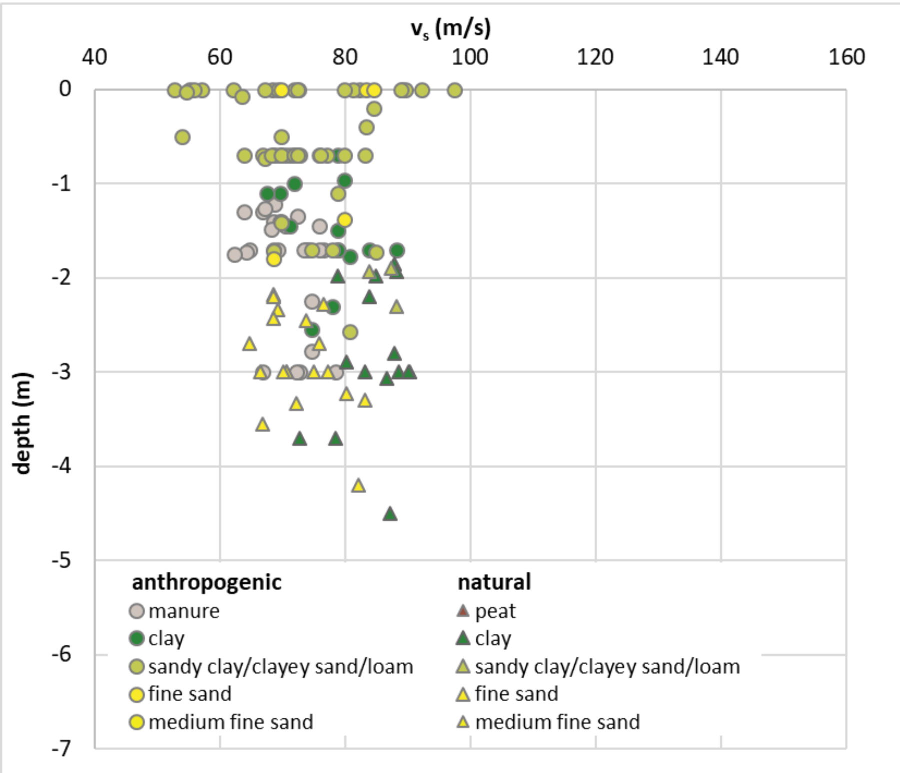


*Figure 4.14: $v_s$ values per lithoclass plotted against depth below soil surface for Biessum*

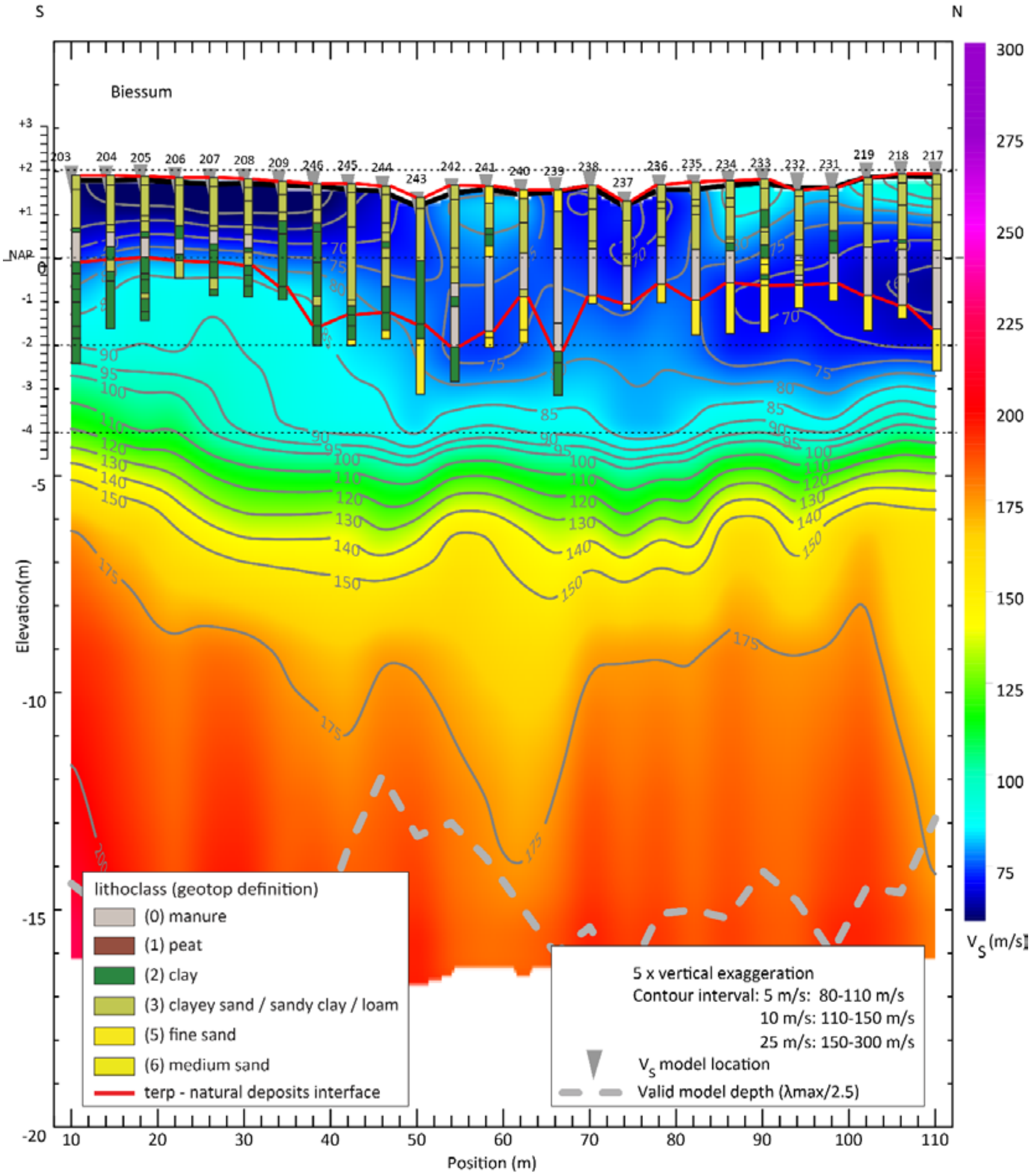


*Figure 4.15: Rayleigh wave 2D profile with archaeo-lithological corings for Biessum (adapted after Geovision, 2019a)*

## 4.6 Ezinge-Zuiderweg 1

### *4.6.1 General terp description*

Location Ezinge-Zuiderweg 1 is an oval terp measuring approximately 120 m along its northwest-southeast axis and 90 m along the axis perpendicular to that. According to the LIDAR data, the highest point at c. 2.75 m +NAP is located in the centre of the terp. The terp appears to be intact, although the southeastern is slightly damaged by digging in the early 1970’s. For a description of the geological and palaeogeographical situation, see location Beswerd and Ezinge-Zuiderweg 3, located at c. 1500 m and 400 m to the east respectively.

From an archaeological point of view, little is known about the location. It is listed as object 7Az104 in the inventory by Miedema (1983), but the entry lists no finds and remarks only that no anthropogenic layers were seen in the coring. Based on the information in ARCHIS3, the terp dates between the Iron Age to Late Middle Ages, while most of the pottery dates from the Roman period.

### 4.6.2 Archaeo-lithological characterisation

There is no lithological information about this location because no coring has taken place as part of this project. The monument description only mentions a 1.1 m to 1.6 m thick anthropogenic layer, but no further details about lithology or the presence of manure.

### 4.6.3 Shear wave velocity variability

The Rayleigh wave 2D profile for Ezinge Zuiderweg 1 (Figure 4.16) shows that horizontal variation in $v_s$ values at greater depths (3 m –NAP to the valid model depth) is limited. The increase in shear wave velocity with depth in this zone visually appears to be rather linear. This is very different at shallow depth, however. Although there are no corings available for this site, we assume that the terp thickness is around 2.5 to 3 m, based on the other terps. That means that the terp-natural subsurface interface is located at around 1.5 m-NAP. On the southern end of the transect, this shows a strong relation with the shear wave velocity, since there is a sharp decrease in vs values here (from 110 to 90 m/s within one metre). Additionally, vs values of the near surface are relatively low here. Near the top of the terp, this pattern is not present however. Vs values here seem to also linearly decrease with decreasing depth.

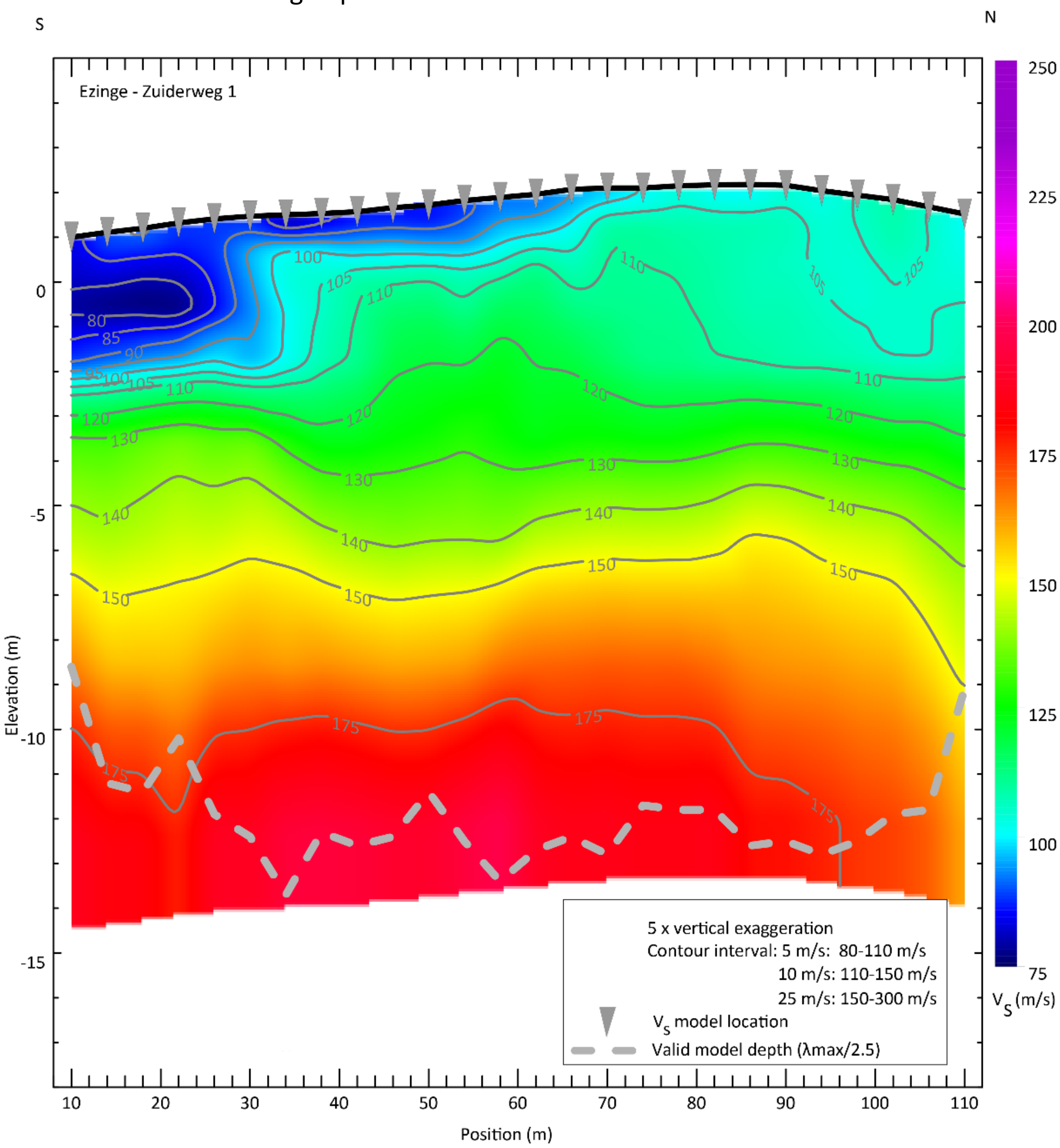


*Figure 4.16: Rayleigh wave 2D profile for Ezinge Zuiderweg 1 (adapted after Geovision, 2019a). Archaeo-lithological corings are not available for this site.*

## 4.7 Ezinge Zuiderweg 3

### *4.7.1 General terp description*

Location Ezinge – Zuiderweg 3 is a more or less round terp with a diameter between 150 m and 175 m. According to LIDAR data, its' highest point is located in the centre, at c. 2.65 m +NAP. From the LIDAR images, aerial photographs and field observations it is apparent that the terp is slightly damaged by the digging of ditches, and by a farmstead on the northeastern flank. This location is situated in almost the same geological and palaeogeographical setting as Beswerd, and for a brief description of the landscape development see Paragraph 4.4.1. It must be noted here however, that this location is situated at a somewhat greater distance from the main tidal channels than Beswerd. The dating of this terp is fairly well known. Miedema (1983) mentions several hundreds of sherds of Iron Age to Roman Age pottery, along with several tens dating from the Middle Ages. Knol (1993) however notes that material from the Early Middle Ages is almost absent from this site.

### *4.7.2 Archaeo-lithological characterisation*

As in location Beswerd, the top of the Pleistocene part and the lower part of the Holocene sedimentary sequences are only known from DINOloket data. In a 12 m deep core, located near the farmstead on the north-eastern flank, the top of the Pleistocene deposits (coversand, Boxtel Fm, Wierden Mbr) lies at c. 10.10 m -NAP. Subsoil variation within this region is demonstrated by a core c. 30 m to the east, where Holocene sediments lie directly on top of fine sands dating from the Eemian (Eem Fm), and another 850 m to the south-west, where a 28 m thick layer of Holocene sediments overlies Saalian deposits (Drente Fm, Schaarsbergen Mbr). The Holocene part of the sequence consists almost entirely of tidal deposits, locally with a thin peat layer at its base (Nieuwkoop Fm, Basisveen Bed).

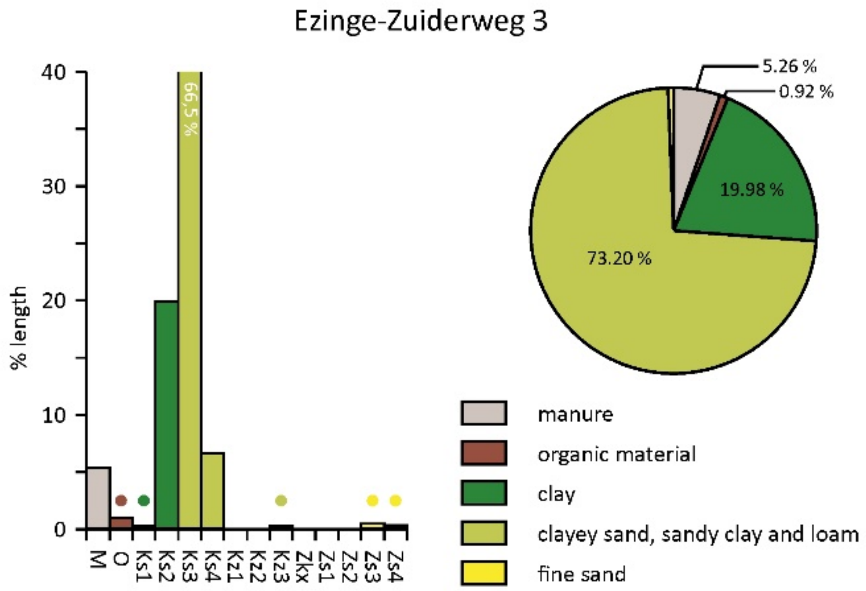


*Figure 4.17: Terp lithoclass proportions of Ezinge Zuiderweg 3. Left: frequency distribution NEN5104 lithoclasses and manure. Dots denote values < 2%; right: percentages of GeoTOP lithoclasses.*

Cores from the current project show that sandy and clayey intertidal deposits prevail up to c. 1.20 m -NAP. The top of the tidal deposits consists of silty clays, interpreted as saltmarsh deposits, and outside the terp these continue up to surface level. The anthropogenic layers constituting the terp body are, in comparison to some of the other locations, fairly homogenous, although the total thickness (up to 3.25 m) is not dissimilar to other locations. Almost all clastic layers consist of strongly silty clay (Ks3), with only minor contributions of other lithologies (Figure 4.17). Only to the east of the centre, the lower part of the terp body appears to consist of less silty clays, but the difference is marginal. West of the centre, a manure layer forms the base of the terp layers. In the main east-west section, this manure layers is up to 1.17 m thick and c. 25 m wide, but based on the results of the cores outside the main line it may well extent at least 30 m to the north and at least 10 m further south. The larger coring intervals outside the main section however do not permit exact conclusions.

Pottery found during the coring dates from two periods, namely the Middle Iron Age to Roman Age and Karolingian period to Late Middle Ages, confirming earlier observations about the occupation of this location.

### *4.7.3 Shear wave velocity variability*

The terp Ezinge Zuiderweg 3 shows a significant difference in $v_s$ values between natural (90 m/s) and anthropogenic deposits (76 m/s), but in absolute sense this difference seems limited (Table 4.7). In terms of lithoclasses, the only class that significantly deviates is manure, which is higher (96 m/s) than the clayey and sandy lithoclasses (78 - 82 m/s on average). This is also valid for within terp samples. Between lithoclasses underneath the terp, no significant differences were demonstrated. This may be explained by the relatively low number of samples and the limited variation in GeoTOP lithoclasses.

There is a general tendency of $v_s$ values to increase with depth, which is statistically significant and strong, with almost half of the variance explained ($R^2$ = 0.47; p < 0.000; Figure 4.18). The within terp increase with depth is similar ($R^2$ = 0.43; p < 0.000).

*Table 4.7: ANOVA results for $v_s$ values per lithoclass for Ezinge Zuiderweg 3*

| Ezinge Zuiderweg 3 | | | | **$v_s$ (m/s)** | | **ANOVA** | |
|---|---|---|---|---|---|---|---|
| | **lithoclass** | **code** | **n** | **mean** | **std.** | **F** | **p** |
| **all samples** | natural | 0 | 43 | 90.2 | 15.0 | 36.650 | 0.000 |
| | anthropogenic | 1 | 99 | 76.1 | 11.7 | | |
| | total | | 142 | 80.4 | 14.3 | | |
| **all samples** | manure | 0 | 11 | 96.0 | 11.3 | 6.781 | 0.000 |
| | organic material (peat) | 1 | | | | *9.524* | *0.000* |
| | clay | 2 | 41 | 81.6 | 11.2 | *(fine sand excl.)* | |
| | clayey sand, sandy clay and loam | 3 | 88 | 77.6 | 14.5 | | |
| | fine sand | 5 | 2 | 91.6 | 18.2 | | |
| | medium fine sand | 6 | | | | | |
| | total | | 142 | 80.4 | 14.3 | | |
| **within terp (anthropogenic)** | manure | 0 | 11 | 96.0 | 11.3 | 32.208 | 0.000 |
| | organic material (peat) | 1 | | | | | |
| | clay | 2 | 22 | 77.5 | 9.4 | | |
| | clayey sand, sandy clay and loam | 3 | 66 | 72.3 | 8.6 | | |
| | fine sand | 5 | | | | | |
| | medium fine sand | 6 | | | | | |
| | total | | 99 | 76.1 | 11.7 | | |
| **under terp (natural)** | manure | 0 | | | | 1.124 | 0.335 |
| | organic material (peat) | 1 | | | | | |
| | clay | 2 | 19 | 86.4 | 11.4 | | |
| | clayey sand, sandy clay and loam | 3 | 22 | 93.4 | 17.3 | | |
| | fine sand | 5 | 2 | 91.6 | 18.2 | | |
| | medium fine sand | 6 | | | | | |
| | total | | 43 | 90.2 | 15.0 | | |

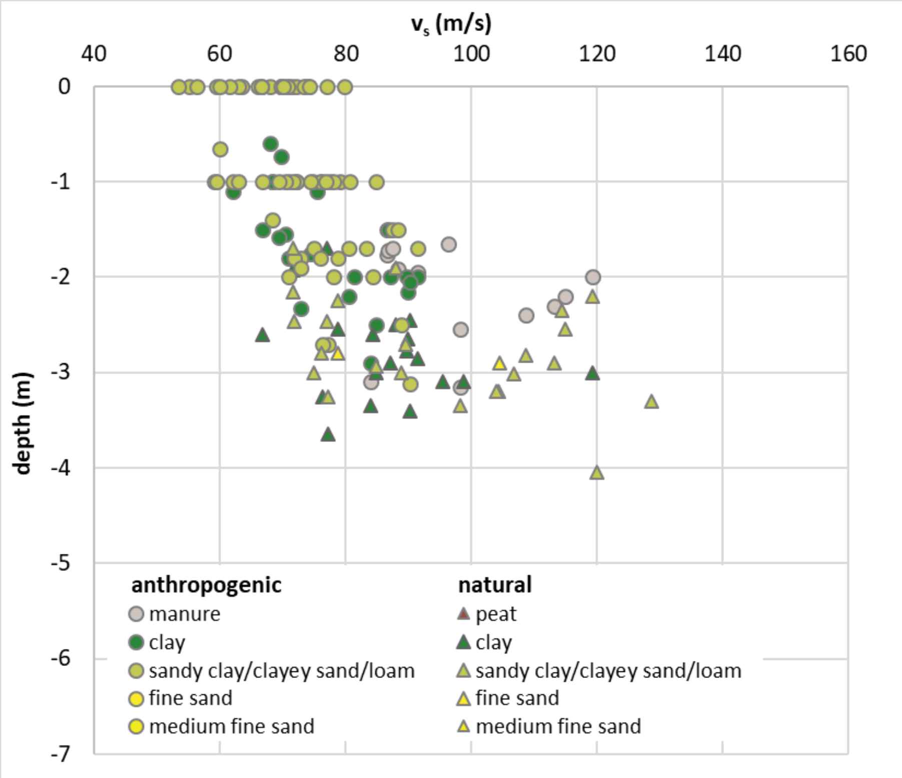


*Figure 4.18: $v_s$ values per lithoclass plotted against depth below soil surface for Ezinge Zuiderweg 3*

Figure 4.19 shows the $v_s$ profile combined with lithoclass profiles. Between the two datasets, there was a slight deviation in altitude and therefore, the altitudes from the $v_s$ profile were taken as leading; the coring data were adjusted accordingly. The horizontal variation in $v_s$ values lower than 3 m -NAP below the terp is very limited and appears to be very stable in horizontal direction, and is nearly linearly increasing with increasing depth (Figure 4.19). At the terp basis, fluctuating at 2 m to 0.5 m -NAP (indicated with the red line in the figure) to just below the terp basis the variability is somewhat higher. The $v_s$ values in the terp generally decrease with decreasing depth in the terp profile. The $v_s$ value are generally 80-90 m/s at the bottom of the terp, at the natural/anthropogenic interface. Towards the south-eastern side of the transect, values appear somewhat lower (60-80 m/s), whereas near the north-western side values are substantially higher (110 m/s). On both side, the decrease in $v_s$ values with depth is much higher than in the central section of the terp body. This results in relatively homogeneous $v_s$ values near the surface of the terp, ranging from 60 to 70 m/s. Upon visual inspection, there is no clear relationship between lithoclasses and $v_s$ values in the terp. Although the ANOVA results show significantly higher values for manure layers, this may be due to higher $v_s$ values below the terp, rather than the lithoclass itself.

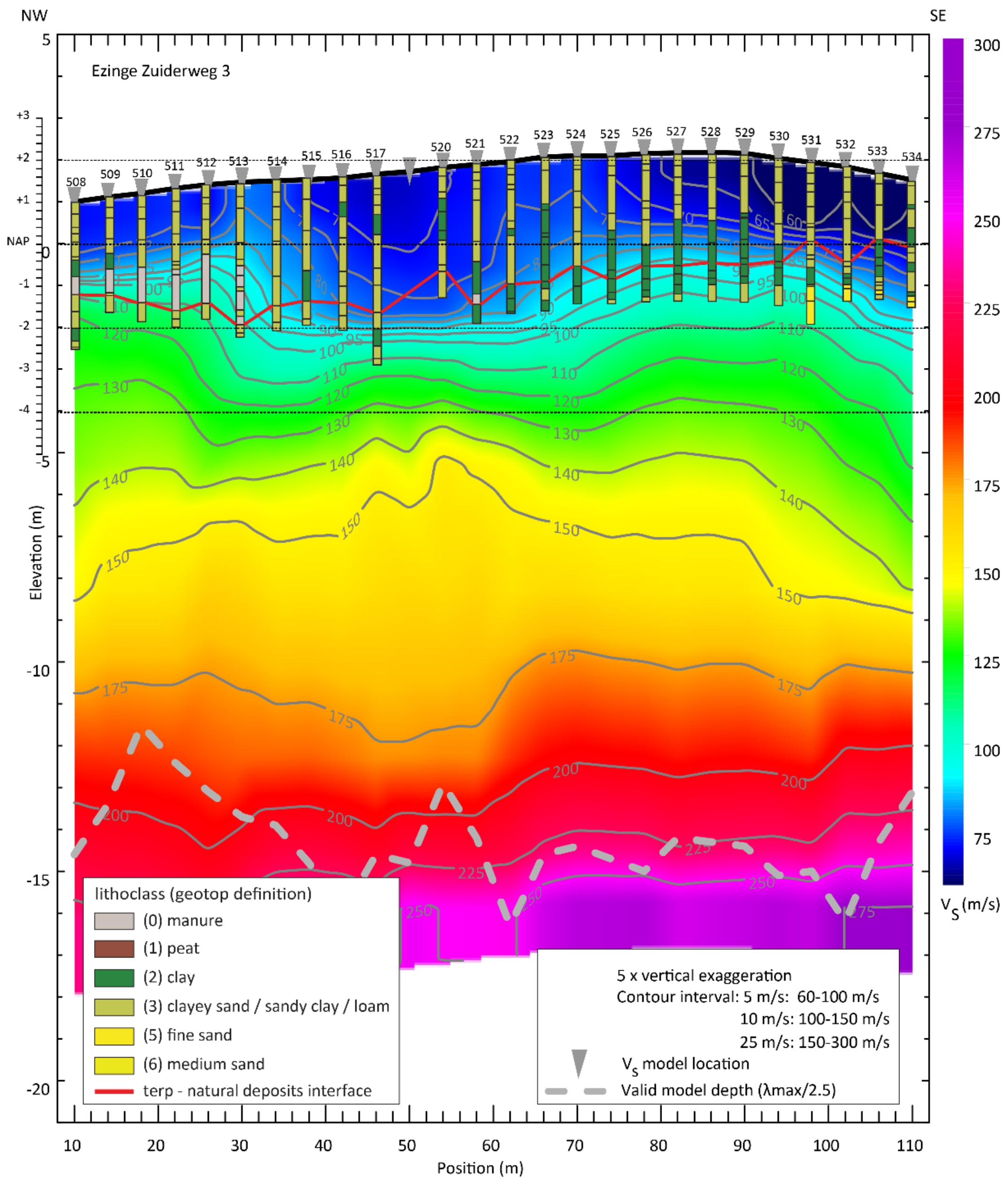


*Figure 4.19: Rayleigh wave 2D profile with archaeo-lithological corings for Ezinge Zuiderweg 3 (adapted after Geovision, 2019a)*

## 4.8 Fransum

### *4.8.1 General terp description*

Fransum is an almost round terp with a 300 m diameter, and a highest point of c. 3.20 m +NAP. Several houses and a farmstead are located on the terp, but the most prominent feature is a restored church with a precursor dating to the 13th century AD. A small moat surrounds the churchyard on three sides. LIDAR images and field observations show that all flanks except the northern are damaged by quarrying to some extent, as has the building of the (historical) farmstead on the eastern flank. This location is situated in almost the same geological and palaeogeographical setting as Beswerd, and for a brief description of the landscape development see Paragraph 4.4.1. In her inventory of terps and other archaeological objects in the western part of the Groningen coastal plain, Miedema (1983) lists Fransum as item number 7Az34, and mentions finds including a single sherd dating from the Iron Age/Roman Age, and twenty fragments from the Late Middle Ages.

Knol (1993) indicates the location was inhabited during almost the entire period between 450 AD and 900 AD. Most finds from this location registered in ARCHIS 3 date from the Middle Ages, although they also include Roman coins.

### *4.8.2 Archaeo-lithological characterisation*

The top of the Pleistocene deposits probably is somewhat shallower than for instance Beswerd, given the proximity of the Noordhorn/Zuidhorn glacial ridge. A lack of deep enough cores in the immediate surroundings of the location however means that this cannot be verified. The majority of the Holocene sequence likely consists of tidal deposits, and cores from this project and DINOloket confirm that this is indeed the case, at least for the uppermost 5 m. Here, intertidal deposits (silty to strongly silty very fine sand and clay, characterised by very thin sand-, silt- and clay layers). From c. 1.60 m -NAP upward, the sediments are interpreted as supratidal saltmarsh deposits (slightly to moderately silty clay, sometimes somewhat bioturbated or subaerially weathered).

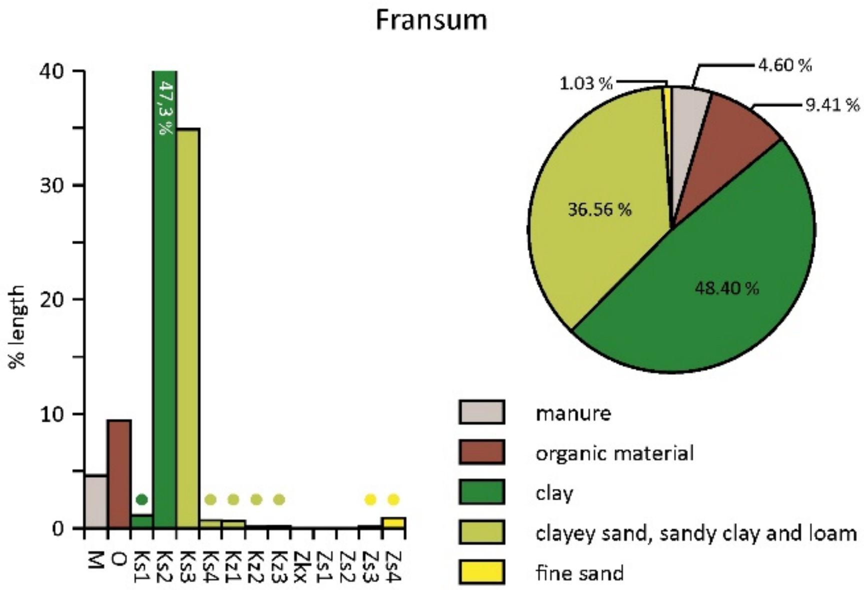


*Figure 4.20: Terp lithoclass proportions of Fransum. Left: frequency distribution NEN5104 lithoclasses and manure. Dots denote values < 2%; right: percentages of GeoTOP lithoclasses.*

The majority of the anthropogenic layers consists of moderately silty clay, but almost every other lithology up to extremely silty very fine sand occurs as well (Figure 4.20). In the central area of the terp, a pattern is hard to discern. Only on the eastern flank and to a lesser extent on the western flank, the top of the anthropogenic sequence seems to be siltier than the basal layers. A substantial manure layer underlies the central terp area. Remarkably, this layer appears to be more degraded than elsewhere, as the characteristic short, straw-like plant remains could not be identified. However, the position of the layer excludes virtually every other (natural) organic material. The manure layer is up to 1.37 m thick and extends for at least 45 m on the upper eastern flank. Outside the main section, several other cores both to the north and (in particular) to the south of the main line, contain manure layers. The wider coring interval however means it remains uncertain whether all these layers are part of a contiguous layer, or that, similar to Biessum, several manure layers are present.

Perhaps with the exception of the Late Roman Age and Migration period, pottery finds from the cores dates from almost every period between the Middle Iron Age and modern time, confirming the dating of the terp by Miedema (1983) and Knol (1993).

### 4.8.3 Shear wave velocity variability

In comparison to other terps, Fransum shows a relatively large difference in $v_s$ values between terp and natural deposits (Table 4.8). Not only is the difference highly significant, but in absolute terms the anthropogenic deposits show an average of 88 m/s, whereas in the natural deposits beneath the terp is much higher with an average of 115 m/s. It striking therefore, that there is no significant difference between GeoTOP lithoclasses, not in all samples, nor within the terp or beneath. This is also visible in Figure 4.21, in which there is a clear cluster on relatively low $v_s$ values within the terp, distinctively separated from the higher $v_s$ values underneath the terp. The change in $v_s$ values with depth appears to be stepwise with a separation at the base level of the terp, rather than a gradual increase, which is visible in some of the other terps. A regression analysis on the $v_s$-depth relationship was not carried out, because this seems meaningless in a stepwise increase in $v_s$ values.

*Table 4.8: ANOVA results for $v_s$ values per lithoclass for Fransum*

| Fransum | | | | $v_s$ (m/s) | | ANOVA | |
|---|---|---|---|---|---|---|---|
| | **lithoclass** | **code** | **n** | **mean** | **std.** | **F** | **p** |
| **all samples** | natural | 0 | 31 | 114.9 | 19.1 | 86.735 | 0.000** |
| | anthropogenic | 1 | 153 | 87.6 | 13.8 | | |
| | total | | 184 | 92.2 | 18.0 | | |
| **all samples** | manure | 0 | 20 | 90.7 | 19.1 | 1.83 | 0.143 |
| | organic material (peat) | 1 | 0 | | | | |
| | clay | 2 | 110 | 94.3 | 19.1 | | |
| | clayey sand, sandy clay and loam | 3 | 50 | 87.7 | 13.6 | | |
| | fine sand | 5 | 4 | 99.0 | 22.4 | | |
| | medium fine sand | 6 | 0 | | | | |
| | total | | 184 | 92.2 | 18.0 | | |
| **within terp (anthropogenic)** | manure | 0 | 20 | 90.7 | 19.1 | 0.544 | 0.643 |
| | organic material (peat) | 1 | 0 | | | | |
| | clay | 2 | 82 | 87.8 | 14.1 | | |
| | clayey sand, sandy clay and loam | 3 | 48 | 86.0 | 11.0 | | |
| | fine sand | 5 | 3 | 88.4 | 8.7 | | |
| | medium fine sand | 6 | | | | | |
| | total | | 153 | 87.6 | 13.8 | | |
| **under terp (natural)** | manure | 0 | 0 | | | 0.896 | 0.419 |
| | organic material (peat) | 1 | 0 | | | | |
| | clay | 2 | 28 | 113.4 | 19.6 | | |
| | clayey sand, sandy clay and loam | 3 | 2 | 128.0 | 4.2 | | |
| | fine sand | 5 | 1 | 130.9 | | | |
| | medium fine sand | 6 | 0 | | | | |
| | total | | 31 | 114.9 | 19.1 | | |

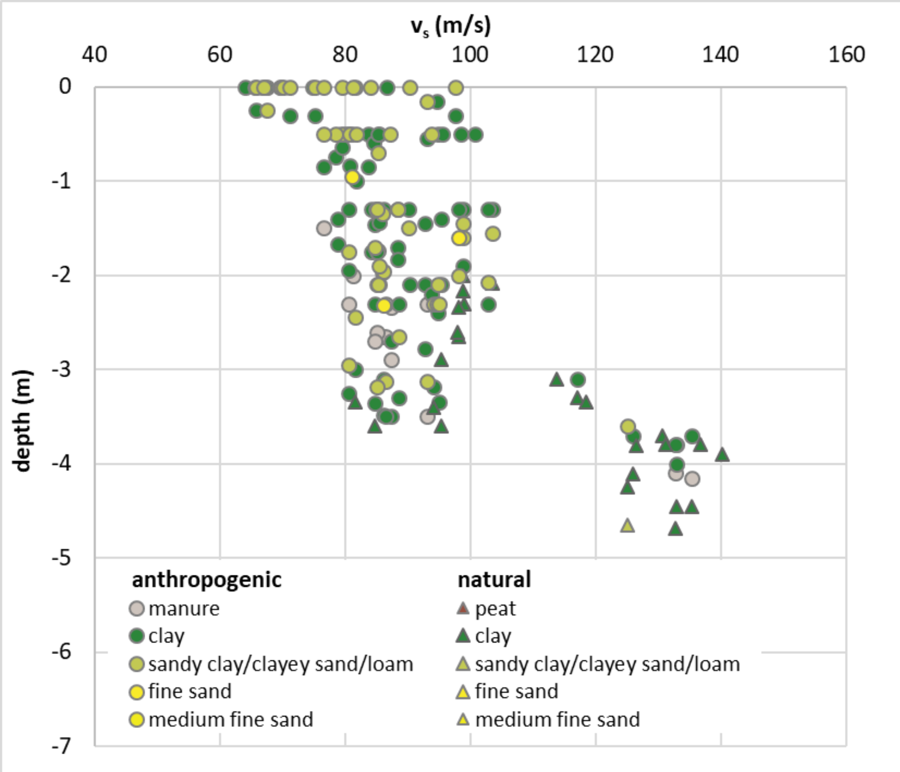


*Figure 4.21: $v_s$ values per lithoclass plotted against depth below soil surface for Fransum*

Visual inspection of the 2D $v_s$ profile in combination with the archaeo-lithoclass cores (Figure 4.22) shows that the north-eastern section of the terp (cores 109 through 126) shows distinctively lower $v_s$ values than the south-western section. This corresponds with a high proportion of manure layers in the terp, which seem to be almost absent in the southwestern section. Although in some terps, $v_s$ values tend to increase again above manure layers (e.g. Ezinge Zuiderweg 3, Biessum), this is not the case here. Below the terp basis, at around 1 m -NAP, or 5 m below the terp surface, $v_s$ values appear rather homogeneous in parallel with the surface ($v_s$ = 130 m/s), although there is a slight tendency towards somewhat lower values towards the southwest, ranging from 100 to 110 m/s.

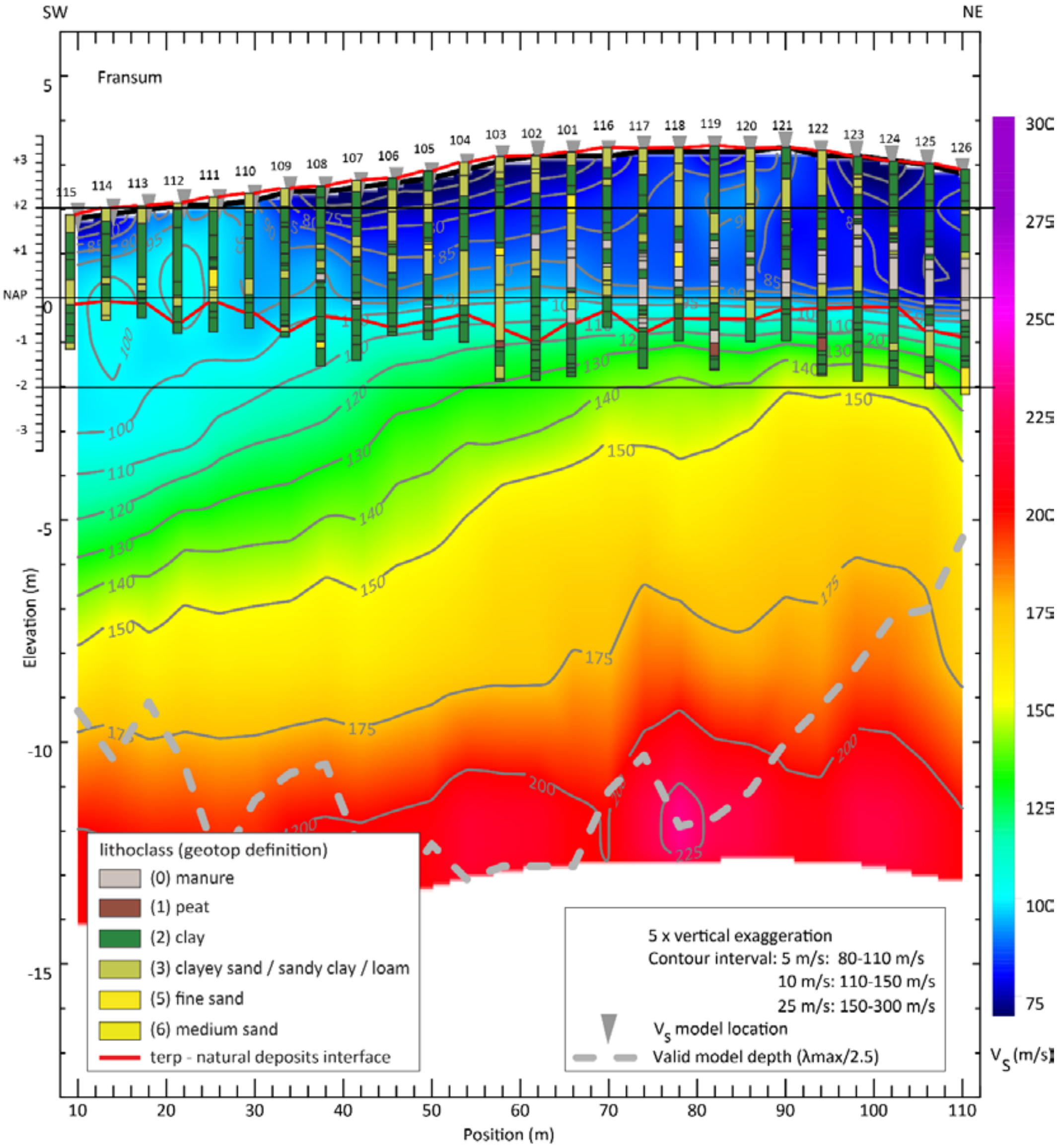


*Figure 4.22: Rayleigh wave 2D profile with archaeo-lithological data for Fransum (adapted after Geovision, 2019a)*

## 4.9 Grote Houw

### *4.9.1 General terp description*

The Grote Houw location is part of a complex of terps situated between Leens and Ulrum. Based on recent LIDAR data, this terp complex consists of at least three parts. The main terp body, and subject of the seismic and archaeo-lithological research reported here, lies south of the Leensterweg and measures approximately 130 x 130 m. Likely, it extends further north of the Leensterweg, but it cannot excluded that this is a separate small, single-farmstead terp located on the flank of the larger, main terp body. Slightly further north, a similar, less distinct mound underlying the present-day farm could also be a single-farmstead terp. A dry ditch separates the main terp and a smaller, c. 110 x 80 m large terp directly to the west of it. Although in the field this division appears artificial and perhaps quite recent, older topographic maps show two distinct mounds. Further west, two more somewhat less distinct mounds form the terp De Houw-West, but these terps have not been included in the current research setup.

Geomorphologically, Grote Houw is located on a pronounced saltmarsh barrier with an east-west orientation which can be traced for c. 9.5 km from Wehe-Den Hoorn to the eastern edge of the Lauwersmeer (Figure 4.1). The palaeo-geographical reconstructions (Roeleveld, 1974; Vos & De Vries, 2013) show the location forming part of the intertidal landscape of the outer Hunze-systeem. Around or slightly before 100 AD, the coastal morphology changes sufficiently to allow the formation of the Vierhuizen-Wehe-Den Hoorn saltmarsh barrier. Once this barrier is in place, the western part of the Groningen coastal plain aggrades in a northerly direction, leading to a succession of smaller saltmarsh barriers and associated lower areas.

In 2013/2014, a project investigating erosion speeds using $^{137}$Cs-measurements, coring and an archaeological survey was carried out on the Grote Houw location (Huisman *et al.*, 2017). The oldest pottery fragments found at the surface date from the 9$^{th}$ century AD, although Knol (1993) indicates occupation may have started somewhat earlier, around the 8$^{th}$ century AD.

### *4.9.2 Archaeo-lithological characterisation*

According to the data available from DINOloket, the depth of the top of the Pleistocene varies, lying between 12 m -NAP and 20 m -NAP. During the earlier part of the Holocene, erosion must have been a dominant process to the west of the terp, because here the Boxtel Fm is absent, and the uppermost Pleistocene deposits are formed by Eemian deposits. The upper part of the Holocene deposits consists of sandy tidal sediments. From c. 4.0 m -NAP to c. 0.7 m -NAP, subtidal and intertidal deposits form the base of the layers in the cores. The upper layers (very fine sand, with little flecks of somewhat coarser sand and other evidence of bioturbation) are predominantly interpreted as saltmarsh barrier deposits, although saltmarsh and creek deposits have been found as well.

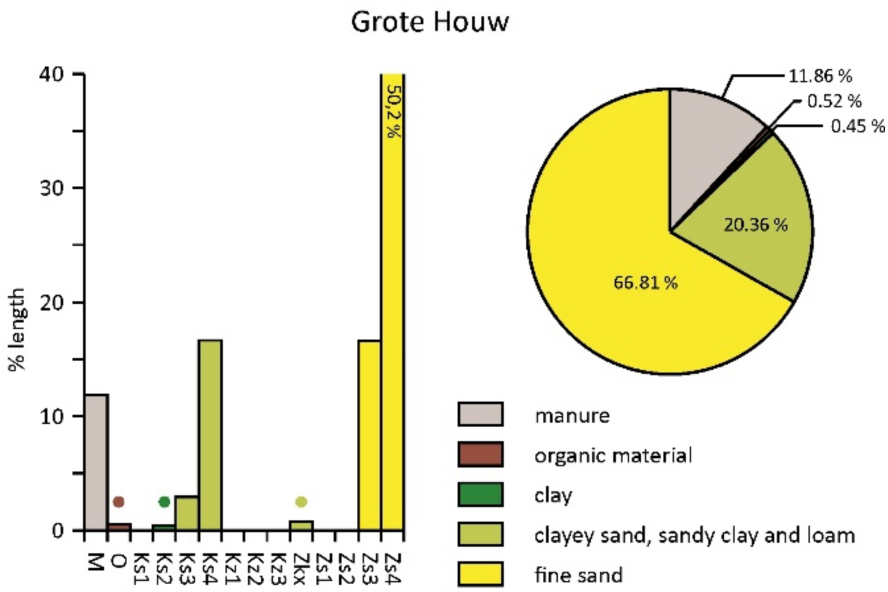


*Figure 4.23: Terp lithoclass proportions of Grote Houw. Left: frequency distribution NEN5104 lithoclasses and manure. Dots denote values < 2%; right: percentages of GeoTOP lithoclasses.*

Unsurprisingly, the anthropogenic layers mostly consist of strongly to extremely silty, very fine to extremely fine sand (Zs3 and Zs4; ‘fine sand’ in the Geotop lithoclass definition; Figure 4.23). Slightly finer deposits (strongly to extremely silty clay) also occur, most notably in the upper part of the profile of the somewhat lower, western mound and the eastern flank of the main mound. In the main part of the terp body however, clay layers are clearly of secondary importance.

In the main section, a substantial manure layer underlies the western part of the terp body. The distribution of cores with manure layers suggests this manure layer extends c. 45 m to the south and at least 48 m to the north, matching the results from the 2013/2014 coring (Huisman *et al.*, 2017). The manure layer is up to 1.45 m thick, and in most cases separated from the natural saltmarsh barrier deposits by a sandy anthropogenic layer. A second, smaller and thinner manure layers is found in three cores on the eastern flank. In comparison to the other terps, finds in the cores were scarce and consist entirely of typical Karolingian to Late Medieval pottery.

### *4.9.3 Shear wave velocity variability*

Comparable to the terps Beswerd and Fransum, Grote Houw also shows a considerable, significant difference in $v_s$ values between the terp and the subsurface (Table 4.9). $V_s$ values of anthropogenic deposits (121 m/s) are substantially lower than below (101 m/s), despite the high standard deviations. Similar to Fransum, there is no significant difference between lithoclasses. $V_s$ values generally increase with depth (Figure 4.24). The regression analysis shows this is significant but weak ($p < 0.000$; $R^2 = 0.25$), although this is mostly explained by the samples below the terp, since the analysis within the terp only shows a very weak ($p = 0.003$; $R^2 = 0.05$) correlation.

*Table 4.9: ANOVA results for $v_s$ values per lithoclass for Grote Houw*

| Grote Houw | | | | $v_s$ (m/s) | | ANOVA | |
|---|---|---|---|---|---|---|---|
| | **lithoclass** | **code** | **n** | **mean** | **std.** | **F** | **p** |
| **all samples** | natural | 0 | 36 | 120.9 | 16.3 | 42.547 | 0.000** |
| | anthropogenic | 1 | 117 | 100.6 | 16.3 | | |
| | total | | 153 | 105.4 | 18.4 | | |
| **all samples** | manure | 0 | 17 | 101.9 | 26.3 | 1.499 | 0.217 |
| | organic material (peat) | 1 | 0 | | | | |
| | clay | 2 | 2 | 119.6 | 0.0 | | |
| | clayey sand, sandy clay and loam | 3 | 21 | 99.7 | 18.5 | | |
| | fine sand | 5 | 113 | 106.7 | 16.9 | | |
| | medium fine sand | 6 | 0 | | | | |
| | total | | 153 | 105.4 | 18.4 | | |
| **within terp (anthropogenic)** | manure | 0 | 17 | 101.9 | 26.3 | 0.081 | 0.922 |
| | organic material (peat) | 1 | 0 | | | | |
| | clay | 2 | 0 | | | | |
| | clayey sand, sandy clay and loam | 3 | 21 | 99.7 | 18.5 | | |
| | fine sand | 5 | 79 | 100.6 | 12.8 | | |
| | medium fine sand | 6 | | | | | |
| | total | | 117 | 100.6 | 16.3 | | |
| **under terp (natural)** | manure | 0 | 0 | | | 0.013 | 0.910 |
| | organic material (peat) | 1 | 0 | | | | |
| | clay | 2 | 2 | 119.6 | 0.0 | | |
| | clayey sand, sandy clay and loam | 3 | 0 | | | | |
| | fine sand | 5 | 34 | 121.0 | 16.8 | | |
| | medium fine sand | 6 | 0 | | | | |
| | total | | 36 | 120.9 | 16.3 | | |

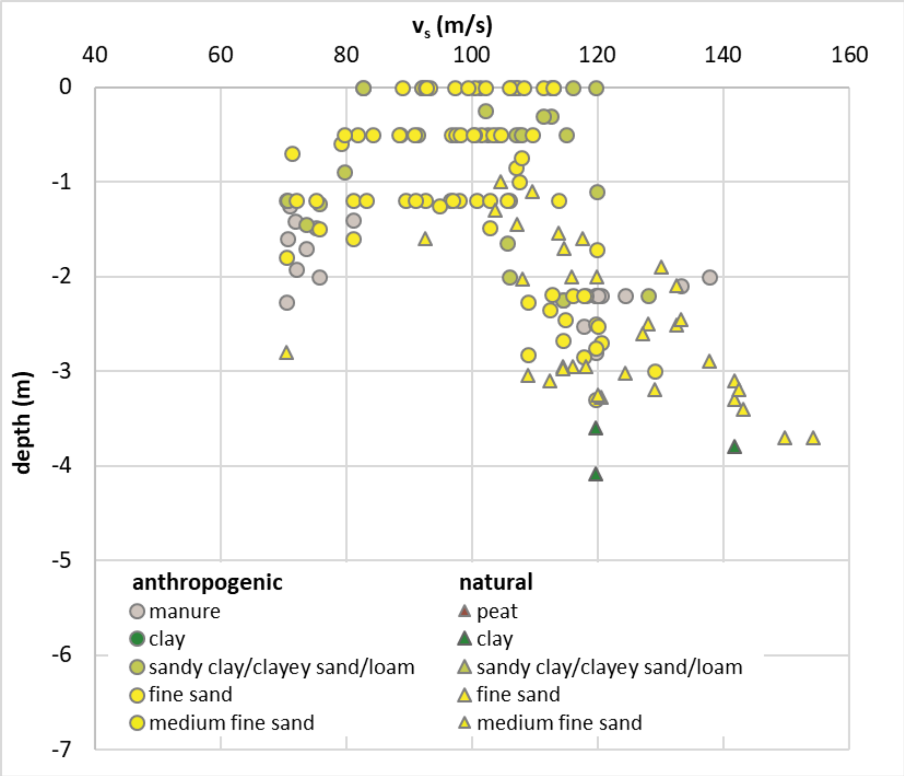


*Figure 4.24: $v_s$ values per lithoclass plotted against depth below soil surface for Grote Houw*

The archaeo-lithological cores combined with the $v_s$ profile (Figure 4.25) shows that at around 6 m below the gently sloping surface $v_s$ values are rather homogeneous (130 to 140 m/s) in the plane parallel to the soil surface. Below, the $v_s$ values are linearly increasing with depth. Closer to the surface, the decline of $v_s$ values with decreasing depth is much more rapid in the centre of the terp (represented by soil cores 710 through 720), which is clearly visible in dark blue. Rates sharply decline from 120 m/s to 75 m/s, which almost perfectly corresponds with the presence of a relatively thick manure layer. The decrease in $v_s$ values starts within the manure layers, but continues to decrease in the layers with clayey sand / sandy clay / loam above. Near the surface, $v_s$ values start to increase again. Towards the eastern section of the terp, the manure layers are fragmented and thinner (cores 724, 725 and 726), which seem to result in a much weaker decrease in $v_s$ values.

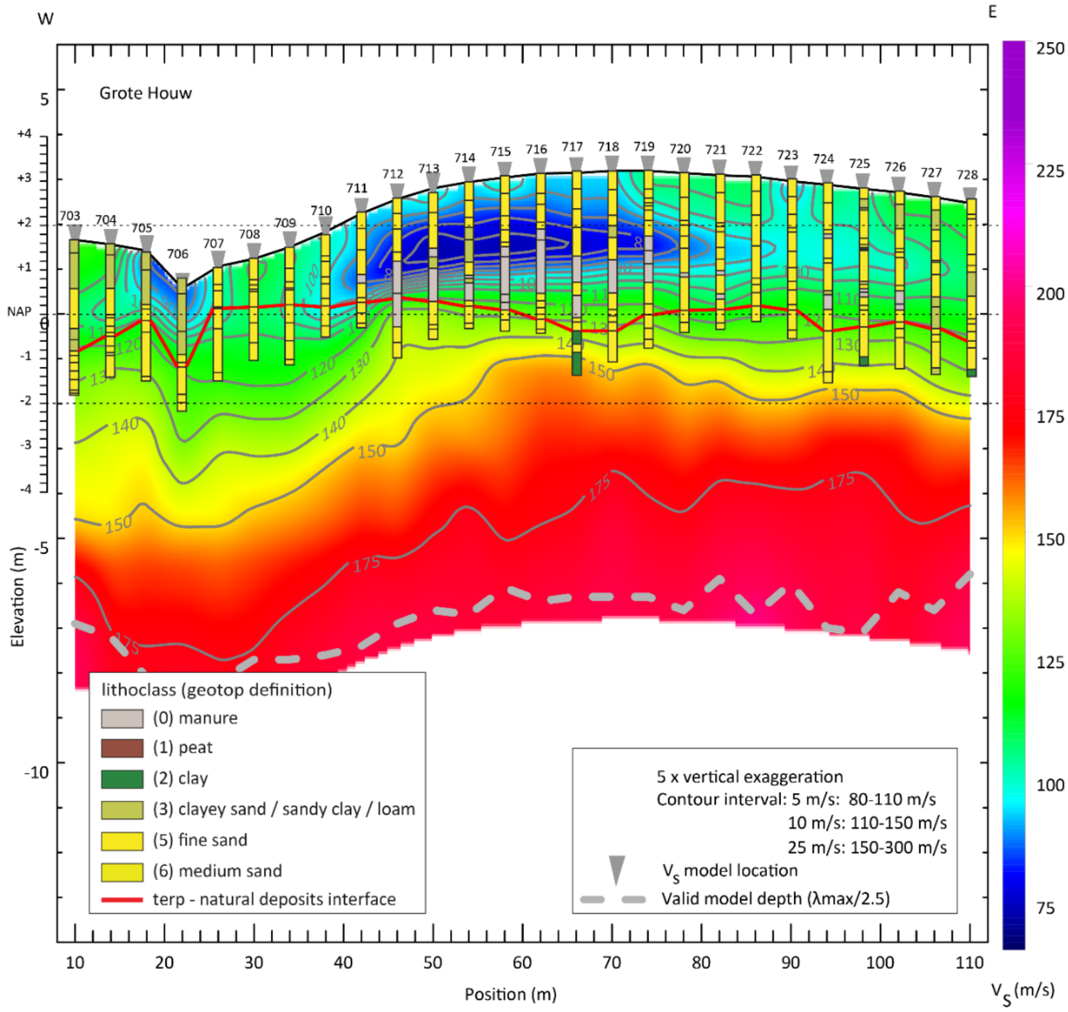


*Figure 4.25: Rayleigh wave 2D profile with archaeo-lithological corings for Grote Houw (adapted after Geovision, 2019a)*

## 4.10 Helwerd

### *4.10.1 General terp description*

Location Helwerd is distinct from the other locations in that it presently consists of two mounds, split by a steep-sided, north-south oriented ditch. Although evidence such as cores or exposures is absent, the terps are generally considered separate mounds. Both are more or less semi-circular in shape and LIDAR data and field observations show that the south flanks are damaged somewhat by quarrying. The highest point of the western and eastern mound lie around 2.60 m +NAP and 2.80 m +NAP, respectively. The location in its entirety measures approximately 250 m x 200 m.

The palaeo-geographical reconstructions (Vos & De Vries 2013) show Helwerd was located on the western shore of the Fivel estuary. Changes in the coastal configuration shortly after 1500 BC led to the development of more west-east oriented saltmarsh barrier, on which amongst others the towns of Baflo, Usquert and Uithuizen are situated, and Helwerd appears to be situated on the southern flank of this barrier. On the geomorphological map however, the saltmarsh barrier is less wide and Helwerd lies in the extensive low-lying area landward of the barrier (Figure 4.1).

No archaeological observations from the location are registered in ARCHIS 3, resulting in a rather wide dating of Iron Age to Early Middle Ages. The inventory by Knol (1993) only mentions a possible occupation phase around the 9$^{th}$ century AD. Archaeological coring prior to the construction of a stable near the farm just to the south of the location yielded neither finds nor anthropogenic layers (Leuvering, 2013), and is clear that the terp does not extend this far southward.

### *4.10.2 Archaeo-lithological characterisation*

Based on information from DINOloket, the top of the Pleistocene deposits at and around location Helwerd lies between 10 m -NAP and 20 m -NAP. In general, the uppermost Pleistocene deposits are correlated with the Boxtel Fm; where the Pleistocene surface lies deeper, the Holocene sequence overlies sands and clays belonging to the Peelo Fm. Because of the depth of the Pleistocene deposits and the fact that most cores in the vicinity are relatively shallow, usually not deeper than 5 m below present-day surface, little is known about the base of the Holocene deposits. Where the entire Holocene sequence is available, a basal peat layer is absent and tidal deposits of the Naaldwijk Fm directly overly the Pleistocene deposits. The top of the Holocene tidal deposits consists of intertidal (slightly sandy clay and extremely silty, very fine sand with shell remains) and supratidal sediments (moderately to strongly silty clay, with traces of bioturbation or subaerial weathering). The contact between intertidal and supratidal deposits lies between 1.20 m -NAP and 1.80 m -NAP.

The anthropogenic layers in the terp body predominantly consist of strongly silty clay, with minor contributions of sand, organic material or less silty clay (Figure 4.26). In the northern half of the section, the base of the anthropogenic layers appears to be somewhat more clayey, but the presence of several deep cut features prevents certain identification of such a pattern.

Thin manure layers were only found in seven cores, and it would seem that a substantial manure layer similar to those found at other locations is not present, at least not on the western part of the location. On the eastern mound, a substantial manure layer could be present, but easily have been missed because of the wider core intervals used here. Although the results from other locations strongly suggest manure layers lie more or less central underneath the terp, Ezinge-Zuiderweg 3 and Biessum show that this is not necessarily the case. Further complicating the pattern are several cores with organic layers, which in the field could not be identified as manure. Whereas in Biessum similar organic layers could be correlated with manure layers and thus interpreted as degraded or oxidised manure, this is not the case in Helwerd. Obviously, it is very unlikely that a peat layer will grow on a terp, but deposition of detritus and other organic sediments in deeper features with standing water is not impossible. In this case therefore, these are treated separately from manure layers.

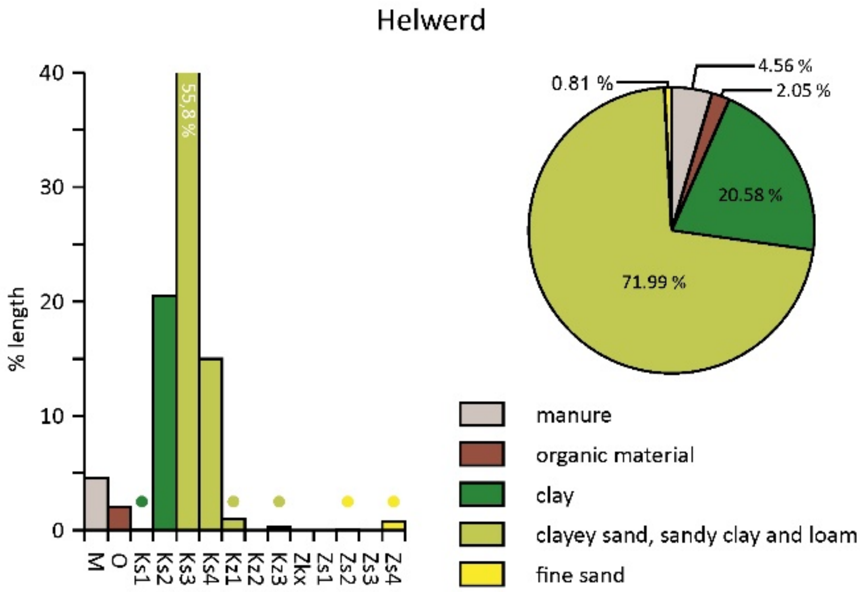


*Figure 4.26: Terp lithoclass proportions of Helwerd. Left: frequency distribution NEN5104 lithoclasses and manure. Dots denote values < 2%; right: percentages of GeoTOP lithoclasses.*

A large number of finds has been made during the coring, yielding pottery fragments from almost all periods between the Middle Iron Age and the Late Middle Ages. A fragment resembling Roman *terra nigra* pottery may, when the identification proves correct, add to the growing evidence of economical and cultural contacts between the northern coastal regions and the Roman Empire.

### *4.10.3 Shear wave velocity variability*

Shear wave velocity values are significantly lower in the anthropogenic deposits than the natural layers between the terp (87 vs. 99 m/s resp.; $p < 0.000$; Table 4.10). The standard deviations are similar. The $v_s$ linearly increases with depth ($R^2 = 0.51$; $p < 0.000$), in which the regression in the natural deposits is slightly stronger than in the anthropogenic deposits (Figure 4.27). According to the post hoc analysis (Bonferroni), the average $v_s$ value for the lithoclass clayey sand, sandy clay and loam (84 m/s) is significantly lower than manure (94 m/s; n = 7), which on its turn is significantly lower than fine sand (102 m/s) within the terp.

*Table 4.10: ANOVA results for $v_s$ values per lithoclass for Helwerd*

| Helwerd | | | | **$v_s$ (m/s)** | | **ANOVA** | |
|---|---|---|---|---|---|---|---|
| | **lithoclass** | **code** | **n** | **mean** | **std.** | **F** | **p** |
| **all samples** | natural | 0 | 44 | 98.7 | 10.1 | 31.950 | 0.000** |
| | anthropogenic | 1 | 112 | 86.1 | 13.3 | | |
| | total | | 156 | 89.6 | 13.7 | | |
| **all samples** | manure | 0 | 7 | 94.4 | 11.4 | 8.575 | 0.000** |
| | organic material (peat) | 1 | | | | | |
| | clay | 2 | 51 | 92.7 | 8.2 | | |
| | clayey sand, sandy clay and loam | 3 | 89 | 85.9 | 14.5 | | |
| | fine sand | 5 | 9 | 105.7 | 16.7 | | |
| | medium fine sand | 6 | | | | | |
| | total | | 156 | 89.6 | 13.7 | | |
| **within terp (anthropogenic)** | manure | 0 | 7 | 94.4 | 11.4 | 7.551 | 0.000** |
| | organic material (peat) | 1 | | | | | |
| | clay | 2 | 27 | 90.9 | 9.0 | | |
| | clayey sand, sandy clay and loam | 3 | 73 | 82.4 | 13.0 | | |
| | fine sand | 5 | 5 | 102.3 | 18.4 | | |
| | medium fine sand | 6 | | | | | |
| | total | | 112 | 86.1 | 13.3 | | |
| **under terp (natural)** | manure | 0 | | | | 6.364 | 0.004** |
| | organic material (peat) | 1 | | | | | |
| | clay | 2 | 24 | 94.7 | 6.7 | | |
| | clayey sand, sandy clay and loam | 3 | 16 | 101.8 | 10.1 | | |
| | fine sand | 5 | 4 | 109.9 | 15.7 | | |
| | medium fine sand | 6 | | | | | |
| | total | | 44 | 98.7 | 10.1 | | |

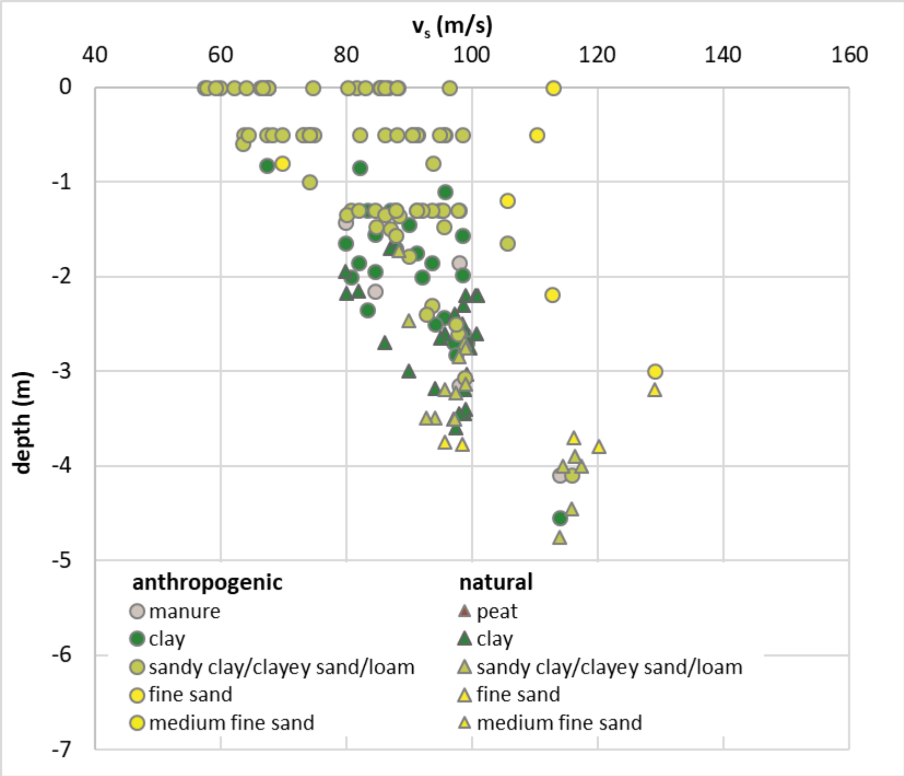


*Figure 4.27: $v_s$ values per lithoclass plotted against depth below soil surface for Helwerd*

The shear wave velocity profile (Figure 4.28) at 2 m –NAP and below shows a homogeneous pattern. There is hardly any horizontal variation and $v_s$ values linearly increase with depth, ranging from 110 m/s at 3 m -NAP (4 m below soil surface) to 250 m/s at 14 m -NAP. Higher in the profile, just below the terp base (indicated by the wavy red line in the figure), there is relatively sharp decline in $v_s$ values in the southern half of the terp, whereas in the northern half, $v_s$ values hardly decrease with decreasing depth. A possible explanation could be the slightly higher proportion of natural clay layers below the terp (soil cores 428 through 476). Higher in the profile, the $v_s$ values continue to decrease sharply. Although there are some peaty layers here, their thickness and fragmented presence do not seem to fully explain the relatively low $v_s$ values here.

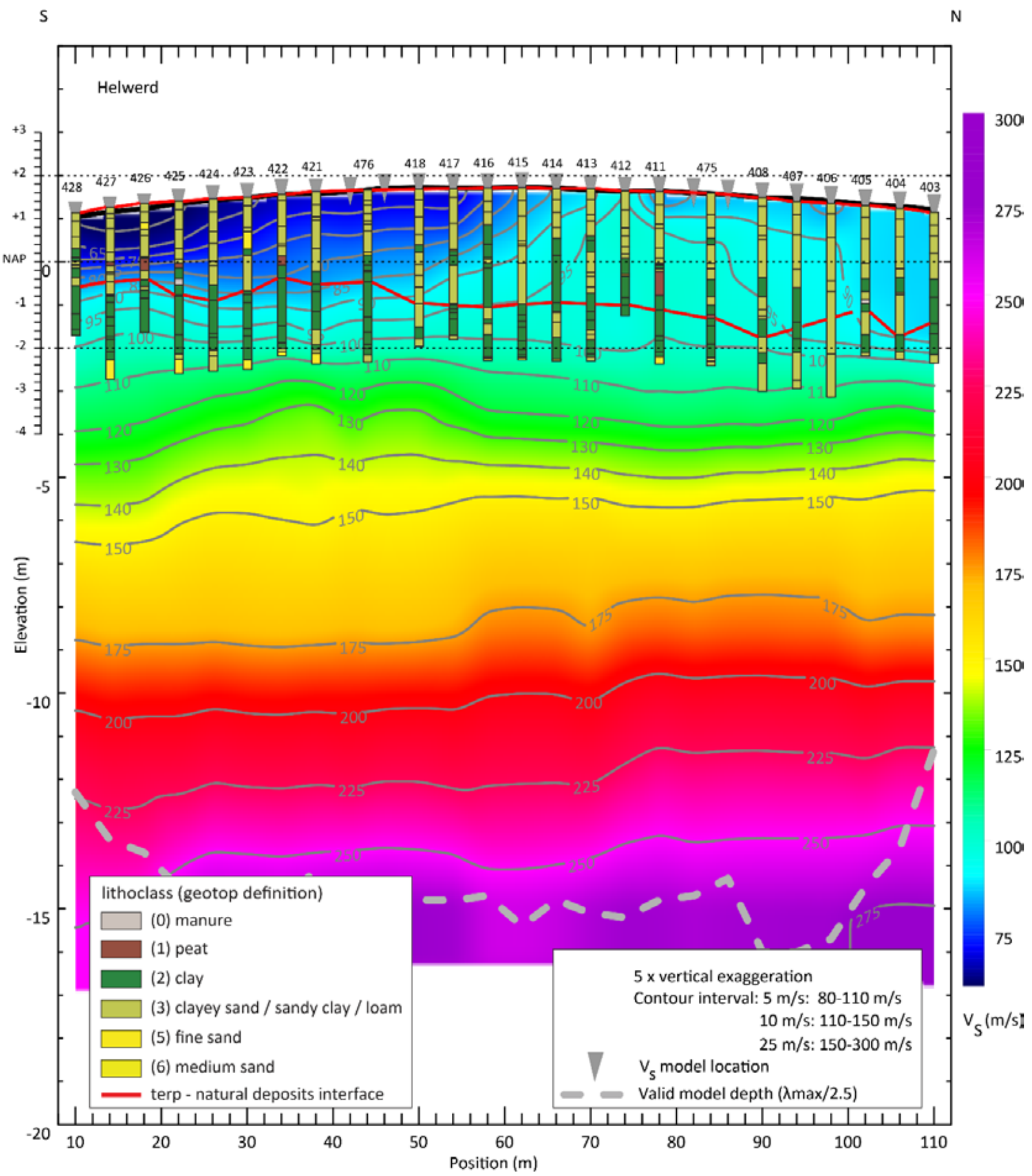


*Figure 4.28: Rayleigh wave 2D profile with archaeo-lithological corings for Helwerd (adapted after Geovision, 2019a)*

# 5 Synthesis

## 5.1 Shear wave velocity lithoclass characterisation

Figure 5.1 and Table 5.1 show the average $v_s$ values per lithoclass over all eight terps combined. It is shown, that taken all samples (in and below terp) into account, the peat lithoclass shows $v_s$ values of around 70 m/s on average, which is significantly lower than all other lithoclasses. Manure, clay and clayey sand, sandy clay and loam (Geotop classes 0, 2 and 3) are similar and not statistically different with values of around 85-90 m/s. Fine sand shows significantly higher $v_s$ values (101 m/s). This is the same for within-terp samples, with manure, clay and clayey sand, sandy clay and loam not being significantly different, but fine sand showing distinctively higher $v_s$ values. Since peat is a natural organic sediment, it is not present in terps by definition. Below the terp, the differences between all lithoclasses are larger and more significant, with peat again being the lowest and fine sand being the highest. Average $v_s$ values of fine sand (class 5) within the terp seem to be slightly lower than the same lithoclass underneath the terp.

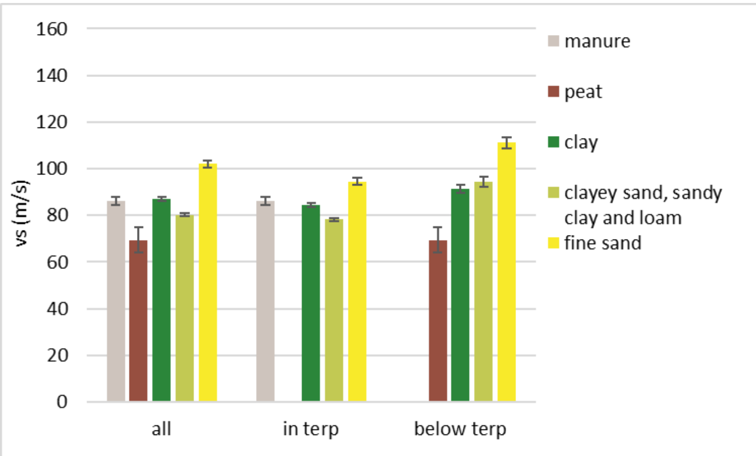


*Figure 5.1: Rayleigh $v_s$ values per lithoclass for all terps combined. Error bars denote standard errors.*

*Table 5.1: ANOVA results for $v_s$ values per lithoclass for all terps combined*

| | | $v_s$ (m/s) | | |
|---|---|---|---|---|
| **lithoclass** | **code** | **n** | **mean** | **std.** |
| natural | 0 | 328 | 96.4 | 23.5 |
| anthropogenic | 1 | 904 | 83.1 | 16.4 |
| | Total | 1232 | 86.6 | 19.5 |
| | | | | |
| ANOVA | F | 125.395 | | |
| | p | 0.000 | | |

| | | all samples | | | within terp | | | under terp | | |
|---|---|---|---|---|---|---|---|---|---|---|
| **lithoclass** | **code** | **n** | **mean** | **std.** | **n** | **mean** | **std.** | **n** | **mean** | **std.** |
| manure | 0 | 123 | 86.1 | 19.9 | 123 | 86.1 | 19.9 | 0 | | |
| organic material (peat) | 1 | 13 | 69.4 | 18.9 | 0 | | | 13 | 69.4 | 18.9 |
| clay | 2 | 391 | 87.1 | 17.9 | 235 | 84.4 | 14.9 | 156 | 91.2 | 21.1 |
| clayey sand, sandy clay and loam | 3 | 487 | 80.2 | 15.1 | 428 | 78.3 | 13.8 | 59 | 94.4 | 16.7 |
| fine sand | 5 | 214 | 102.0 | 21.5 | 118 | 94.5 | 16.6 | 96 | 111.2 | 23.4 |
| medium fine sand | 6 | 4 | 67.1 | 22.9 | 0 | | | 4 | 67.1 | 22.9 |
| | Total | 1232 | 86.6 | 19.5 | 904 | 83.1 | 16.4 | 328 | 96.4 | 23.5 |
| | | | | | | | | | | |
| ANOVA | F | 58.532* | | | 37.502 | | | 26.239* | | |
| | p | 0.000 | | | 0.000 | | | 0.000 | | |

**excl. medium fine sand*

## 5.2 Shear wave velocities characterisation between terps

In Table 5.2 we show all average $v_s$ values of all terps. Note that the terps are ordered by increasing shear wave velocity. Clearly, average $v_s$ values range from 72 m/s (Amsweer) to 107 m/s (Grote Houw) with an overall average of 87 m/s. Between the terps, the ANOVA analysis shows that these differences are significant. The general picture of the samples within the terp is similar, in which the order of terps in terms of $v_s$ values is virtually the same (with Fransum and Beswerd as exceptions). Generally, $v_s$ values within the terp are around 5 m/s lower than the entire sample.

*Table 5.2: ANOVA results for $v_s$ values between terps. Terps are ordered by increasing $v_s$.*

| | | all samples (in & under terp) | | | in terp samples | | |
|---|---|---|---|---|---|---|---|
| | | | $v_s$ (m/s) | | | $v_s$ (m/s) | |
| **Terp** | **nr.** | **n** | **mean** | **std.** | **n** | **mean** | **std.** |
| Amsweer | 1 | 165 | 71.9 | 13.3 | 89 | 68.2 | 4.3 |
| Biessum | 3 | 154 | 74.7 | 8.8 | 112 | 72.9 | 8.4 |
| Ezinge Zuiderweg 3 | 4 | 142 | 80.4 | 14.3 | 99 | 76.1 | 11.7 |
| Groot Maarslag | 6 | 102 | 81.5 | 13.5 | 79 | 77.7 | 9.1 |
| Helwerd Rottum | 8 | 156 | 89.6 | 13.7 | 112 | 86.1 | 13.3 |
| Fransum | 5 | 204 | 92.0 | 17.8 | 171 | 87.5 | 13.6 |
| Beswerd | 2 | 154 | 93.3 | 24.0 | 123 | 85.7 | 19.9 |
| Grote Houw | 7 | 155 | 106.5 | 18.8 | 119 | 101.1 | 16.1 |
| | Total | 1232 | 86.6 | 19.5 | 904 | 83.1 | 16.4 |
| ANOVA | F | 76.348 | | | 66.130 | | |
| | p | 0.000 | | | 0.000 | | |

When breaking down in lithoclasses per terp (Table 5.3), it becomes clear that the variation between lithoclasses is substantial and statistically significant. $V_s$ values of manure range from 69 to 105 m/s, depending on the terp, with Biessum, Amsweer and Groot Maarslag showing the lowest, and Grote Houw and Beswerd showing relatively high values. For clay, values range from 68 to 106 m/s within the terp, with Amsweer, Ezinge and Biessum showing relatively low values in comparison to Groot Maarslag and Beswerd. For clayey sand and sandy clay, again Amsweer, Ezinge and Biessum appear to be showing the lowest values and Grote Houw, Fransum and Helwerd the highest. For fine sand, Amsweer and Biessum have the lowest values, and Grote Houw and Helwerd the largest. Since the order of the $v_s$ values per terp seems to be similar (Amswer, Biessum consistently being on the low side, and Grote Houw and Helwerd on the high side), we may observe some 'terp effect' rather than a lithoclass effect. To test this, we carried out a regression analysis, described in the following paragraph.

*Table 5.3: ANOVA results for $v_s$ lithoclass values between terps*

| | | | In terp (anthropogenic) | | | | Below terp (natural deposits) | | | | |
|---|---|---|---|---|---|---|---|---|---|---|---|
| | | | $v_s$ (m/s) | | ANOVA | | | $v_s$ (m/s) | | ANOVA | |
| **manure (0)** | **nr** | **n** | **mean** | **std.** | **F** | **p** | **n** | **mean** | **std.** | **F** | **p** |
| Amsweer | 1 | 3 | 68.9 | 3.8 | 13.516 | 0.000 | | | | | |
| Beswerd | 2 | 11 | 103.9 | 21.9 | | | | | | | |
| Biessum | 3 | 30 | 71.1 | 4.4 | | | | | | | |
| Ezinge Z. 3 | 4 | 11 | 96.0 | 11.3 | | | | | | | |
| Fransum | 5 | 23 | 88.6 | 18.6 | | | | | | | |
| Groot Maarslag | 6 | 21 | 74.5 | 6.9 | | | | | | | |
| Grote Houw | 7 | 17 | 105.1 | 25.5 | | | | | | | |
| Helwerd Rottum | 8 | 7 | 94.4 | 11.4 | | | | | | | |
| Total | | 123 | 86.1 | 19.9 | | | | | | | |

*(Table continues on next page)*

| | | In terp (anthropogenic) | | | | | Below terp (natural deposits) | | | | |
|---|---|---|---|---|---|---|---|---|---|---|---|
| | | | $v_s$ (m/s) | | ANOVA | | | $v_s$ (m/s) | | ANOVA | |
| **clay (2)** | **nr** | **n** | **mean** | **std.** | **F** | **p** | **n** | **mean** | **std.** | **F** | **p** |
| Amsweer | 1 | 44 | 68.7 | 4.7 | 24.975 | 0.000 | 54 | 78.1 | 18.1 | 24.625 | 0.000 |
| Beswerd | 2 | 30 | 97.5 | 17.1 | | | | | | | |
| Biessum | 3 | 15 | 78.4 | 6.3 | | | 21 | 85.3 | 4.5 | | |
| Ezinge Z. 3 | 4 | 22 | 77.5 | 9.4 | | | 19 | 86.4 | 11.4 | | |
| Fransum | 5 | 96 | 88.1 | 13.6 | | | 29 | 113.7 | 19.3 | | |
| Groot Maarslag | 6 | 1 | 106.2 | . | | | 7 | 99.1 | 22.6 | | |
| Grote Houw | 7 | | | | | | 2 | 156.3 | 0.0 | | |
| Helwerd Rottum | 8 | 27 | 90.9 | 9.0 | | | 24 | 94.7 | 6.7 | | |
| Total | | 235 | 84.4 | 14.9 | | | 156 | 91.2 | 21.1 | | |
| **clayey sand, sandy clay, loam (3)** | | | | | | | | | | | |
| Amsweer | 1 | 41 | 67.8 | 3.8 | 23.538 | 0.000 | 4 | 77.3 | 10.2 | 4.664 | 0.001 |
| Beswerd | 2 | 78 | 78.8 | 16.4 | | | | | | | |
| Biessum | 3 | 63 | 72.2 | 9.7 | | | 3 | 86.5 | 2.3 | | |
| Ezinge Z. 3 | 4 | 66 | 72.3 | 8.6 | | | 22 | 93.4 | 17.3 | | |
| Fransum | 5 | 49 | 85.9 | 11.0 | | | 2 | 128.0 | 4.2 | | |
| Groot Maarslag | 6 | 36 | 79.1 | 7.4 | | | 12 | 88.4 | 16.7 | | |
| Grote Houw | 7 | 22 | 99.3 | 18.2 | | | | | | | |
| Helwerd Rottum | 8 | 73 | 82.4 | 13.0 | | | 16 | 101.8 | 10.1 | | |
| Total | | 428 | 78.3 | 13.8 | | | 59 | 94.4 | 16.7 | | |
| **fine sand (5)** | | | | | | | | | | | |
| Amsweer | 1 | 1 | 68.3 | . | 11.774 | 0.000 | 1 | 91.6 | . | 36.163 | 0.000 |
| Beswerd | 2 | 4 | 81.5 | 29.9 | 57.821* | 0.000 | 31 | 123.3 | 13.0 | *119.84*** | *0.000* |
| Biessum | 3 | 4 | 75.4 | 7.4 | *Groot Maarslag | | 18 | 72.1 | 4.9 | ** Beswerd, Biessum | |
| Ezinge Z. 3 | 4 | | | | and Grote Houw only | | 2 | 91.6 | 18.2 | & Grote Houw only | |
| Fransum | 5 | 3 | 88.4 | 8.7 | | | 2 | 127.3 | 5.2 | | |
| Groot Maarslag | 6 | 21 | 77.3 | 11.2 | | | 4 | 103.3 | 5.5 | | |
| Grote Houw | 7 | 80 | 100.7 | 12.8 | | | 34 | 122.6 | 14.2 | | |
| Helwerd Rottum | 8 | 5 | 102.3 | 18.4 | | | 4 | 109.9 | 15.7 | | |
| total | | 118 | 94.5 | 16.6 | | | 96 | 111.1 | 23.4 | | |

## 5.3 Regression analysis

For the regression analysis, we assumed that shear wave velocity is explained by the independent variables depth, lithoclass and the terp. We have used $v_s$ as dependent variable. Depth was defined as the top of each functional horizon, lithoclass followed the GeoTOP classification and terps are assigned a dummy number. We defined three models to assess which factor contribute to $v_s$ values for all eight terps combined. Model 1 includes depth and lithoclass. Since lithoclasses are nominal values, we have used dummies for each lithoclass. Sandy clay loam was chosen to be the reference, since this lithoclass has the average largest grain size in the spectrum and is generally associated with the highest $v_s$ values (Kruiver *et al.*, 2017b). Model 2 has depth and the terps as explaining variable to test the terp effect. Each terp (nominal value) is a dummy with Grote Houw being the reference because it shows the highest $v_s$ values in the range of terps. In model 3 we have combined all independent variables (depth, lithoclass and terp). We ran the regression model for all soil corings to a depth within the natural layers below the terp (models 1-3), and ran the model for terp samples only (models 4-6). The results are shown in Table 5.4 and Table 5.5.

Model 1 shows, that depth and lithoclass alone explain over 30% of the variation in $v_s$ values ($R^2$ = 0.350). All lithoclasses are significant ($p<0.01$), with manure, peat, clay and sandy clay all being negatively correlated with $v_s$ respective to sandy clay loam. Standardized betas show that the lithoclass contributions to the $v_s$ are similar. Depth is also significantly contributing to the variation in $v_s$ with a larger relative impact, since the standardized beta is about twice as high as from the lithoclasses. Using the same model but for the in-terp corings only (model 4), we observe that the explained variation is reduced by depth and lithoclasses only ($R^2$ = 0.266). There is a clear variation in lithoclass effects, as manure and clay are associated with lower $v_s$ values than sandy clay, all in respect to sandy clay loam (reference).

Different terps have different effects on $v_s$ values. Model 2 shows that all terps contribute significantly to the variation in $v_s$ values, and there is substantial variation in the strength of the effect of each individual independent variable. Amsweer is the strongest and Beswerd the weakest in respect to the reference terp (Grote Houw). The combination of depth and terp dummies explains 55% of the variation in $v_s$. Model 5, with only the in-terp samples shows a similar pattern ($R^2$ = 0.489), in which the terp effect seems to be more dominant (with standardized beta coefficient ranging from -0.32 to -0.57) than depth (-0.39). For the combined models (3 and 6, resp.), nearly 60% of the variation is explained by depth, lithoclass and terp ($R^2$ = 0.574 and 0.495, resp.). For model 3, all independent variables except clay and sandy clay lithoclasses contribute significantly to the $v_s$ ($p<0.01$), with depth contributing most strongly, followed by the terps. The lithoclass effect is less strong and only significant for peat and manure. When only considering in-terp samples, none of the lithoclass variables are significant. Depth is comparable to terp variables in terms of strength.

*Table 5.4: Multiple linear regression model results for explained variable $v_s$ for all samples (in and under terp) (n=1231)*

| Dependent variable: $v_s$ | Model 1 | | | | | Model 2 | | | | | Model 3 | | | | |
|---|---|---|---|---|---|---|---|---|---|---|---|---|---|---|---|
| All samples. all terps | Unstandardised | | Standardised | | | Unstandardised | | Standardised | | | Unstandardised | | Standardised | | |
| Variables | B | se | Beta | t | p | B | se | Beta | t | p | B | se | Beta | t | p |
| (Constant) | 86.1 | 1.33 | | 64.9 | 0.000 | 94.8 | 1.14 | | 83.6 | 0.000 | 95.4 | 1.21 | | 78.8 | 0.000 |
| Depth_top | -8.1 | 0.42 | -0.50 | -19.3 | 0.000 | -8.2 | 0.31 | -0.51 | -26.4 | 0.000 | -8.6 | 0.35 | -0.53 | -24.8 | 0.000 |
| manure (dummy) | -17.3 | 1.78 | -0.27 | -9.8 | 0.000 | | | | | | -7.6 | 1.55 | -0.12 | -4.9 | 0.000 |
| peat (dummy) | -44.5 | 4.54 | -0.23 | -9.8 | 0.000 | | | | | | -21.0 | 3.91 | -0.11 | -5.4 | 0.000 |
| clay (dummy) | -15.4 | 1.33 | -0.37 | -11.6 | 0.000 | | | | | | -2.4 | 1.38 | -0.06 | -1.7 | 0.088 |
| sandy clay (dummy) | -13.9 | 1.34 | -0.35 | -10.4 | 0.000 | | | | | | -2.0 | 1.33 | -0.05 | -1.5 | 0.136 |
| sandy clay loam (ref.) | | | | | | | | | | | | | | | |
| Amsweer (dummy) | | | | | | -37.1 | 1.46 | -0.65 | -25.5 | 0.000 | -34.6 | 1.75 | -0.61 | -19.8 | 0.000 |
| Beswerd (dummy) | | | | | | -14.0 | 1.48 | -0.24 | -9.4 | 0.000 | -13.1 | 1.60 | -0.22 | -8.2 | 0.000 |
| Biessum (dummy) | | | | | | -32.4 | 1.48 | -0.55 | -21.9 | 0.000 | -30.7 | 1.62 | -0.52 | -18.9 | 0.000 |
| Ezinge Zuiderweg (dummy) | | | | | | -28.1 | 1.51 | -0.46 | -18.6 | 0.000 | -26.9 | 1.76 | -0.44 | -15.3 | 0.000 |
| Fransum (dummy) | | | | | | -17.9 | 1.39 | -0.34 | -12.9 | 0.000 | -16.4 | 1.67 | -0.31 | -9.8 | 0.000 |
| Groot Maarslag (dummy) | | | | | | -26.1 | 1.66 | -0.37 | -15.7 | 0.000 | -24.6 | 1.74 | -0.35 | -14.1 | 0.000 |
| Helwerd (dummy) | | | | | | -19.1 | 1.48 | -0.33 | -12.9 | 0.000 | -18.1 | 1.71 | -0.31 | -10.6 | 0.000 |
| Grote Houw (ref) | | | | | | | | | | | | | | | |
| N | 1231 | | | | | 1231 | | | | | 1231 | | | | |
| $R^2$ | 0.350 | | | | | 0.556 | | | | | 0.574 | | | | |
| F | 131.81 | | | | | 191.49 | | | | | 136.79 | | | | |
| p | 0.000 | | | | | 0.000 | | | | | 0.000 | | | | |

*Table 5.5: Multiple linear regression model results for explained variable $v_s$ for in-terp samples (n = 903)*

| Dependent variable: $v_s$ | Model 4 | | | | | Model 5 | | | | | Model 6 | | | | |
|---|---|---|---|---|---|---|---|---|---|---|---|---|---|---|---|
| All samples. all terps | Unstandardised | | Standardised | | | Unstandardised | | Standardised | | | Unstandardised | | Standardised | | |
| Variables | B | se | Beta | t | p | B | se | Beta | t | p | B | se | Beta | t | p |
| (Constant) | 86.0 | 1.43 | | 60.0 | 0.000 | 94.0 | 1.16 | | 80.8 | 0.000 | 93.9 | 1.29 | | 73.0 | 0.000 |
| Depth_top | -7.8 | 0.57 | -0.46 | -13.8 | 0.000 | -6.6 | 0.41 | -0.39 | -16.1 | 0.000 | -7.1 | 0.48 | -0.42 | -14.7 | 0.000 |
| manure (dummy) | -16.6 | 1.91 | -0.35 | -8.7 | 0.000 | | | | | | -3.3 | 1.79 | -0.07 | -1.9 | 0.063 |
| peat (dummy) | | | | | | | | | | | | | | | |
| clay (dummy) | -13.4 | 1.60 | -0.36 | -8.4 | 0.000 | | | | | | 1.3 | 1.80 | 0.04 | 0.7 | 0.459 |
| sandy clay (dummy) | -13.4 | 1.48 | -0.41 | -9.1 | 0.000 | | | | | | 0.4 | 1.62 | 0.01 | 0.2 | 0.813 |
| sandy clay loam (ref.) | | | | | | | | | | | | | | | |
| Amsweer (dummy) | | | | | | -31.2 | 1.65 | -0.57 | -18.9 | 0.000 | -32.2 | 2.00 | -0.59 | -16.1 | 0.000 |
| Beswerd (dummy) | | | | | | -16.3 | 1.51 | -0.34 | -10.8 | 0.000 | -17.1 | 1.84 | -0.36 | -9.3 | 0.000 |
| Biessum (dummy) | | | | | | -27.9 | 1.55 | -0.56 | -18.1 | 0.000 | -27.8 | 1.83 | -0.56 | -15.2 | 0.000 |
| Ezinge Zuiderweg (dummy) | | | | | | -25.7 | 1.60 | -0.49 | -16.1 | 0.000 | -26.3 | 1.93 | -0.50 | -13.6 | 0.000 |
| Fransum (dummy) | | | | | | -16.5 | 1.41 | -0.40 | -11.6 | 0.000 | -17.5 | 1.81 | -0.42 | -9.7 | 0.000 |
| Groot Maarslag (dummy) | | | | | | -23.9 | 1.71 | -0.41 | -14.0 | 0.000 | -23.7 | 1.81 | -0.41 | -13.1 | 0.000 |
| Helwerd (dummy) | | | | | | -15.6 | 1.55 | -0.32 | -10.1 | 0.000 | -16.4 | 1.86 | -0.33 | -8.8 | 0.000 |
| Grote Houw (ref) | | | | | | | | | | | | | | | |
| N | 903 | | | | | 903 | | | | | 903 | | | | |
| $R^2$ | 0.266 | | | | | 0.489 | | | | | 0.495 | | | | |
| F | 81.309 | | | | | 106.979 | | | | | 79.470 | | | | |
| p | 0.000 | | | | | 0.000 | | | | | 0.000 | | | | |

## 5.4 Shear wave velocities from literature

For the Groningen area, in preparation for GMM version 5, Kruiver *et al.* (2015) compiled a shear wave velocity database, based on literature (Wassing *et al.*, 2013), a parametrisation of $v_s$ values based on 60 seismic cone penetration tests (SCPTs) and expert judgement (Kruiver *et al.*, 2015). The data were classified using lithoclass definitions and lithostratigraphic units, both as defined according to the GeoTOP model. To further improve the GMM, Kruiver *et al.* (2017b) used field $v_s$ measurements to obtain representative $v_s$ values for the different Groningen-specific natural sediment lithoclasses. The improved model (GMM v6) was used to calculate $v_s$ values based on the lithoclass profile obtained in this study.

The lithoclass profiles as obtained in this study were entered in the GMM v6 model. Consequently, we carried out a paired t-test in order to compare modelled and measured shear wave velocities. Lithoclass averaged $v_s$ values from all eight terps combined were compared against the modelled vs values per lithostratigraphic unit in and below the terps. This included a comparison of in-terp $v_s$ values with anthropogenic deposits (which are not further defined into lithoclasses by Kruiver et al. (2015) which were first modelled using the Kruiver et al., 2017 GMM v6 model.

*Table 5.6: Paired t-test results for $v_s$ values per lithoclass compared with modelling results based on Kruiver et al., 2017.*

| | | | **mean $v_s$ (m/s)** | | **std.** | | | |
|---|---|---|---|---|---|---|---|---|
| **lithoclass** | code | N | GMM v6 | this study | GMM v6 | this study | t | p |
| **All** | | | | | | | | |
| all samples | | 1009 | 145.9 | 84.4 | 37.3 | 17.6 | 46.2 | 0.000 |
| within terp | | 837 | 153.8 | 83.6 | 34.5 | 16.9 | 50.9 | 0.000 |
| under terp | | 172 | 107.8 | 88.1 | 24.5 | 20.7 | 10.0 | 0.000 |
| **Manure** | **0** | | | | | | | |
| all samples | | n/a | | | | | | |
| within terp | | 107 | 65.2 | 88.0 | 8.6 | 20.7 | -10.3 | 0.000 |
| under terp | | n/a | | | | | | |
| **Peat** | **1** | | | | | | | |
| all samples | | n/a | | | | | | |
| within terp | | n/a | | | | | | |
| under terp | | 17 | 65.1 | 70.4 | 9.0 | 18.4 | -1.0 | 0.349 |
| **Clay** | **2** | | | | | | | |
| all samples | | 339 | 147.7 | 84.5 | 30.8 | 15.8 | 33.9 | 0.000 |
| within terp | | 243 | 166.6 | 84.6 | 7.3 | 15.4 | 75.6 | 0.000 |
| under terp | | 96 | 99.8 | 84.2 | 3.9 | 16.9 | 9.2 | 0.000 |
| **clayey sand, sandy clay and loam** | **3** | | | | | | | |
| all samples | | 420 | 163.9 | 79.3 | 11.9 | 14.8 | 83.6 | 0.000 |
| within terp | | 392 | 167.1 | 78.4 | 0.0 | 14.4 | 122.3 | 0.000 |
| under terp | | 28 | 120.2 | 91.8 | 7.3 | 15.8 | 11.4 | 0.000 |
| **Fine sand** | **5** | | | | | | | |
| all samples | | 125 | 159.7 | 100.0 | 14.4 | 17.8 | 26.5 | 0.000 |
| within terp | | 94 | 167.1 | 97.6 | 0.0 | 15.7 | 42.9 | 0.000 |
| under terp | | 31 | 137.5 | 107.5 | 13.2 | 21.8 | 6.5 | 0.000 |
| **Medium fine sand** | **6** | | | | | | | |
| all samples | | n/a | | | | | | |
| within terp | | n/a | | | | | | |
| under terp | | n/a | | | | | | |

The results in Table 5.6 show that for all samples, $v_s$ values as measured in this study are statistically significantly lower than $v_s$ values as modelled by the GMM v6 model, with an average measured $v_s$ value of 84 m/s and an average modelled vs values of 146 m/s. This is also the case for within-terp values, with modelled $v_s$ values nearly twice as high as measured (154 against 84 m/s, resp.). When considering in-terp lithoclass $v_s$ values, manure layers are measured slightly but significantly higher than modelled (88 vs 65 m/s, resp). However, the field measurements of the lithoclasses clay, clayey sand and fine sand are consistently lower than modelled, roughly with typical average values twice as low. This difference is substantially higher than lithoclasses from sub-terp locations. Although the field $v_s$ measurements are still significantly lower than modelled, the difference is much less. Shear wave velocities from natural peat deposits do not show significantly different values (65 vs 70 m/s). However, we have only found peat at a single terp location (Amsweer), and with n=17, the number of $v_s$ measurements is relatively low here.

## 5.5 Soil map-based modelling

In phase 1 of the project, a method was proposed to predict the terp composition based on readily available maps and spatial databases. In this section, we compare the results using this method with the actual coring results of phase 2 of the project. Using the protocol outlined in Meijles *et al.* (2016), the lithological composition of the eight locations was modelled with the soil map as the source for lithological information, with the following changes and additions:

- terp height, or rather the thickness of the anthropogenic terp layers was calculated from the core data;
- for comparison with the actual terp height, maximum terp height and the average surface elevation of the surrounding area were calculated from AHN3 data;
- a sod thickness of 0,1 m rather than 0,15 m was used;
- after calculation of the percentage for each texture class, the (known) percentage of manure was added, and percentages recalculated. This allows better comparisons with the percentages of GeoTOP lithoclasses derived from the core data.

The results of the soil map modelling are presented for each location as piecharts in Figures 5.2 through 5.9.

*Table 5.7: Observed and estimated terp thicknesses.*

| | height (m) | | | geomorphological position |
|---|---|---|---|---|
| | calculated (AHN3) | observed | difference | |
| Amsweer | 2,64 | 2,63 | -0,01 | inversion ridge |
| Beswerd | 2,65 | 3,38 | 0,74 | |
| Biessum | 3,82 | 2,75 | -1,07 | inversion ridge |
| Ezinge Zuiderweg 3 | 2,39 | 3,00 | 0,61 | |
| Fransum | 3,35 | 3,84 | 0,94 | |
| Groot Maarslag | 4,12 | 3,15 | -0,97 | levee |
| Grote Houw | 3,19 | 3,19 | 0,00 | saltmarsh barrier |
| Helwerd | 2,76 | 2,77 | 0,01 | |

The availability of core data allows a direct comparison between observed terp thickness from core data and the estimated value from LIDAR data. The results are shown in Table 5.7 below. Surprisingly, some of the values, in particular those of Amsweer, Grote Houw and Helwerd, are virtually similar; among the other locations the LIDAR-derived values show the values to be either an overestimate or underestimate of up to 1,0 m. For some sites, the overestimation of terp thickness can be attributed to the geomorphological position of the terp. In the case of Groot Maarslag, the presence of a tidal channel levee underneath the terp body adds several dm to the thickness. Something similar appears to be the case at Biessum, although the LIDAR data also show that the immediate surroundings of the terp are lowered possibly as a result of clay extraction for bricks. In general, the estimation of terp thickness from LIDAR data appears to give a reasonable alternative for measured data, although the geomorphological position must be taken into account somehow.

In the analysis, we created proportional distributions of the texture from the soil map (phase 1) and GeoTOP lithoclass proportions (phase 2). However, since manure is added on the terp body itself and by definition cannot be estimated from soil maps, we added the volume of manure from the coring data to the soil map texture proportion, resulting in three piecharts per terp. The results and visual analyses are described below.

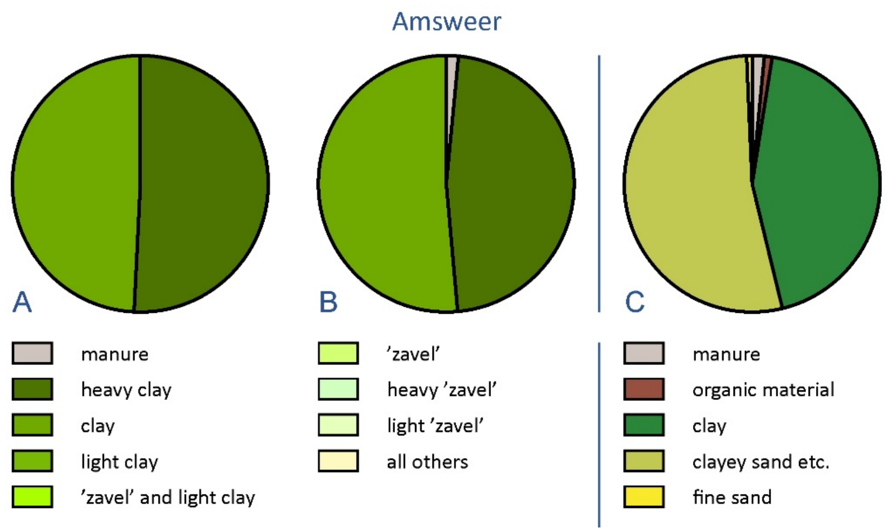


*Figure 5.2: Soil map modelling results for Amsweer. Left: percentage composition soil texture classes; centre: percentage composition soil texture classes including manure; right: GeoTOP lithoclasses.*

The results for Amsweer show a clear similarity between the calculated texture class percentages (Figure 5.2A) and the observed GeoTOP-lithoclasses (Figure 5.2C), with the 'clay' and 'heavy clay' texture classes matching the percentages for GeoTOP lithoclasses 'clayey sand' and 'clay' respectively. However, there is a mismatch between between 'clay' from the soil map data and 'clayey sand' from the coring data. This is not observed in other terps, where the 'clayey sand' category usually correlates with one of the lighter soil texture classes.

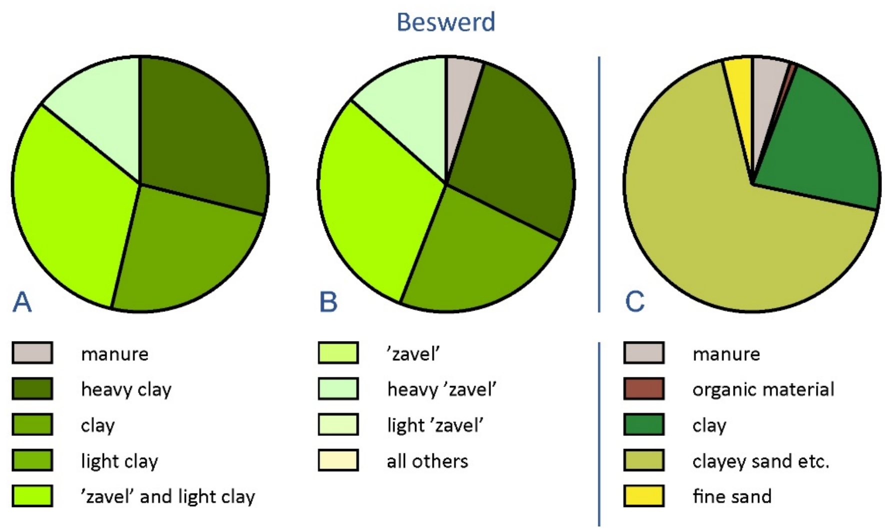


*Figure 5.3: Soil map modelling results for Beswerd. Left: percentage composition soil texture classes; centre: percentage composition soil texture classes including manure; right: GeoTOP lithoclasses.*

In Beswerd, a clear correlation between texture class 'heavy clay' and lithoclass 'clay' can be seen. Other texture classes seem to be included in lithoclass 'clayey sand'. The relatively small amount of fine sand in the cores has no equivalent in the soil texture classes.

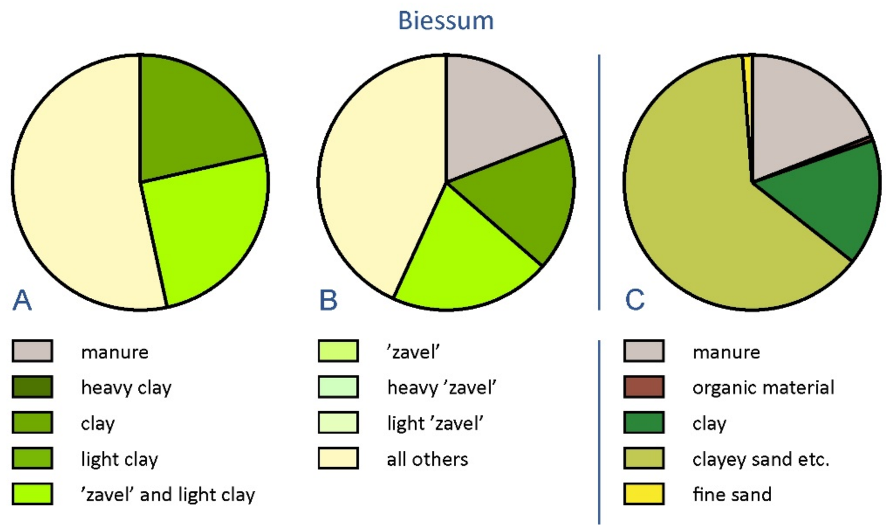


*Figure 5.4: Soil map modelling results for Biessum. Left: percentage composition soil texture classes; centre: percentage composition soil texture classes including manure; right: GeoTOP lithoclasses.*

Although the results for Biessum show some similarity, there are several problems associated with the analysis of the location. First of all, as the coring transect shows, the Biessum wierde is not lens-shaped like all the other locations, and its' highest point is not located in the centre. A cone, or in fact any other simple 3D- geometry, therefor is not a good representation of the volume. Furthermore, a considerable amount of the source area zone around Biessum consists of built-up residential areas. For these areas, amounting to more than 50% of total sod source area, no soil texture information is available. The results for Biessum therefore must be disregarded.

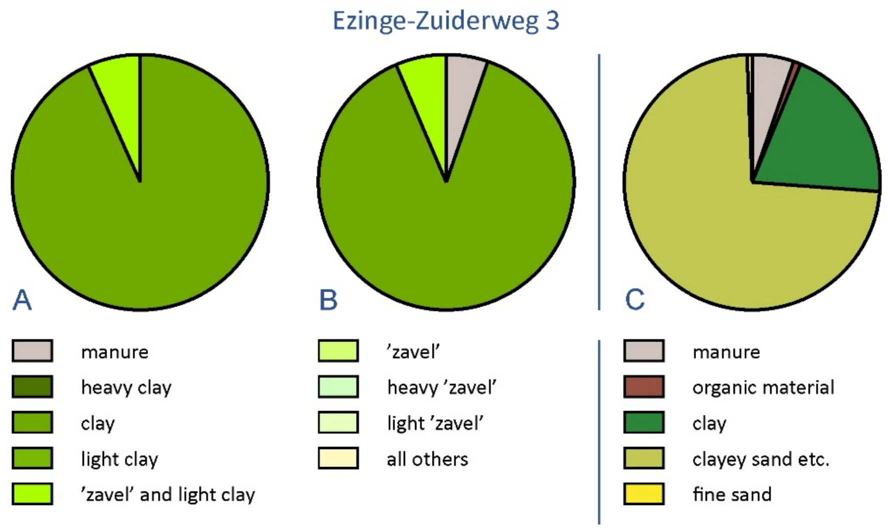


*Figure 5.5: Soil map modelling results for Ezinge-Zuiderweg 3. Left: percentage composition soil texture classes; centre: percentage composition soil texture classes including manure; right: GeoTOP lithoclasses.*

The Ezinge Zuiderweg 3 shows a relatively large correspondence between soil map texture and GeoTOP lithoclasses. From the cores, it is shown that around 75% of the terp material consists of clayey sands and sandy clays, with only around 20% of heavier clay. Data from the soil map show a very large proportion of light clay. However, the soil map method here shows a somewhat reduced variability than measured by the cores.

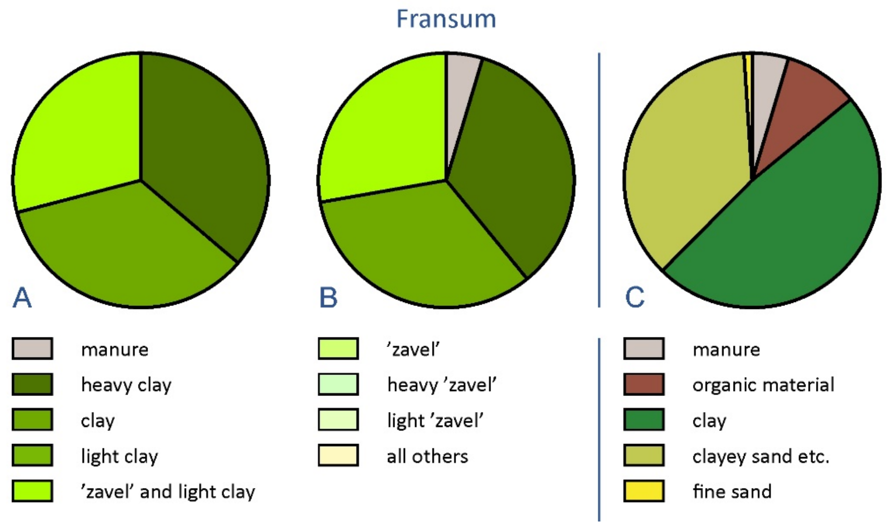


*Figure 5.6: Soil map modelling results for Fransum. Left: percentage composition soil texture classes; centre: percentage composition soil texture classes including manure; right: GeoTOP lithoclasses.*

The Fransum terp roughly shows 25-30% to be consisting of 'zavel' and light clays from the soil map analysis, whereas the cores show a somewhat higher proportion of the clayey sands and sandy clays. Soil map analysis suggest a slightly larger proportion of (heavy) clays than observed from the soil cores.

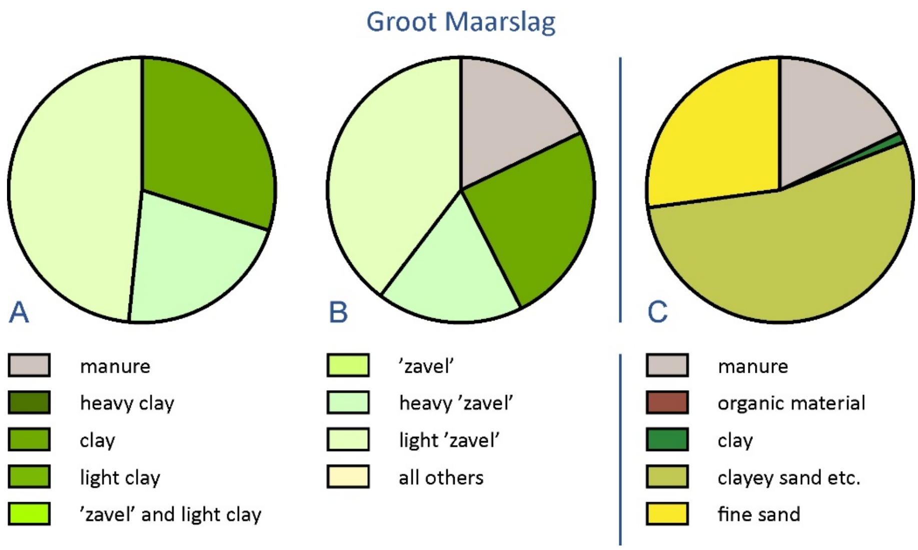


*Figure 5.7: Soil map modelling results for Groot Maarslag. Left: percentage composition soil texture classes; centre: percentage composition soil texture classes including manure; right: GeoTOP lithoclasses.*

The soil map modelling results confirm the dominance of relative coarse-grained sediments (fine sand and clayey sand lithoclasses) at Groot Maarslag. However, the soils on clay, amounting to almost 30% of the source area, are absent from the terp itself. A cause for this difference is not immediately apparent. Neither the pattern in which these soils occur on the soil map nor the geomorphological map give any clear indication. It is possible however, that these clayey soils in part or entirely post-date terp construction. The location of Groot Maarslag near a major active tidal channel, even when it's position shifted from the northerly course to the present-day Reitdiep system, may have resulted in deposition of predominantly sandy sediments throughout until embankment reduced flooding frequency but more importantly allowed standing water from which fine-grained sediments could settle.

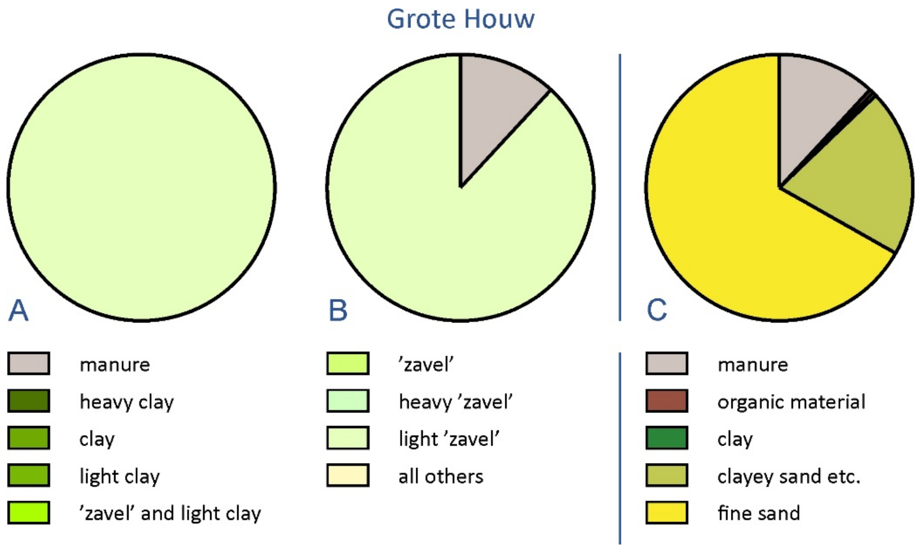


*Figure 5.8: Soil map modelling results for Grote Houw. Left: percentage composition soil texture classes; centre: percentage composition soil texture classes including manure; right: GeoTOP lithoclasses.*

A lack of differentiation in soil types and textures around Grote Houw results in diagrams with only a single texture class (light 'zavel'). This compares well with the GeoTOP lithoclass percentages; here, too, the fine sand lithoclass dominates with a minor contribution of the clayey sand class.

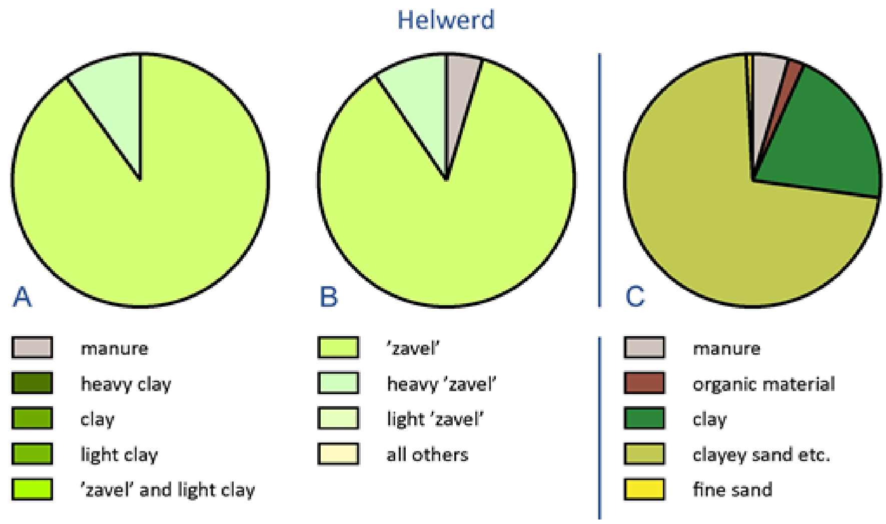


*Figure 5.9: Soil map modelling results for Helwerd. Left: percentage composition soil texture classes; centre: percentage composition soil texture classes including manure; right: GeoTOP lithoclasses.*

At Helwerd, a clear discrepancy between soil texture classes and GeoTOP lithoclass percentages can be seen. In contrast to Groot Maarslag however (where fine-grained sediments are absent from the terp body), the terp body contains c. 20% clay, which appears to be absent from the immediate surrounding area. However, the description of the soil types indicates that although the upper part consists of relatively coarse-grained sediments (in this case, 'zavel'), the part below c. 0.5 m to 0.7 m below surface level of the soil profile consists of clay and heavy clay (see for instance Kuijer, 1987).

The above results show that soil map modelling provides a fairly quick way of determining terp lithology and, to some extent, lithological variability. However, the presence of substantial but varying amounts of manure in terps (as demonstrated by the archaeo-lithological coring) is one of the drawbacks, which is hard to factor in into this method. Another, the fact that the present-day surface sediments are not necessarily coeval with terp formation, sometimes requires further analysis of the soil profile information. Using the data of a certain level below surface from GeoTOP model voxel stacks instead of the soil map could provide a better or more detailed result.
Using a cone to approximate the volumes of terps leads to a clear underestimation of the actual volume. However, given the horizontal resolution of the soil map (the area of the smallest soil unit is 0.4 ha), this probably has only a minor effect on the reconstructed percentages. Using an ellipsoid instead of a cone may provide an alternative which possibly could also compensate for non-circular or irregularly shaped terps. This is worth exploring, but falls outside the scope of the current project.
Finally, there is mounting evidence that sods with certain lithologies or lithological characteristics were used for specific purposes, in other words, a form of source area selection. Such selective use of natural resources cannot be represented by taking a simple buffer around a location. However, using a buffer remains an unavoidable simplification.

# 6 Conclusions and discussion

The shear wave velocity measurements in the eight investigated terps show substantially lower values than expected based on GMM modelling outcomes (GMM v6, Kruiver et al., 2017b). The difference is in the order of 1.5 to 2 lower. This is important, since earthquakes with the same energy with lower near-surface shear wave velocities will have a larger amplification effect on ground motions. The observation is valid for the in-terp anthropogenic deposits, as well as the natural deposits below the terp.

All investigated terps show significantly lower $v_s$ values in the terp (anthropogenic deposits) than in natural deposits below the terp. Average $v_s$ values of the anthropogenic deposits range from 68 m/s in Amsweer to 101 m/s in Grote Houw (Table 6.1), averaging at 85 m/s. The average $v_s$ of the natural subsurface is 102 m/s, which is substantially higher. The absolute difference between natural subsurface and terp deposits differ substantially, ranging from just 5 m/s in Biessum to 38 m/s in Beswerd. In seven out of eight terps $v_s$ increases with depth. In some terps, this gradually increases with depth, whereas in a couple of cases (Groot Maarslag, Beswerd and Fransum) this is stepwise, with the increment in $v_s$ values usually at or just below the terp base. This suggests that at least in some terps, the interface from natural deposits to the terp body acts as a transition from higher to lower shear wave velocities. This could have important implications for peak acceleration on the terp.

In all cases, the horizontal variation in $v_s$ values is higher in the terp than below, based on visual inspection. In general, it appears that the $v_s$ profile beneath the terp is showing much more homogeneous variation with depth than in the terp, and the $v_s$ values below terps show similar values, roughly 130 m/s at 5 m depth. Amsweer and Biessum are exceptions though, with much lower values of 90 and 110 m/s, respectively. This could suggest, that generally speaking, the terp composition has a strong influence on the passage of shear waves, since $v_s$ values near the surface show a higher degree in variation than at depth. This may also indicate, that the high variation should be reflected in updates in the GMM.

*Table 6.1: Overview of $v_s$ values of natural and anthropogenic lithoclasses.*

| Terp | $v_s$ average (m/s) natural | anthr. | difference (absolute) | $v_s$ with depth | ANOVA lithocl. p (in terp) | % clay in terp | % organic in terp |
|---|---|---|---|---|---|---|---|
| Amsweer | 76.8 | 68.2 | + 8.6 | increase | 0.095 | 46% | 4% |
| Beswerd | 123.3 | 85.7 | + 37.6 | stepwise | < 0.000** | 24% | 9% |
| Biessum | 78.2 | 73.1 | + 5.1 | not sign. | < 0.000** | 12% | 30% |
| Ezinge Z. 3 | 90.2 | 76.1 | + 14.1 | linear | 0.000** | 19% | 8% |
| Fransum | 114.9 | 87.6 | + 27.3 | stepwise | 0.643 | 51% | 14% |
| Groot Maarslag | 94.3 | 77.7 | + 17.6 | stepwise | 0.143 | 2% | 27% |
| Grote Houw | 120.9 | 100.6 | + 20.3 | linear | 0.922 | 0% | 15% |
| Helwerd | 98.7 | 86.1 | + 12.6 | linear | < 0.000** | 15% | 5% |
| average | 101.8 | 84.8 | | | | | |

It was shown that in most cases, manure has an impact on shear wave propagation, although this is a bit unambiguous. In the majority of the terps, $v_s$ values for manure differ significantly from other anthropogenic lithoclasses. Most often, values are lower but in two cases, values appeared higher (i.e. Beswerd and Ezinge Zuiderweg 3). On visual inspection, it becomes clear that in (thick) manure layers, generally substantial lower $v_s$ values are observed. This ‘manure effect’ also seems to appear higher in the profile, where substantially lower $v_s$ values are visible within or above relatively thick manure layers (e.g. Groot Maarslag, Ezinge Zuiderweg 3 and Fransum) or sometimes only above the manure layer (Beswerd and Grote Houw). In cases where the manure layers are overlain by relatively thick (clastic) anthropogenic layers, $v_s$ values tend to increase again closer to the terp surface, as for example in Biessum and Grote Houw.

Lithoclasses show significantly different shear wave velocities, with peat (69 m/s) being the lowest for all-in-terp and below-terp samples. Clayey sand, clay and manure are significantly higher (80-87 m/s). Fine sand shows the highest values (102 m/s). Within the terp body, however, this seems to be slightly different, with sandy clay providing the lowest values, increasing via manure and clay to fine sand being the highest. For natural deposits in the immediate area surrounding the terp, only measured at Groot Maarslag, we do not see significant difference between lithoclasses.

Based on multiple linear regression models, shear wave velocities can be explained by depth, lithoclass and the terp. Depth is a very strong predictor, which is strongly correlated with shear wave velocity in the profile. As for lithoclasses, peat and manure and to a lesser extent clay contributes to the explanation of $v_s$, with all three classes tending to lower $v_s$-values in respect to the sand lithoclass. We also observe that the terp itself is a predictor for $v_s$, with all terps contributing significantly to the shear wave velocity as dummy variable. However, it is as yet unclear what the 'terp effect' represents. Subsurface conditions may play a role here. Since it is apparent from the regression models that the explained variance within the terp is lower than the variance of both in-terp and under-terp samples, it is highly likely that the 'terp effect' originates below the terp basis. Possible, the lithology of the Pleistocene subsoil plays a role here, or the thickness and composition of the Holocene deposits. More research using deeper coring may shed light on this.

Since we can model the shear wave velocity based on depth and lithoclass, it may be possible to extrapolate the work to other terps in the area. By first assessing the lithology of individual terps, either by coring or by the method presented by Meijles et al. (2016) and secondly using the regression equation as model, it would be possible to calculate typical $v_s$ values for each individual terp.

By measuring shear wave velocities and detailed lithoclass composition, we now have a good overview of the 'typical' terp and the possible variations between different terps. With this study, we have created a characterisation of typical terps in the province of Groningen area, which can be used as input for an updated GMM to further assess the possible impact of the anthropogenic terp composition on earthquake amplification.

# 7 References

Aalbersberg, G. & H.W. Veenstra (in prep.). Archeologisch en seismisch onderzoek naar de lithologie en opbouw van acht wierden in de provincie Groningen (Gemeenten Het Hogeland, Delfzijl en Westerkwartier). RAAP Archeologisch Adviesbureau b.v., Weesp, The Netherlands.

Bazelmans, J., D. Meier, A. Nieuwhof, T. Spek, P. Vos. 2012. Understanding the cultural historical value of the Wadden Sea region. The co-evolution of environment and society in the Wadden Sea area in the Holocene up until early modern times (11,700 BC–1800 AD): An outline. Ocean & Coastal Management 68, 114-126, https://doi.org/10.1016/j.ocecoaman.2012.05.014

Bommer, J., Dost, B., Edwards, B., Kruiver, P., Ntinalexis, M., Rodriguez-Marek, A., Stafford, P.J., Van Elk, J. (2017). Developing a model for the prediction of ground motions due to earthquakes in the Groningen gas field. Netherlands Journal of Geosciences, 96(5), S203-S213. https://doi.org/10.1017/njg.2017.28

Elk, J. van, Doornhof, D., Bommer, J., Bourne, S., Oates, S., Pinho, R., & Crowley, H. (2017). Hazard and risk assessments for induced seismicity in Groningen. Netherlands Journal of Geosciences, 96(5), S259-S269. https://doi.org/10.1017/njg.2017.37

DINOloket, 2020. https://www.dinoloket.nl/ondergrondgegevens. Last accessed 20-8-2020.

Geovision, 2019a. Report surface wave data reduction and modeling. Fransum, Grote-Houw, Beswerd, Amsweer, Ezinge, Rottum and Biessum on wierde surveys. GEOVision Project No. 19172. 194 p.

Geovision, 2019b. Report surface wave data reduction and modeling. Groot Maarslag on wierde survey. GEOVision Project No. 18285. 67 p.

Geovision, 2019c. Report surface wave data reduction and modelling. Wierde Groot Maarslag off star 1 survey. GEOVision Project No. 17314. 163 p.

Giffen AE van. 1926. Resumé van de in de laatste vereenigingsjaren verrichte werkzaamheden ten behoeve van de Terpenvereeniging. *Jaarverslagen van de Vereeniging voor Terpenonderzoek* 9-10 (1924-1926), pp. 9-32.

Giffen AE van. 1928. Mededeeling omtrent de systematische onderzoekingen, verricht in de jaren 1926 en 1927, ten behoeve van de Terpenvereeniging in Friesland en Groningen. *Jaarverslagen van de Vereeniging voor Terpenonderzoek* 11-12 (1926-1928), pp. 30-48.

Huisman, D.J., Van der Heiden, M., Derickx, W., Kort, J.W. de, Reimann, T., Schoorl, J., Thasing, S., Egmond, F. van, Soest, M., Verplanke, P. & Wallinga, J., 2017. Erosie-onderzoek op de Grote Houw Oost in het kader van TOPsites. *Rapportage Archeologische Monumentenzorg* 238. Rijksdienst voor het Cultureel Erfgoed, Amersfoort.

Knol, E., 1993. De Noordnederlandse kustlanden in de Vroege Middeleeuwen. Academisch proefschrift Vrije Universiteit Amsterdam, Amsterdam/Groningen.

Koomen, A.J.M. and Maas, G.J. 2004. Geomorfologische Kaart Nederland (GKN). Achtergronddocument bij het landsdekkende digitale bestand. Wageningen, Alterra. Alterra rapport 1039.

Kruiver, P., de Lange G., Wiersma, A., Meijers, P., Korff, M., Peeters, P., Stafleu, J., Harting, R., Dambrink, R., Busschers, F., Gunnink, J. 2015. Geological schematisation of the shallow subsurface of Groningen. Deltares report 1209862-005. Deltares, Utrecht, The Netherlands, 227 p.

Kruiver, P., Wiersma, A., Kloosterman, F.H., De Lange, G., Korff, M., Stafleu, J. Busschers, F.S., Harting, R., Gunnink, J.L., Green, R.A., Van Elk, J., Doornhof, D. (2017a). Characterisation of the Groningen subsurface for seismic hazard and risk modelling. Netherlands Journal of Geosciences, 96(5), S215-S233. https://doi.org/10.1017/njg.2017.11

Kruiver, P.P., van Dedem, E., Romijn, R., de Lange, G., Korff, M., Stafleu, J., Gunnink, J.L., Rodriguez-Marek, A., Bommer, J.J., van Elk, J. & Doornhof, D., 2017b. An integrated shear-wave velocity model for the Groningen gas field, The Netherlands. Bulletin of Earthquake Engineering 15 (9): 3555–3580.

Kuijer, P.C. (1987). Bodemkaart van Nederland schaal 1:50.000. Toelichting bij de kaartbladen 3 West Uithuizen en 3 Oost Uithuizen. Stichting voor Bodemkartering Wageningen.
Leuvering, J.H.F., 2013. Inventariserend veldonderzoek, karterend booronderzoek, Usquerderweg 21 te Rottum. Synthegra Rapport S130060. Synthegra b.v., Doetinchem.

Langen, G.J. de & Mol, H. (2016). Terpenbouw en dorpsvorming tussen Vlie en Eems in de Volle Middeleeuwen. In: Nieuwhof (red.) (2016) Van Wierhuizen tot Achlum. Honderd jaar archeologisch onderzoek in terpen en wierden. Jaarverslagen van de Vereniging voor Terpenonderzoek 98, 99-128.

Meijles E.W. Aalbersberg G. and Groenendijk HA. 2016. Terp composition in respect to earthquake risk in Groningen. Rijksuniversiteit Groningen.

Meijles, E.W., Kiden, P., Streurman, H-J., van der Plicht, J., Vos, P.C., Gehrels, W.R., & Kopp, R.E. (2018). Holocene relative mean sea-level changes in the Wadden Sea area, northern Netherlands. Journal of Quaternary Science, 33(8), 905-923. https://doi.org/10.1002/jqs.3068

Miedema, M., 1983. Vijfentwintig eeuwen bewoning in het terpenland ten noordwesten van Groningen. Academisch proefschrift Vrije Universiteit Amsterdam. Drukkerij Doevendans, Dieren.

Miedema, M., 1990. Oost-Fivelingo 250 vC-1850 nC. Archeologische kartering en beschrijving van 2100 jaar bewoning in Noordoost-Groningen, Palaeohistoria 32, 111-1245.

Nieuwhof, A., & Schepers, M. (2016). Living on the edge: synanthropic salt marshes in the coastal area of the Northern Netherlands from around 600 BC. Archaeological Review from Cambridge, 31, 48-74

Nieuwhof, A., M. Bakker, E. Knol, G. J. de Langen, J. A. W. Nicolay, D. Postma, M. Schepers, T. W. Varwijk, and P. C. Vos. 2019. Adapting to the sea: Human habitation in the coastal area of the northern Netherlands before medieval dike building. Ocean & Coastal Management 173 (2019): 77-89. https://doi.org/10.1016/j.ocecoaman.2019.02.014

Rappol, M. (1984) - Till in Southeast Drente and the origin of the Hondsrug complex, the Netherlands. Eiszeitalter und Gegenwart 34, p. 7-27.

Roeleveld, W., 1974. The Holocene evolution of the Groningen marine-clay district. ). Berichten van de Rijksdienst voor het Oudheidkundig Bodemonderzoek 24 (supplement).

Stafleu, J. and Dubelaar CW. 2016. Product specification subsurface model GeoTOP. TNO report R10311 1.3. TNO Utrecht, The Netherlands, 53 p. https://www.DINOloket.nl/sites/default/files/file/DINOloket_toelichtingmodellen_20160606_tno_2016_r10133_geotop_v1r3_english.pdf. Last accessed 31-3-2020.

Stafleu J, Maljers D, Busschers FS, Gunnink JL, Schokker J, Dambrink RM, Hummelman, JH, Schijf, ML. 2012. GeoTOP modellering. TNO rapport TNO-2012-R10991. 214 p. Available at DINOloket.nl.

Stafleu J, Maljers D, Busschers FS, Gunnink JL, Schokker J, Hummelman, JH. 2019. Totstandkomingsrapport GeoTOP. TNO report R11655. TNO, Utrecht, The Netherlands. 132 p. https://www.DINOloket.nl/sites/default/files/Totstandkomingsrapport-GeoTOP.pdf

Vos, P.L. & Vries, S. de, 2013. *2^e^ generatie palaeogeografische kaarten van Nederland (versie 2.0)*. Deltares, Utrecht.

Van den Berg, M.W., Beets, D.J. (1987) - Saalian glacial deposits and morphology in the Netherlands. In: Van der Meer, J.J.M. (Ed), Tills and Glaciotectonics. Balkema, Rotterdam, 235–251.

Wassing, B.B.T., Maljers, D., Westerhoff, R.S., Bosch, J.H.A. & Weerts, H.J.T. (2003). Seismisch hazard van geïnduceerde aardbevingen, Rapportage fase 1. Report nr. NITG-03-185-C-def.